

การพัฒนาตัวรับเซรีซินจากไหมที่บรรจุในไฮโดรเจล และการประเมินฤทธิ์ทางชีวภาพ

นางสาวพนิดา เกทิพย์

วิทยานิพนธ์นี้เป็นส่วนหนึ่งของการศึกษาตามหลักสูตรปริญญาเภสัชศาสตรมหาบัณฑิต

สาขาวิชาเภสัชกรรม ภาควิชาวิทยาการเภสัชกรรมและเภสัชอุตสาหกรรม

คณะเภสัชศาสตร์ จุฬาลงกรณ์มหาวิทยาลัย

ปีการศึกษา 2554

ลิขสิทธิ์ของจุฬาลงกรณ์มหาวิทยาลัย  
บทคัดย่อและแฟ้มข้อมูลฉบับเต็มของวิทยานิพนธ์ตั้งแต่ปีการศึกษา 2554 ที่ให้บริการในคลังปัญญาจุฬาฯ (CUIR)

เป็นแฟ้มข้อมูลของนิสิตเจ้าของวิทยานิพนธ์ที่ส่งผ่านทางบัณฑิตวิทยาลัย

The abstract and full text of theses from the academic year 2011 in Chulalongkorn University Intellectual Repository (CUIR) are the thesis authors' files submitted through the Graduate School.

FORMULATION OF SILK SERICIN LOADED IN NIOSOMES AND  
EVALUTION OF BIOLOGICAL ACTIVITIES

Miss Panida Kethip

A Thesis Submitted in Partial Fulfillment of the Requirements  
for the Degree of Master of Science in Pharmacy Program in Pharmaceutics  
Department of Pharmaceutics and Industrial Pharmacy  
Faculty of Pharmaceutical Sciences  
Chulalongkorn University  
Academic Year 2011  
Copyright of Chulalongkorn University



พินิดา เกทิพย์: การพัฒนาตำรับเซริซินจากไหมที่บรรจุในนิโอโซม และการประเมินฤทธิ์ทางชีวภาพ. (FORMULATION OF SILK SERICIN LOADED IN NIOSOMES AND EVALUATION OF BIOLOGICAL ACTIVITIES) อ.ที่ปรึกษาวิทยานิพนธ์หลัก: รศ. ดร. สุชาดา ชุตติมาวรินทร์, อ.ที่ปรึกษาวิทยานิพนธ์ร่วม: รศ. ดร.ดวงเดือน เมฆสุริเยนทร์, 172 หน้า.

การศึกษานี้ตอนแรกสกัดเซริซินจากไหมพันธุ์นางน้อยศรีสะเกษ เพื่อศึกษาวิธีที่เหมาะสมในการสกัดเซริซิน พบว่าวิธีที่ 1 ซึ่งคัดเลือกเป็นวิธีที่เหมาะสมที่สุดโดยใช้การสกัดด้วยความร้อนภายใต้ความดัน เซริซินจากไหมที่สกัดด้วยวิธีที่ 1 ให้ฤทธิ์ต้านอนุมูลอิสระซูเปอร์ออกไซด์และฤทธิ์ต้านไทโรซิเนสสูงกว่าวิธีที่ 2 อย่างมีนัยสำคัญทางสถิติ ( $p < 0.05$ ) จากนั้นได้ศึกษาสภาวะการพ่นแห้งที่เหมาะสมที่สุดด้วยวิธีที่ 1 นี้ด้วยตัวเอง ได้ศึกษาผลของปัจจัยเกี่ยวกับกระบวนการได้แก่ ความเข้มข้นของรังไหม และ อุณหภูมิลมเข้าต่อปริมาณผลผลิตและปริมาณความชื้นโดยใช้วิธีการออกแบบส่วนประกอบกลางที่ผิวพบว่าโมเดลเชิงเส้นเหมาะสมเข้ากับร้อยละปริมาณผลผลิต และโมเดลกำลังสองเหมาะสมเข้ากับร้อยละปริมาณความชื้น ( $p < 0.05$ ) โดยใช้การพล็อตโอเวอร์เลย์สามารถหาสภาวะที่เหมาะสมที่สุดได้ และทดลองซ้ำพบว่าค่าเฉลี่ยของเปอร์เซ็นต์ปริมาณผลผลิตและร้อยละความชื้นที่ได้อยู่ในช่วงที่คาดการณ์ไว้ที่ระดับความเชื่อมั่น 95 เปอร์เซ็นต์ โดยมีค่า  $11.64 \pm 0.62$  เปอร์เซ็นต์ และ  $6.38 \pm 0.23$  เปอร์เซ็นต์ตามลำดับ แสดงว่าโมเดลดังกล่าวเข้ากันได้ดีกับผลการทดลอง การศึกษาคุณสมบัติของผงพ่นแห้งเซริซิน พบว่าปริมาณโปรตีนเท่ากับ  $21.83 \pm 1.71$  เปอร์เซ็นต์ ฤทธิ์ต้านอนุมูลอิสระพบว่ามีการยับยั้งอนุมูลอิสระดีพีพีเฮกซ์ที่ 50% ( $EC_{50}$ ) เท่ากับ 0.82 มิลลิกรัมต่อมิลลิลิตร และค่าการยับยั้งอนุมูลซูเปอร์ออกไซด์ที่ 50% เท่ากับ 0.43 มิลลิกรัมต่อมิลลิลิตร และมีค่าการยับยั้งไทโรซิเนสที่ 50% เท่ากับ 0.40 มิลลิกรัมต่อมิลลิลิตร การเตรียมนิโอโซมโดยบรรจุเซริซินจากไหม 1.0% โดยน้ำหนักต่อปริมาตร โดยวิธีระเหยแบบกลีบวัตภาค สามารถเตรียมได้ 4 สูตรตำรับโดยใช้ สเปน 20 สเปน 40 สเปน 60 และสเปน 80 โดยอัตราส่วนระหว่างสารลดแรงตึงผิวและคอเลสเตอรอล เท่ากับ 1:1 และใช้โซลูแลนซี<sup>®</sup>-24 เป็นสารเพิ่มความคงตัว ขนาดเวสิเคิลที่ได้จากทุกสูตรตำรับซึ่งวัดโดยเทคนิคโฟตอนคอร์ริเลชัน สเปกโทรสโกปี มีขนาดระหว่าง 181-341 นาโนเมตร ประสิทธิภาพการกักเก็บสารมีค่าระหว่าง 84.22-93.88 เปอร์เซ็นต์ และทุกสูตรตำรับยังคงมีฤทธิ์ทางชีวภาพ ขนาดเวสิเคิลมีการเปลี่ยนแปลงใหญ่ขึ้นเมื่อเก็บไว้ที่อุณหภูมิ 4<sup>o</sup>ซ นาน 8 สัปดาห์ ค่าเปอร์เซ็นต์ปริมาณเซริซินในสูตรตำรับนิโอโซมที่เก็บที่อุณหภูมิ 4<sup>o</sup>ซ นาน 8 สัปดาห์มีค่าลดลงแต่ไม่มีนัยสำคัญทางสถิติในสูตรที่ประกอบด้วยสเปน 40 และสเปน 60 ( $p > 0.05$ ) การศึกษาการซึมผ่านผิวหนังแบบนอกกายใช้ผิวหนังหน้าท้องของสุกรแรกเกิดเป็นโมเดล พบว่าตำรับนิโอโซมซึ่งบรรจุเซริซินสามารถเพิ่มการซึมผ่านผิวหนังได้เมื่อเทียบกับสารละลายเซริซิน แสดงให้เห็นว่ารูปแบบการนำส่งด้วยนิโอโซมสามารถเพิ่มการนำส่งเซริซินผ่านผิวหนังได้ โดยมีค่าสัมประสิทธิ์การซึมผ่านระหว่าง 0.0043-0.0051 ซม/ชั่วโมง

ภาควิชา วิทยาการเภสัชกรรมและเภสัชอุตสาหกรรม ลายมือชื่อ.....  
 สาขาวิชา เภสัชกรรม..... ลายมือชื่อ.....ที่ปรึกษาวิทยานิพนธ์หลัก.....  
 ปีการศึกษา 2554..... ลายมือชื่อ.....ที่ปรึกษาวิทยานิพนธ์ร่วม.....

# # 5276581433 : MAJOR PHARMACEUTICS

KEYWORDS : SILK SERICIN / SPRAY DRAYING / NIOSOMES /  
ANTI-OXIDANT ACTIVITIES / ANTI-TYROSINASE ACTIVITY /  
SKIN PERMEATION

PANIDA KETHIP: FORMULATION OF SILK SERICIN LOADED IN NIOSOMES AND EVALUATION OF BIOLOGICAL ACTIVITIES. ADVISOR: ASSOC. PROF. SUCHADA CHUTIMAWORAPAN, Ph.D., CO-ADVISOR: ASSOC. PROF. DUANGDEUN MEKSURIYEN, Ph.D., 172 pp.

The process of extraction of sericin from silkworm, *Bombyx mori* Linn (Nang-noi Sisaket 1), was investigated for the appropriate method for silk sericin extraction. Method I which was performed by using a high temperature and pressure degumming technique, yielded silk sericin with a significantly higher superoxide scavenging and antityrosinase activities than method II ( $p < 0.05$ ). In addition, the optimized spraying condition was estimated using response surface methodology. The effect of two process parameters, inlet temperature and cocoon concentration solution on yield and moisture content was studied. A face centered design showed a linear model fitted for %yield and a quadratic model for %moisture content ( $p < 0.05$ ). The optimum region by overlay plot was carried out using the best condition to evaluate the repeatability of the spray-drying technique. The observed means obtained for %yield and %moisture content were in range of the prediction intervals at 95% confidence level as,  $11.64 \pm 0.62\%$  and  $6.38 \pm 0.23\%$ , respectively. The result clearly showed that the model fitted the experimental data well. The properties of silk sericin spray dried powder were determined. The protein content of silk sericin was  $21.83 \pm 1.71\%$  (w/w). The scavenging activities of sericin against DPPH and superoxide free radicals exhibited the  $EC_{50}$  values of 0.82 and 0.43 mg/ml, respectively. The antityrosinase activity of sericin exhibited an  $EC_{50}$  value of 0.40 mg/ml. Consequently, niosomes loaded with 1.0% weight by volume silk sericin could be prepared by reverse phase evaporation technique. Niosomes could be achieved by four formulations using Span 20, Span 40, Span 60 and Span 80 with surfactant: cholesterol ratio of 1:1 and with Solulan<sup>®</sup> C-24 as a stabilizer. Vesicular sizes of all formulations determined by photon correlation spectroscopy technique were between 181-341 nanometers. Entrapment efficiency of all niosomes formulation was between 84.22-93.88%. All of silk sericin loaded in niosomes formulations have biological activities. Vesicular size showed a larger mean size at 4 °C for 12 weeks. The percentage of silk sericin in niosomes that composed of Span 40 and Span 60 were non-significantly decreased at 4 °C for 8 weeks ( $p > 0.05$ ). The in vitro permeation using newborn abdominal porcine skin as skin model revealed that niosomes loaded with sericin could enhance the skin penetration of sericin through pig skin as compared with sericin solution. The result demonstrated that niosomes could enhance the delivery of sericin through skin. The permeability coefficient of sericin loaded niosome formulations were between 0.0043-0.0051 cm/h.

Department : Pharmaceutics and Industrial Pharmacy Student's Signature .....

Field of Study : Pharmaceutics..... Advisor's Signature .....

Academic Year : 2011..... Co-advisor's Signature .....

## ACKNOWLEDGEMENTS

I wish to express sincere gratitude to my advisor, Associate Professor Suchada Chutimaworapan, Ph.D. for her wide knowledge and logical ways of thinking, which have been of great value for me. I am most grateful for her meaningful advice, patience, and encouragement, all of which made the completion of this study possible.

My great appreciation is due to my co-advisor, Associate Professor Duangdeun Meksuriyen, Ph.D. for her kindness, valuable guidance and continual support during the biochemical and biological testing.

I sincerely thank to the reviewers of this thesis, Associate Professor Parkpoom Tengamnuay, Ph.D., the chairman of my thesis examination committee, as well as other committee members. I am grateful to Assistant Professor Angkana Tantituvanont, Ph.D. and Assistant Professor Panida Asavapichayont, Ph.D. for their constructive criticism and for giving me valuable suggestions for improvement.

I am very grateful to Dr. Dusadee Charnvanich for spending her valuable time and helpful guidance for the statistical program.

My deep gratitude is given to the Faculty of Pharmaceutical Sciences for the research which supports to this investigation.

My gratitude is given to the Faculty of Medicine Siriraj Hospital, Mahidol University for partially financial support the course of my education.

I would like to thank Pathom-Kaset Farm for giving the dead newborn pigs.

Sincere thanks are also given to my friends for their friendship, all staffs of the Department of Pharmaceutics and Industrial Pharmacy, Department of Biochemistry and Microbiology, Faculty of Pharmaceutical Sciences, Chulalongkorn University and other people whose names have not been mentioned here for their assistance and great helpful support during the time of my study.

Finally, greatest thanks to my family for their everlasting love, understanding, encouragement, and continued support during the course of my education.

## CONTENTS

	PAGE
ABSTRACT [THAI].....	iv
ABSTRACT [ENGLISH].....	v
ACKNOWLEDGEMENTS.....	vi
CONTENTS.....	vii
LIST OF TABLES.....	ix
LIST OF FIGURES.....	xi
LIST OF ABBREVIATIONS.....	xv
CHAPTER	
I INTRODUCTION.....	1
II LITERATURE REVIEW.....	4
Silk sericin.....	4
Free radical scavenging activities .....	10
Anti-tyrosinase activity.....	19
Niosomes .....	22
III MATERIALS AND METHODS.....	29
Materials.....	29
Apparatus.....	31
Accessories.....	32
Methods.....	34
A. Preparation of silk sericin.....	34
B. Optimization of spray drying condition.....	46
C. Determination of physicochemical and biological activities of silk sericin power.....	48
D. Preparation and evaluation of niosomes verified in compositions.....	50

CHAPTER	PAGE
E. Detection of biological activities of niosome loaded with sericin.....	53
F. Skin permeation study of niosomes loaded with sericin comparing with sericin in other system .....	53
IV RESULTS AND DISCUSSION.....	55
A. Comparision of extraction methods for silk sericin.....	55
B. Optimization of spray drying condition.....	67
C. Determination of physicochemical and biological activities of silk sericin powder (from the optimized condition).....	83
D. Preparation and evaluation of niosomes verified in compositions.....	88
E. Determination of biological activities of niosomes loaded with sericin.....	98
F. Skin permeation study of niosomes loaded with sericin.....	99
V CONCLUSIONS.....	105
REFERENCES.....	108
APPENDICES.....	119
Appendix A Molecular structure and physical properties of material.....	120
Appendix B Comparison of extraction methods for silk sericin.....	124
Appendix C Determination of entrapment efficiency and stability of niosomes.....	138
Appendix D Skin permeation study.....	161
VITA.....	172



## LIST OF TABLES

TABLE		PAGE
1	Amino acid composition of silk sericin and fibroin.....	8
2	Reactive oxygen and nitrogen species .....	11
3	Component of separating gel and stacking gel.....	40
4	Factor and level of studied variables.....	46
5	A face-centered composite design with observed responses.....	47
6	Composition of lipid in formulations in various ratios of cholesterol and surfactant.....	51
7	Comparison of percentage yield, percentage moisture content and physical appearances silk sericin spray dried powder from two different methods.....	56
8	A face-centered composite design with observed responses.....	67
9	ANOVA for response surface linear model of %yield.....	69
10	ANOVA for response surface quadratic model of %moisture content.....	69
11	Model summary statistics of %yield and %moisture.....	70
12	Coefficients of the regression equation linking the response to the experimental factors and major interactions (coded units).....	70
13	Optimum region by overlay plot of two parameters and the observed responses .....	76
14	Observed responses and 95% CI (confidence interval) of optimization spray dried condition.....	76
15	The particle size distributions of silk sericin spray dried particles (mean $\pm$ SD; n=3).....	82
16	Particles size and polydispersity index (mean $\pm$ SD) of silk sericin loaded niosome formulations under storage in refrigerator (4-8 °C) (n=3).....	91
17	Entrapment efficiency of silk sericin loaded in niosome when storage in refrigerator (4-8 °C) for 8 weeks.....	94

TABLE		PAGE
18	Particle size* and polydispersity index* of silk sericin loaded in noisome formulations under storage in refrigerator (4-8 °C) for 8 weeks.....	95
19	The membrane permeability coefficient of various formulation of silk sericin.....	104

## LIST OF FIGURES

FIGURE		PAGE
1	Silk cocoons of <i>Bombyx mori</i> Nang-Noi Sisaket 1.....	5
2	Cellular redox homeostasis.....	12
3	Structure of DPPH before and after reacted with antioxidant (AH).....	14
4	Structure of nitro-blue tetrazolium (NBT) reaction with $O_2^{\bullet-}$ into formazan.....	15
5	Reaction of guaiacol with hydrogen peroxide in the presence of peroxidase to produce tetraguaiacol .....	16
6	Reaction of deoxyribose with hydroxyl radical in the presence of thiobarbituric acid to produce pink chromogen .....	17
7	The L-arginine/nitric oxide pathway.....	18
8	The Griess reaction. Under acidic condition, nitrite reacts with the amino group of sulfanilamide to form the diazonium cation, which couples to N-(1-naphthyl)ethylenediamine in <i>para</i> -position to form the azo dye.....	19
9	Biosynthetic pathway of melanin .....	20
10	Structure of niosomes.....	23
11	Chemical structure of Span series.....	24
12	Chemical structure of cholesterol.....	25
13	Spray dryer .....	35
14	Procedure of setting up gel cassettes.....	39
15	Silk sericin spray dried powder from two different methods.....	56
16	Morphology of particles of spray dried products from method I and II.....	57
17	Standard curve of BSA, n=5.....	58

FIGURE	PAGE
18 SDS-PAGE (10% ) analysis of BSA, sericin (method I) and sericin (methodII), compared with the rainbow marker.....	59
19 SDS-PAGE (8%) analysis of BSA, (method I), sericin (method II) and sericin (optimization), compared with the rainbow marker	60
20 SDS-PAGE (6%) analysis of BSA, (method I), sericin (method II) and sericin (optimization), compared with the rainbow marker	60
21 DPPH scavenging activity of silk sericin obtained from method I and II. L-ascorbic acid was used as a positive control (n=3).....	61
22 Superoxide radical scavenging activity of silk sericin obtained from method I and II. Quercetin was used as a positive control (n=3).....	62
23 Hydrogen peroxide scavenging activity of silk sericin obtained from method I and II. Quercetin was used as a positive control (n=4).....	63
24 Hydroxyl radicals scavenging activity of silk sericin obtained from method I and II. Mannitol was used as a positive control (n=3).....	64
25 Nitric oxide radical scavenging activity of silk sericin obtained from method I and II. Quercetin was used as a positive control (n=3).....	65
26 Anti-tyrosinase activity of silk sericin obtained from method I and II. Alpha-arbutin and kojic acid were used as a positive control (n=3).....	66
27 Linear regression plot of %yield and response surface plot of the %moisture content.....	72
28 Contour plots of the %yield and %moisture content.....	73
29 Normal probability plot of the %yield and %moisture content.....	74
30 Optimum region by overlay plot of two responses (%yield and %moisture content) evaluated as a function of inlet temperature and %cocoon concentration.....	76

FIGURE	PAGE
31	Silk sericin spray dried powder of optimal spray dried condition... 77
32	Morphology of particles of spray dried products under 3% cocoon concentration and three levels of inlet temperature, 100, 120 and 140°C..... 78
33	Morphology of particles of spray dried products under 6.5% cocoon concentration and three levels of inlet temperature, 100, 120 and 140°C..... 79
34	Morphology of particles of spray dried products under 10% cocoon concentration and three levels of inlet temperature, 100, 120 and 140°C..... 80
35	Morphology of particles of spray dried products under 4.6% cocoon concentration and 140°C of inlet temperature (optimum condition)..... 81
36	DSC thermogram of optimized silk sericin spray-dried powder.... 84
37	X-ray diffractograms of optimized silk sericin spray-dried powder 84
38	DPPH scavenging activity of optimized silk sericin (n=3)..... 85
39	Superoxide radical scavenging activity of optimized silk sericin (n=3)..... 86
40	Anti-tyrosinase activity of optimized silk sericin (n=3)..... 87
41	X-cross bilayer formation of niosomes loaded silk sericin by X-cross light polarization microscopy with magnification 10X100... 89
42	Transmission electron microscope (TEM) photomicrograph of silk sericin loaded niosomes prepared by Span <sup>®</sup> 20 (A), Span <sup>®</sup> 40 (B), Span <sup>®</sup> 60 (C), and Span <sup>®</sup> 80 (D)..... 92
43	Particle size of silk sericin loaded niosome formulations under storage in refrigerator (4-8 °C) for 8 weeks..... 95
44	%Entrapment efficiency of silk sericin loaded niosome formulations under storage in refrigerator (4-8 °C) for 8 weeks.... 97

FIGURE		PAGE
45	Superoxide radicals scavenging activity of silk sericin loaded niosome formulations (n=4).....	98
46	Anti-tyrosinase activity of silk sericin loaded niosome formulations (n=3).....	99
47	Cumulative amount of silk sericin from silk sericin solution in permeation study in vitro.....	100
48	Cumulative amount of silk sericin from silk sericin loaded niosomes that compose of Span <sup>®</sup> 20, Span <sup>®</sup> 40, Span <sup>®</sup> 60 and Span <sup>®</sup> 80 in permeation study in vitro (n = 3-4).....	101
49	Cumulative amount of silk sericin loaded in niosomes in permeation study in vitro for obtained slope (A, B, C and D: silk sericin loaded in niosomes that compose of Span <sup>®</sup> 20, Span <sup>®</sup> 40, Span <sup>®</sup> 60 and Span <sup>®</sup> 80, respectively).....	102

## LIST OF ABBREVIATIONS

ANOVA	=	analysis of variance
Abs	=	absorbance
APS	=	ammonium persulfate
BSA	=	bovine serum albumin
°C	=	degree Celcius
$C_d$	=	concentration of drug in donor
cm	=	centimeter
conc	=	concentration
$D$	=	diffusion coefficient
DMSO	=	dimethyl sulfoxide
DSC	=	differential scanning calorimetry
Da	=	dalton
DPPH	=	2,2-Diphenyl-1-picrylhydrazyl
EC <sub>50</sub>	=	half maximum effective concentration
EDTA	=	ethylenediaminetetra acetic acid
EE	=	entrapment efficiency
et al.	=	<i>et alii</i> , and others
FCCD	=	face-centered composite design
g	=	gram
h	=	hour
$h$	=	thickness of membrane
$K$	=	partition coefficient
kDa	=	kilodalton
LUVs	=	large unilamellar vesicles
M	=	molar
mbar	=	millibar
mg	=	milligram
min	=	minute
mL	=	milliliter
MLV	=	multilamellar vesicles

mm	=	millimeter
mM	=	millimolar
MW	=	molecular weight
n	=	sample size
NADH	=	$\beta$ -nicotinamide adenine dinucleotide
NBT	=	nitroblue tetrazolium chloride
nm	=	nanometer
P	=	permeation coefficient
PBS	=	phosphate buffered saline
PdI	=	polydispersity index
pH	=	the negative logarithm of the hydrogen ion concentration
PMS	=	phenazine methosulfate
R <sup>2</sup>	=	coefficient of determination
ROS	=	reactive oxygen species
rpm	=	round per minute
RT	=	room temperature
sec	=	second
SD	=	standard derivation
SDS	=	sodium dodecyl sulfate
SDS-PAGE	=	sodium dodecyl sulfate polyacrylamide gel electrophoresis
SEM	=	scanning electron microscopy
S.E.M.	=	standard error of means
SPSS	=	statistical package for the social science
t	=	time
T <sub>c</sub>	=	transition temperature
TBA	=	thiobarbituric acid
TCA	=	trichloroacetic acid
TEM	=	transmission electron microscopy
TEMED	=	tetramethylethylenediamine
$\mu$ g	=	microgram



$\mu\text{g/mL}$	=	microgram per millilitre
$\mu\text{L}$	=	microliter
$\mu\text{m}$	=	micrometer
$\mu\text{mol}$	=	micromole
UV	=	ultraviolet
w/o	=	water in oil
w/v	=	weight by volume
w/w	=	weight by weight

# CHAPTER I

## INTRODUCTION

Silk derived from silkworm *Bombyx mori* Linn., a family of Bombycidae. The cocoons of silk are composed of two major types of proteins: fibroin and sericin. Fibroin, a hydrophobic the core glycoprotein, constitutes over 70% of the cocoon. Sericin, water-soluble glue glycoprotein constitutes 20-30% of the cocoon. Sericin is made of 18 amino acids such as serine and aspartic acid approximately 33.4% and 16.7% of sericin, respectively (Wu, Wang and Xu, 2007; Zhang, 2002). Its molecular weight ranges widely from about 10 to over 300 kDa. Sericin is useful in various fields such as biodegradable material, membrane material, functional biomaterial, medical biomaterial, functional fiber (Kundu et al., 2008). Sericin can be antioxidant (Fan et al., 2009), antibacterial, UV resistant and able to absorb and release moisture easily (Zhang, 2002), antityrosinase (Aramwit et al., 2010), and wound healing (Aramwit and Sangcakul, 2007). Most of the sericin must be removed during raw silk production at the reeling mill and the other stages of silk processing. Sericin is mostly discarded in silk processing wastewater. The cocoon production is about 1 million tons (fresh weight) worldwide and this is equivalent to 400,000 tons of dry cocoon. Processing of this raw silk produces about 50,000 tons of sericin. If sericin is recovered and recycled, it can represent a significant economic and social benefit (Wu et al., 2007).

Extraction methods significantly affect the biochemical activities of silk proteins. Conventionally, removal of sericin is achieved in boiling water but boiling water alone is ineffective. Alternatively, the process could be used hydrothermal and catalyzed by the addition of acid, alkali or  $MgCl_2$ /ethanol/ $H_2O$ , however acid and alkali are considered toxic chemical. Additionally, the severe conditions make the process unfavorable (Lamoolphak, De-eknamkil and Shotipruk, 2008). The development of an effective degumming process is based on enzymes, however the higher cost of enzymes themselves has so far limited the development of industrial processes (Vaithanomsat and Kitpreechavanich, 2008). The extraction process of silk

sericin catalyzed by  $\text{Na}_2\text{CO}_3$  gave higher free radical scavenging activity (DPPH assay) than by  $\text{MgCl}_2/\text{ethanol}/\text{H}_2\text{O}$  (หฤทัย ฐานนันท์และอริษฎาภรณ์ เชื้อคำจันทร์, 2552).

Antioxidant sericin prepared by heating at  $95\text{ }^\circ\text{C}$  for 120 min (Fan et al., 2009) had strong scavenging capacity against DPPH, superoxide and hydroxyl radicals. This study, aimed to evaluate and compare the antioxidant and anti-tyrosinase activities of silk sericin prepared by high temperature and pressure degumming technique and  $\text{Na}_2\text{CO}_3$ .

Nowadays, silk sericin is usually used in cosmetics, despite low stratum corneum permeability limits the usefulness of topical drug delivery. Its molecular weight about 10-300 kDa (Zhang, 2002) may results in low penetration through skin. Recently, vesicular delivery systems (such as liposome, deformable liposome (Puangmalai, 2005), and non-ionic surfactant vesicles or noisome) have attracted considerable attention in transdermal drug delivery. These penetration enhancers are biodegradable, non-toxic, amphiphilic, and effective in the modulation of drug release properties. Their effectiveness is strongly dependent on composition, size, charge, lamellarity (Choi and Maibach, 2005).

Niosomes are now widely studied as an alternative to liposomes. These vesicles appear to be similar to liposomes in terms of their physical properties, being prepared in the same way and, under a variety of conditions, forming unilamellar or multilamellar structures. Niosomes alleviate the disadvantages associated with liposomes such as chemical instability, variable purity of phospholipids and high cost (New, 1990; Uchegbu and Vyas, 1998). Many drugs, using this system to enhance delivery, are enoxacin (Fang et al., 2001), kojic oleate (Manosroi et al., 2005) and colchicine (Hao et al., 2002)

This study aimed to investigate the preparation of silk sericin powder. The evaluation of biological activities of silk sericin and niosomes containing silk sericin was performed. This study also focused on development of formulation and characterization of niosomes containing silk sericin for skin delivery.

**The purposes of this study were as follows:**

1. To evaluate and compare the biological activities of silk sericin, prepared by extraction using  $\text{Na}_2\text{CO}_3$  and high temperature and pressure degumming technique.
2. To optimize the spray drying conditions for silk sericin powder.
3. To formulate niosomes preparation loaded with silk sericin by reverse phase evaporation technique.
4. To study the effect of type of surfactants to physicochemical properties and stability of niosomes.
5. To study the in vitro permeation of silk sericin from niosome formulation.

## CHAPTER II

### LITERATURE REVIEWS

#### A. SILK SERICIN

##### 1. Sources of sericin

Silk is classified by source that one is mulberry silkworms (*Bombyx mori* Linn. belong to Family Bombycidae) and the other one is wild non-mulberry silkworms such as *Antheraea mylitta* (Indian tropical tasar), *Antheraea pernyi* (Chinese temperate oak tasar), *Antheraea assamensis*, *Philosamia* spp. (*Samia* spp.) (Kundu et al., 2008). Silk gland of *B. mori*. is a typical exocrine gland secreting large amount of silk proteins (Mondal, Trivedy and Kumar, 2007). Silk is a continuous stand of two-filaments cemented together forming the cocoon of silkworm, mainly made of sericin and fibroin proteins. Silk filament is a double strand of fibroin, which is held together by a gummy substance called silk sericin or silk gum. Fibroin is a fibrous protein, present as a delicate twin thread linked by disulfide bonds, enveloped by successive sticky layers of sericin that help in the formation of cocoon (Ki et al., 2007; Wu, Wang and Xu, 2007). Silk adapts various secondary structures, including  $\alpha$ -helix,  $\beta$ -sheet, and crossed  $\beta$ -sheet (Padamwar and Pawar, 2004). Figure 1 shows silk cocoons of *Bombyx mori* Linn. (Nang-Noi Srisaket 1) and component of silk.

Fibroin, the core protein constituent over 70% of the cocoon, is a hydrophobic glycoprotein secreted from the posterior part of the silk gland. Fibroin composed of two equimolar protein subunit of heavy chain (370 kDa) and light chain (25 kDa) covalently linked by disulfide bond. The amino acid composition of fibroin consists of glycine (43%), alanine (30%), and serine (12%). Fibroin filament is made of both crystalline and amorphous domains (Kundu et al., 2008; Padamwar and Pawar, 2004; Vepari and Kaplan, 2007).



Figure 1. Silk cocoons of *Bombyx mori* Nang-Noi Srisaket 1 (a) and fibroin wrapped up in sericin (b) (<http://www.dermasilk.com.au>).

Sericin, a second type of silk protein, is glue protein constitute 20-30% of the cocoon and are hot water soluble glycoproteins. Sericin, secreted in the mid-region of the silk gland, comprises different polypeptides ranging in weight from 10 to 300 kDa and are characterized by unusually high serine content (40%) along with significant amounts of glycine (16%) (Aramvit, Siritientong and Srichana, 2011; Kundu et al., 2008; Zhang, 2002).

Most of sericin must be removed during raw silk production at reeling mill and the other stages of silk processing, which mostly discarded in silk processing wastewater. The cocoon production is about 1 million tons (fresh weight) or equivalent to 400,000 tons (dry cocoon), which about 50,000 tons of sericin discarded in processing of raw silk production. If this protein is recoverd and recycled, it can represent a significant economic, social benefit and add more value of sericin (Zhang, 2002).

## 2. Extraction of sericin

The structure of sericin also depends on the casting temperature. There are several methods to remove sericin in degumming process of cocoons.

### 2.1 Boiling water

Conventionally, removal of sericin is achieved in boiling water but boiling water alone is ineffective and time-consuming. Degumming by boiling water

has an advantage because it results in no impurity (Lamoolphak, De-Eknamkul, and Shotipruk, 2008).

### **2.2 Acid or alkaline hydrolysis**

The process could be catalyzed by the addition of acid or alkaline. Almost all industrialized removal methods now involve extraction with soaps and detergents. It is now the most widely used industrial technique since it causes no fibre degradation and is a relatively simple process. However, the process makes it very difficult to gain high quality sericin. Acids or alkali, soap and detergent are considered toxic chemicals and the severe conditions used make the process unfavorable (Aramwit et al., 2011; Lamoolphak et al., 2008). This method is the requirement of time consuming steps to remove the impurities. หฤทัย ฐานันท์และอริษฎาภรณ์ เชื้อคำจันทร์ (2552) found that sericin extraction by using  $\text{Na}_2\text{CO}_3$  gave higher antioxidant efficiency than sericin extraction by using  $\text{MgCl}_2/\text{EtOH}/\text{H}_2\text{O}$ .

### **2.3 High temperature and pressure degumming technique (autoclaving method)**

When sericin is extracted from cocoons by autoclaving, it is obtained with good gelling property and yield (Padamwar and Pawar, 2004). Extraction by autoclaving has an advantage because it results in no impurity (Lamoolphak et al., 2008; Lee et al., 2003; Aramwit et al., 2009; Aramwit et al., 2011).

### **2.4 Ethanol precipitation**

Wu et al (2007) developed a novel extraction procedure to recover sericin from silk industry wastewater by using a chilled ethanol precipitation method, which was an effective, simple method. The yield was enhanced as the ethanol was increased. However, this technique did not sound economically and environmental friendly when applied on an industrial scale (Aramwit et al., 2011).

### **2.5 Enzyme hydrolysis**

The development of degumming process based on enzymes was an effective method because of saving in terms of water, energy, chemicals, and effluent treatment. The recovered sericin by this method into sericin hydrolysate (MW 1046-

2976 Da) which is mostly suitable for cosmetic application (Vaithanomsat and Kitpreechavanich, 2008). However, the higher cost of enzymes themselves has so far limited the development of industrial processes.

### **3. Physicochemical properties of sericin**

#### **3.1 Structure of sericin**

Sericin contains 18 amino acids, most of which have strongly polar side groups such as hydroxyl, carboxyl, and amino groups, especially serine and aspartic acid. Amino acid compositions of silk sericin are demonstrated in Table 1. Sericin takes on a globular shape, with 35%  $\beta$ -sheet and 63% random coil structure, and with no  $\alpha$ -helical content, which results in sol-gel property (Kundu et al., 2008; Padamwar and Pawar, 2004). X-ray diffraction analysis and differential thermal analysis indicate that the assembled structure of sericin powder is amorphous structure (Aramwit et al., 2011).

#### **3.2 Solubility of sericin**

Sericin is a water soluble protein, which is dissolved in a polar solvent. Small sericin peptides are soluble in cold water and large sericin peptides are soluble in hot water (Zhang, 2002). Sericin has sol-gel property as it easily dissolves in water at 50-60°C and again returns to gel on cooling. Solubility of sericin in water decreases when sericin molecules are transformed from random coil to the  $\beta$ -sheet structure (Padamwar and Pawan, 2004; Teramoto, Nakajima and Takabayashi, 2005).

#### **3.3 Molecular weight**

The size of sericin molecules depends on extraction methods, temperature, pH, and the processing time (Aramvit et al., 2011; Zhang, 2002). Its molecular weight ranges widely from 10 to over 400 kDa.



Table 1 Amino acid composition of silk sericin and fibroin (modified from Puangmalai, 2007; Sothornvit, Chllakup and Suwanruji, 2010)

Amino acid	Percent of gram amino acid in 100 g protein				
	Sericin from silk waste <sup>a</sup>	Sericin from raw material <sup>b</sup>	Sericin from degumming solution <sup>c</sup>	Hot water-soluble sericin <sup>d</sup>	Fibroin
Aspartic acid	17.64	15.47	18.80	17.97	0.77
Serine	32.74	31.99	27.30	28.00	13.02
Glutamic	7.31	6.28	7.20	6.25	0.68
Glycine	9.89	14.20	10.70	16.29	40.62
Histadine	1.81	1.49	1.70	1.32	ND
Arginine	6.16	4.29	4.90	3.52	0.85
Threonine	5.51	7.73	7.50	7.78	0.80
Alanine	3.86	4.85	4.30	5.20	29.32
Proline	0.59	0.71	1.20	ND	ND
Cystine	ND	0.20	0.30	0.69	ND
Tyrosine	4.63	3.01	4.60	2.87	10.79
Valine	3.14	3.30	3.80	3.77	2.59
Methionine	0.11	ND	0.50	0.79	ND
Lysine	3.05	4.17	2.10	1.21	0.17
Isoleucine	1.04	0.72	1.30	0.64	0.43
Leucine	1.44	0.96	1.70	1.21	0.32
Phenylalanine	1.08	0.37	1.60	0.64	0.57

<sup>a</sup>Silk waste (pierced cocoon) of *B. mori* Multivoltine strain (Sothornvit et al., 2010)

<sup>b</sup> Raw material sericin of *B. mori* Bivoltine strain (Vaithamsat and Kitprechavanich, 2008)

<sup>c</sup> Degumming solution of *B. mori* Bivoltine strain (Wu et al., 2007)

<sup>d</sup> Hot water-soluble sericin of *B. mori* Bivoltine strain (Zhang et al., 2004)

#### 4. Application of sericin

Molecular weight of sericin was found to be related to its functions. Sericin in range of lower molecular weight ( $\leq 20$  kDa) or sericin hydrolyzate is used in cosmetics but sericin in range of higher molecular weight ( $\geq 20$  kDa) is modified as a coating material, degradable biomaterial, functional membrane, hydrogel, fiber and fabric. Sericin can be cross-linked, copolymerized and blended with other artificial materials (Zhang, 2002). Due to its proteinous nature, silk sericin is

susceptible to the action of proteolytic enzymes present in body and hence it is digestible. This property makes it biocompatible and biodegradable. Because of some additional properties like gelling ability, moisture retention, and skin adhesion, sericin has wide applications in medical, pharmaceutical, and cosmetics.

#### **4.1 Medical and pharmaceutical applications**

Sericin has many medical applications, such as antioxidants, anticancer drugs (Tamada et al., 2004), and anticoagulants (Aramwit et al., 2011). Due to its high content of serine and glycine, sericin has been used as a dietary fiber with antioxidant activity (Kundu 2009). Consumption of sericin can reduce serum lipids, ameliorate glucose tolerance and elevate serum adiponectin in rats fed with a high-fat diet including protective effect against alcohol-mediated liver damage in mice (Aramwit et al., 2011).

Sericin shows more hydrophilicity than fibroin and can activate collagen synthesis in dermal tissue. It was used to form a scaffold which was a good candidate for tissue engineering application such as neural tissue engineering or skin substitution (Aramwit et al., 2011; Mandal, Priya and Kundu, 2009). Sericin has been a promising biomaterial because it promotes cell proliferation and the attachment of cultured human skin fibroblasts. It was considered for a role in the healing process of skin lesions (Aramwit and Sangcakul, 2007; Kundu et al., 2008).

Bioconjugation of sericin with polymers has provided new drug delivery methods with reduced immunogenicity and increased drug stability. Due to the presence of surface-active groups (-OH, -COOH, and -NH<sub>2</sub>), sericin can form covalent links with the conjugate such as L-asparaginase,  $\beta$ -glucosidase and insulin. The effect of conjugated L-asparaginase with sericin is found to retain activity with lower  $K_m$  value, higher thermo-stability, lower immunological response, prolonged half-life, and greater stability in human serum (Zhang et al., 2004). Sericin-insulin conjugated with polyethylene glycol shows good bioavailability, longer half-life in the blood and increases pharmacological activity with no immunogenicity and antigenicity (Kundu et al., 2008). Sericin films, forming gel and sponges can also be used in drug delivery systems since it can be produced to exhibit a sustained-release

profile for a charged protein-fluorescein isothiocyanate-albumin (Aramwit et al., 2011).

In recent years, several studies have suggested sericin's potential as a wound dressing agent (Schneider et al., 2009; Teramoto et al., 2005) and wound healing (Aramwit and Sangcakul, 2007; Nagai et al., 2009). Its hydrophilicity assists to maintain a moist environment and to absorb excess exudates from wounds. Both two dimensional (films, membranes) and three-dimensional (hydrogel and porous scaffolds) matrices from sericin have been reported (Mandal and Kundu, 2008). In wound healing, sericin instillation has a potent effect in promoting wound healing and wound size reduction in rats (Aramwit et al., 2011).

#### **4.2 Cosmetics**

Sericin has been used in cosmetics for skin, hair, and nails. Sericin helps to enhance the elasticity of skin and has anti-wrinkle and anti-aging effects via collagen promoting activity when used as a lotion, cream, or ointment (Aramwit et al., 2011; Padamwar and Pawan, 2004). Sericin gel shows moisturizing properties with an increase in hydroxyproline content in the stratum corneum and a decrease in skin impedance (Kundu et al., 2008). Sericin gel with pluronic and cabopol restores natural moisturizing factors (restoration of amino acids and its occlusive effect) as well as prevents transepidermal water loss from skin (Padamwar et al., 2005). Sericin in sunscreen composition enhances the light screening effect of UV filter like triazine, and cinnamic acid ester (Kundu et al., 2008; Padamwar and Pawan, 2004). Moreover, it is a potent natural antioxidant with high reducing power, ferrous ion chelating ability (Fan et al., 2009), free radical scavenging activity (Manosroi et al., 2010; Wu et al., 2007), lipid peroxidation inhibition (Kato et al., 1998), and tyrosinase inhibition (Kato et al., 1998; Manosroi et al., 2010; Wu et al., 2007).

#### **B. FREE RADICAL SCAVENGING ACTIVITY**

During respiration in biological systems, a significant fraction of oxygen is incompletely reduced. Such partially reduced oxygen and their derivatives are known as reactive oxygen species (ROS) which are highly reactive pro-oxidants and toxic. ROS also include free radicals and non-radical derivatives of oxygen. The reactivity

of ROS can cause functional damage to cellular protein, lipid and genetic material, leading to trigger a number of degenerative diseases, like mutagenesis, carcinogenesis, circulatory disturbance, and aging. This results in tissue oxidative stress and multiple-system organ failure (Moreno, 2002; Park, 1999).

Oxidative stress can be regarded as an imbalance between pro-oxidative/free radical production and opposing antioxidant defense. The oxidative stress can cause process of aging and degenerative diseases such as atherosclerosis, diabetes mellitus, ischemia/reperfusion (I/R) injury, Alzheimer's disease, inflammatory diseases (rheumatoid arthritis, inflammatory bowel disease, and pancreatitis), carcinogenesis, neurodegenerative disease, hypertension, ocular diseases, pulmonary diseases, and hematological diseases (Singh and Singh, 2008).

### 1. Free radicals

Free radical is defined as any species capable of independent existence with one or more unpaired electrons. Free radicals including ROS and reactive nitrogen species (RNS) are unstable and react readily with other groups or substances in the body (Singh and Singh, 2008) (Table 2) (Wiseman and Halliwell, 1996; Perron and Brumaghim, 2009).

Table 2. Reactive oxygen and nitrogen species (Wiseman and Halliwell, 1996; Perron and Brumaghim, 2009).

Radicals	Reactive Oxygen Species	Reactive Nitrogen Species
	Superoxide ( $O_2^{\cdot-}$ )	Nitric oxide ( $NO^{\cdot}$ )
	Hydroxyl ( $OH^{\cdot}$ )	Nitrogen dioxide ( $NO_2^{\cdot}$ )
	Peroxyl ( $ROO^{\cdot}$ )	
	Alkoxy ( $RO^{\cdot}$ )	
	Hydroperoxyl ( $HO_2^{\cdot}$ )	
<b>Non-radicals</b>	Hydrogen peroxide ( $H_2O_2$ )	Nitrous acid ( $HNO_2$ )
	Hypochlorous acid ( $HOCl$ )	Dinitrogen tetraoxide ( $N_2O_4$ )
	Ozone ( $O_3$ )	Dinitrogen trioxide ( $N_2O_3$ )
	singlet oxygen ( $^1O_2$ )	Peroxynitrite ( $ONOO^-$ )
		Peroxynitrous acid ( $ONOOH$ )
		Nitronium cation ( $NO_2^+$ )
		Alkyl peroxy nitrates ( $ROONO$ )

Living cells have a biological defense system consisting of enzymatic antioxidants that convert ROS to harmless species. During respiration, mitochondria generates superoxide anion ( $O_2^{\bullet-}$ ), which is converted to oxygen ( $O_2$ ) and hydrogen peroxide ( $H_2O_2$ ) by superoxide dismutase (SOD) or reacts with nitric oxide ( $NO^{\bullet}$ ) to form peroxynitrite ( $ONOO^-$ ). Then  $ONOO^-$  can decompose into hydroxyl ( $OH^{\bullet}$ ).  $H_2O_2$  can be converted to water and oxygen by catalase (Karadag, Ozcelik and Saner, 2009) or reduced by either  $Fe^{2+}$  or  $Cu^+$  to form  $OH^{\bullet}$  via Fenton reaction (Perron and Brumaghim, 2009). The mechanism of oxidation in cell (Figure 2) is the complex interactions which begin with the formation of superoxide from different vascular cell oxidases. It includes the formation of lipid free radicals ( $LOO^{\bullet}$ ) and their scavenging of  $NO^{\bullet}$  as well as NOS decoupling, SOD scavenging of  $O_2^{\bullet-}$ , and the formation of  $OH^{\bullet}$ .

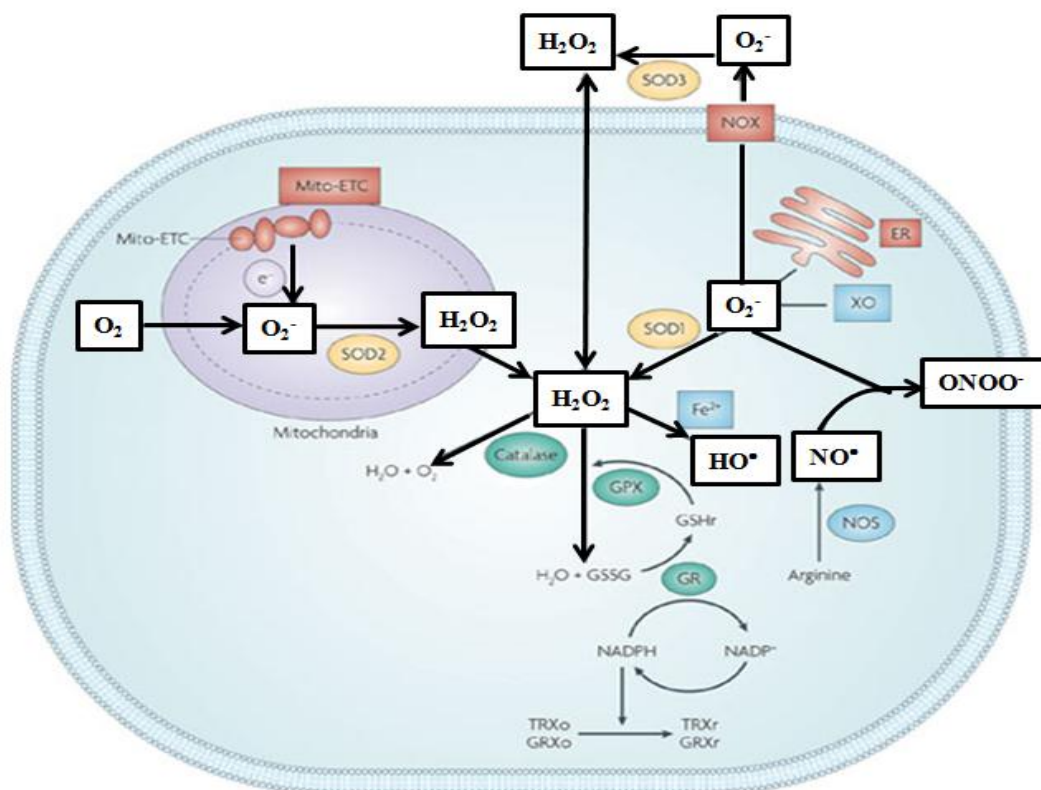


Figure 2 Cellular redox homeostasis (modified from Trachootham, Alexandre and Huang, 2009).

Moreover, the skin region which always contact with oxygen including exposure to ultraviolet (UV) irradiation. Skin damage induced by ROS has increased from the risk of photo-oxidation. ROS and RNS are major sources of cellular oxidative stress, damaging proteins, lipids, and DNA. Thus, determination of the antioxidant status in biological systems could contribute to prevention and evaluation of diseases related to aging. Antioxidant testing is classified into two groups: those assays used to evaluate lipid peroxidation and those assays used to measure free radical scavenging ability (Sanchez-Moreno, 2002).

## **2. Methodology for testing radical scavenging species**

### **2.1 Scavenging of stable radical 2,2-diphenyl-1-picryl-hydrazyl**

#### **(DPPH<sup>•</sup> assay)**

The DPPH<sup>•</sup> (2, 2-diphenyl-1-picryl-hydrazyl) is a stable free radical and the assay is based on the measurement of the DPPH<sup>•</sup> scavenging ability of antioxidants. DPPH<sup>•</sup> reacts with hydrogen donors or antioxidant to the corresponding hydrazine (Figure 3). The scavenging ability is evaluated using electron spin resonance spectroscopy on the basic that the DPPH<sup>•</sup> signal intensity is inversely related to the antioxidant concentration and reaction time. However, the more frequently used technique is the discoloration assay, which evaluates the absorbance decrease at 515-528 nm produced by the addition of the antioxidant to DPPH<sup>•</sup> solution in ethanol or methanol. It has been used to evaluate the antioxidant activity of phenolic compounds by measuring the change in absorbance at 515 to 517 (Sanchez-Moreno, 2002). The antioxidant activity is calculated by determining the decrease in absorbance at different concentrations and comparing it with absorbance in absence of the compound.

The DPPH method is a valid, easy, accurate, sensitive, and economic method to evaluate scavenging activity of antioxidant of fruits and vegetables juices or extracts, since the radical compound is stable and does not have to be generated as in other radical scavenging assays (Singh and Singh, 2008). DPPH is also sensitive to some Lewis bases and solvents. Oxygen may react with DPPH<sup>•</sup> directly in presence of light and decrease its absorbance (Molyneux, 2004).

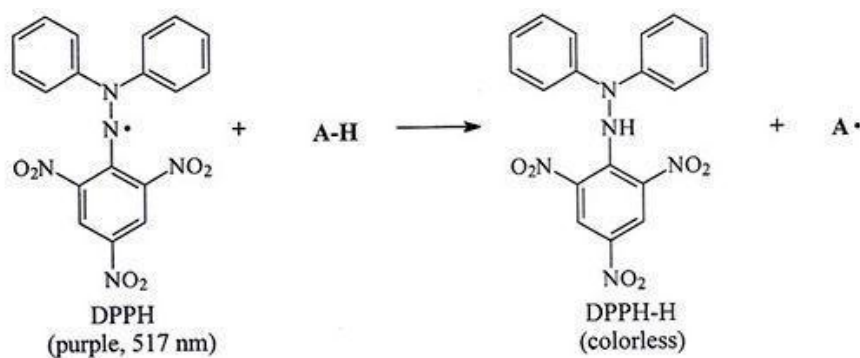


Figure 3 Structure of DPPH before and after reacted with antioxidant (AH).

## 2.2 Scavenging of superoxide radical ( $O_2^{\bullet-}$ )

Pathological processes are known to involve complex mechanisms. Xanthine oxidase is one of the main enzymatic sources of ROS in vivo. Xanthine oxidase present in normal tissue is a dehydrogenase enzyme that transfers electrons to nicotinamide adenine dinucleotide (NAD). Although, xanthine or hypoxanthine are oxidized by xanthine oxidase to uric acid, under certain stress conditions the dehydrogenase is converted to an oxidase enzyme. This conversion the enzyme reacts with the same electron donors, but reducing oxygen instead of NAD, thus producing superoxide and hydrogen peroxide, and contributing to the initiation and progression of a number of pathological processes (Sanchez-Moreno, 2002).

The scavenging activity towards  $O_2^{\bullet-}$  is measured in terms of inhibition of generation of  $O_2^{\bullet-}$  with hypoxanthine-xanthine oxidase superoxide generating system. To a minor extent,  $O_2^{\bullet-}$  is generated using a non-enzymatic reaction of phenazine methosulphate in the presence NADH and molecular oxygen. In both strategies,  $O_2^{\bullet-}$  reduces nitro-blue tetrazolium (NBT) into formazan at pH 7.4 and room temperature (Figure 4), and formazan generation is followed by spectrophotometer at 560 nm. Any added molecule capable of reacting with  $O_2^{\bullet-}$ , inhibits the production of formazan.

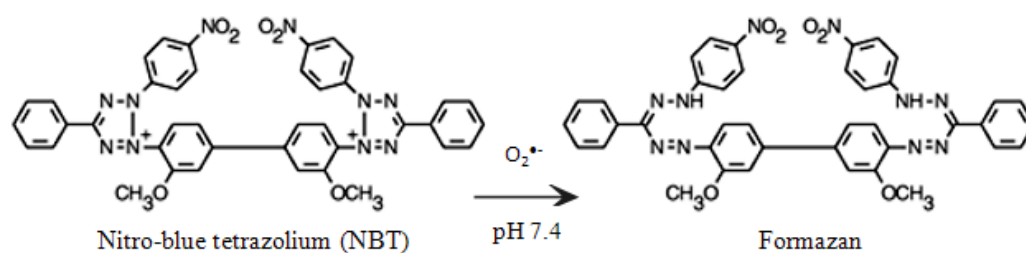


Figure 4 Structure of nitro-blue tetrazolium (NBT) reaction with  $\text{O}_2^{\bullet-}$  into formazan (modified from Kaur and Arora, 2010)

### 2.3 Scavenging of hydrogen peroxide ( $\text{H}_2\text{O}_2$ )

$\text{H}_2\text{O}_2$  is generated *in vivo* by several oxidase enzymes. There is increasing evidence that  $\text{H}_2\text{O}_2$ , either directly or indirectly via its reduction product  $\text{OH}^-$ , acts as a messenger molecule in the synthesis and activation of inflammatory mediators.

$\text{H}_2\text{O}_2$  scavenging activity is easily and sensitively measured by using peroxidase-based assay systems. The most common employs horseradish peroxidase, which uses  $\text{H}_2\text{O}_2$  to oxidize scopoletin into a nonfluorescent product. In the presence of a putative scavenger, the oxidation of scopoletin is inhibited and the  $\text{H}_2\text{O}_2$  scavenging can be monitored (Sanchez-Moreno, 2002). Other assays have been used to minor extent. The assay for  $\text{H}_2\text{O}_2$  is carried out by measuring the direct reaction of  $\text{H}_2\text{O}_2$  and guaiacol. When guaiacol becomes oxidized by horseradish peroxidase in the presence of  $\text{H}_2\text{O}_2$  it forms tetraguaiacol. The tetraguaiacol solution turns a red brown color but begins to fade a few minutes after its formation (Figure 5). Measurements must be made using a spectrophotometer at 450 nm with one or two minutes after initiating the reaction (Choi et al., 2007; Weinheimer and White, 2003). Any added molecule capable of reacting with  $\text{H}_2\text{O}_2$  inhibits the production of tetraguaiacol.



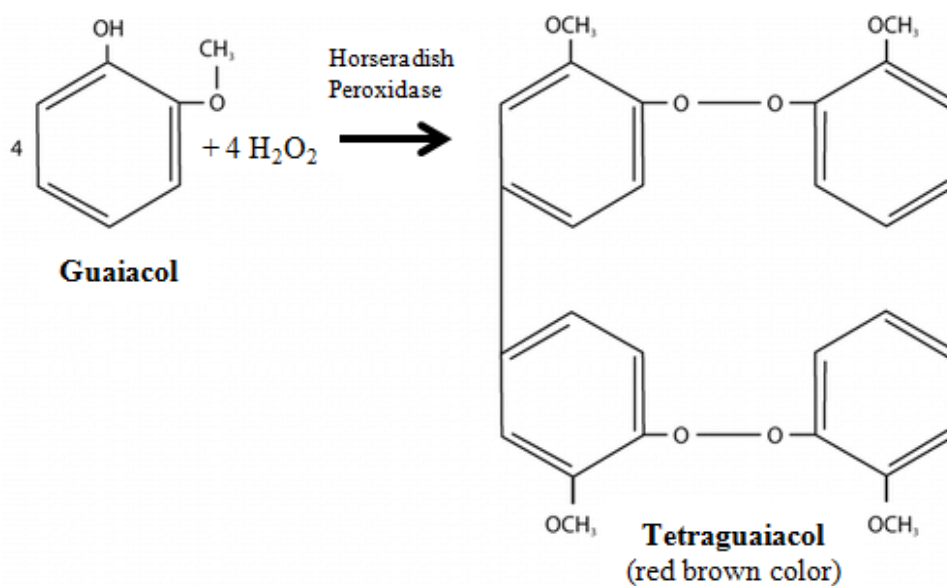


Figure 5 Reaction of guaiacol with hydrogen peroxide in the presence of peroxidase to produce tetraguaiacol (modified from Weinheimer and White, 2003).

#### 2.4 Scavenging of hydroxyl radical ( $\text{HO}^\bullet$ )

Hydroxyl radical ( $\text{HO}^\bullet$ ) scavenging can often be calculated using the deoxyribose assay. A mixture of ferric chloride ( $\text{FeCl}_3$ ) and ethylenediamine tetraacetic acid (EDTA) in the presence of ascorbate reacts to form iron(II)-EDTA plus oxidized ascorbate,  $\text{H}_2\text{O}_2$  then reacts with iron(II)-EDTA to generate iron(III)-EDTA plus  $\text{HO}^\bullet$  in the so-called Fenton reaction ( $\text{Fe}^{2+} + \text{H}_2\text{O}_2 \rightarrow \text{OH}^- + \text{HO}^\bullet$ ). Those radicals not scavenged by other components of the reaction mixture attack the sugar deoxyribose, which degrades into a series of fragments (malonaldehyde). Some or all fragments react on heating with thiobarbituric acid at low pH to give a pink chromogen (Figure 6). Thus the scavenging activity towards  $\text{HO}^\bullet$  of a substance added to the reaction mixture is measured on the basis of the inhibition of the degradation of deoxyribose (Fernandes et al., 2004; Sanchez-Moreno, 2002). Any added molecule capable of reacting with  $\text{HO}^\bullet$  inhibits the production of pink chromogen.

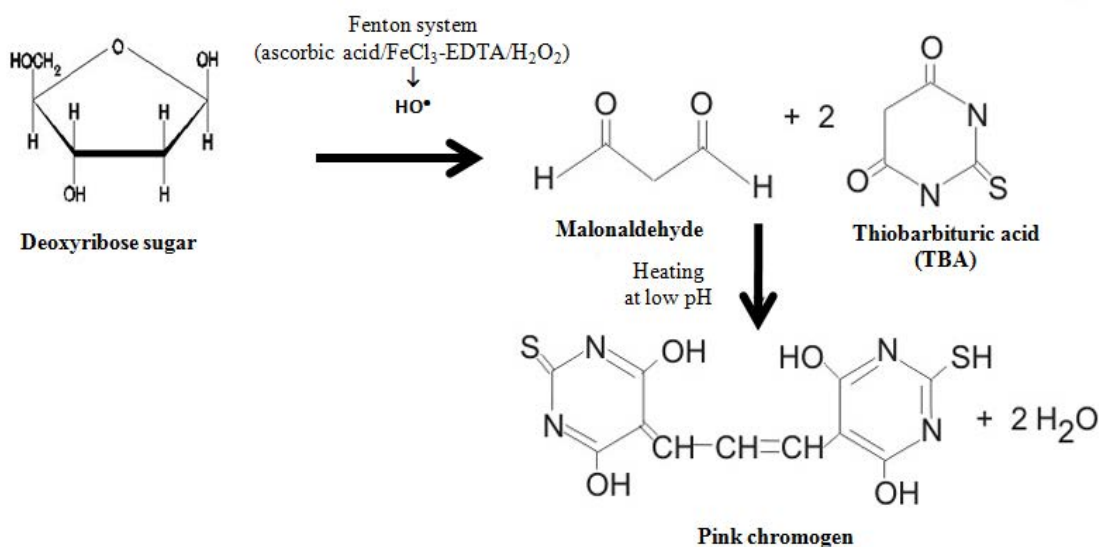


Figure 6 Reaction of deoxyribose with hydroxyl radical in the presence of thiobarbituric acid to produce pink chromogen (modified from Fernandes et al., 2004).

### 2.5 Scavenging of nitric oxide (NO•)

NO• is an important physiological regulator of cellular functions such as vasodilation and neurotransmission. Nevertheless, under pathological conditions, high concentration of NO• can be either beneficial or detrimental, leading to inflammatory reaction and host tissue injury. Such detrimental effects can be mediated by reaction of persistent high amounts of NO• with concomitantly produced superoxide anions, generating highly toxic species, such as peroxynitrite and hydroxyl radicals. Thus, NO• scavenger seems to be an attractive therapeutic approach in some disease. NO• is generated from the terminal guanido nitrogen atom of L-arginine by various NADPH-dependent enzymes called nitric oxide synthase (NOS) (Figure 7).

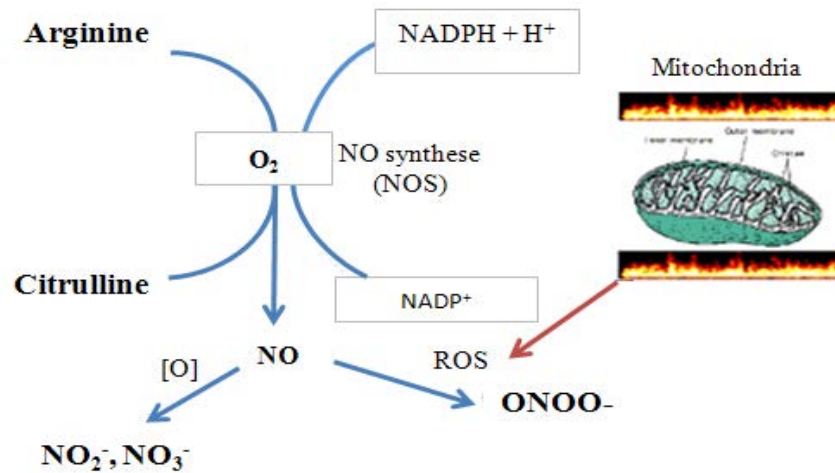


Figure 7 The L-arginine/nitric oxide pathway (modified from Hensley, Mou and Pye, 2003).

The most famous and most frequently used method of analysis of nitrite and nitrate is based on the Griess reaction (Johann Peter Griess). The Griess reaction is a diazotization reaction that used to quantitate the major metabolites of NO<sup>•</sup> such as nitrite. Griess reagents are composed of sulfonamide and N-(1-naphthyl)ethylenediamine in acidic condition to form a diazonium cation which couples to N-(1-naphthyl)ethylenediamine to form a readily water soluble, red-violet color azo dye (Figure 8). Measurement must be made using a spectrophotometer at 540 nm (Hensley, Mou and Pye, 2003; Tsikas, 2007). Scavenging activity against NO<sup>•</sup> is reproducibility, greater rapidity of coupling, increased sensitivity, increased acid-solubility of the azo dye, and pH-dependence of the color using Griess reaction. Thus the scavenging activity towards NO<sup>•</sup> of a substance added to the reaction mixture is measured on the basis of the inhibition of the metabolite of NO<sup>•</sup> (nitrite). Any added molecule capable of reacting with NO<sup>•</sup> inhibits the production of azo dye (Tsikas, 2007).

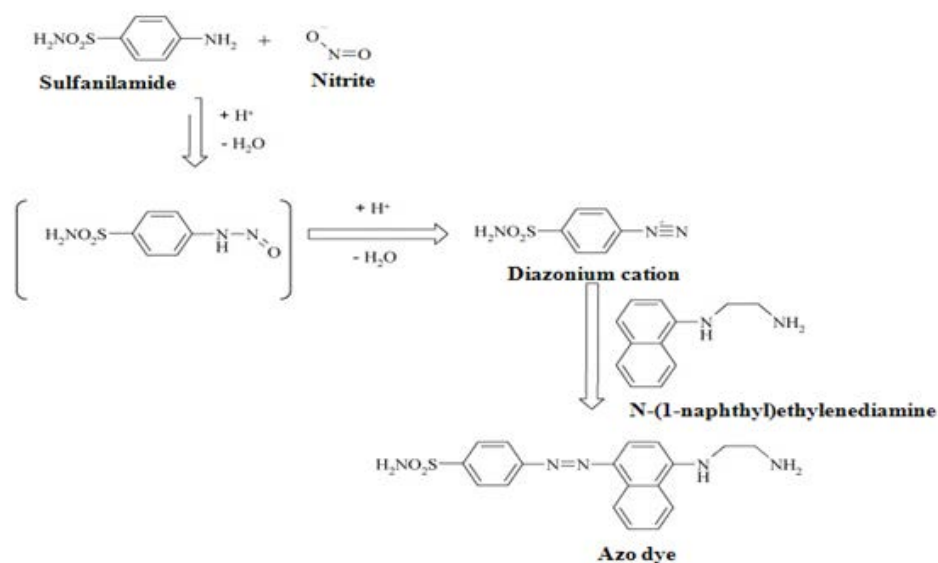


Figure 8 The Griess reaction. Under acidic condition, nitrite reacts with the amino group of sulfanilamide to form the diazonium cation, which couples to N-(1-naphthyl)ethylenediamine in *para*-position to form the azo dye (modified from Tsikas, 2007).

### C. ANTI-TYROSINASE ACTIVITY

Skin color is determined by a mixture of four biochromes: oxyhemoglobin (red), reduced hemoglobin (blue), carotenoids (yellow) and, most importantly, the amounts and types of melanin (brown) produced and their distribution in the skin. Melanin is secreted by melanocyte cells distributed in the basal layer of the dermis. (Brenner and Hearing, 2008). The type and amount of melanin synthesized by the melanocyte and its distribution in the surrounding keratinocytes determine the actual color of the skin. Melanin is formed through a series of oxidative reactions involving the amino acid tyrosine in the presence of tyrosinase.

#### 1. Melanin formation

Pathway of melanin biosynthesis in mammalian (Figure 9) consists of the enzymatic oxidation of tyrosine or L-DOPA to its corresponding o-dopaquinone catalyzed by tyrosinase. Dopaquinone is highly reactive and tends to polymerize spontaneously to form brown pigments of melanin. Two types of melanin are eumelanins (black-brown) and pheomelanins (yellow-brown). According to

melanogenesis pathway, tyrosinase activity is thought to be a major regulatory factor in the initial rate-limiting step of this pathway (Kim and Uyama, 2005).

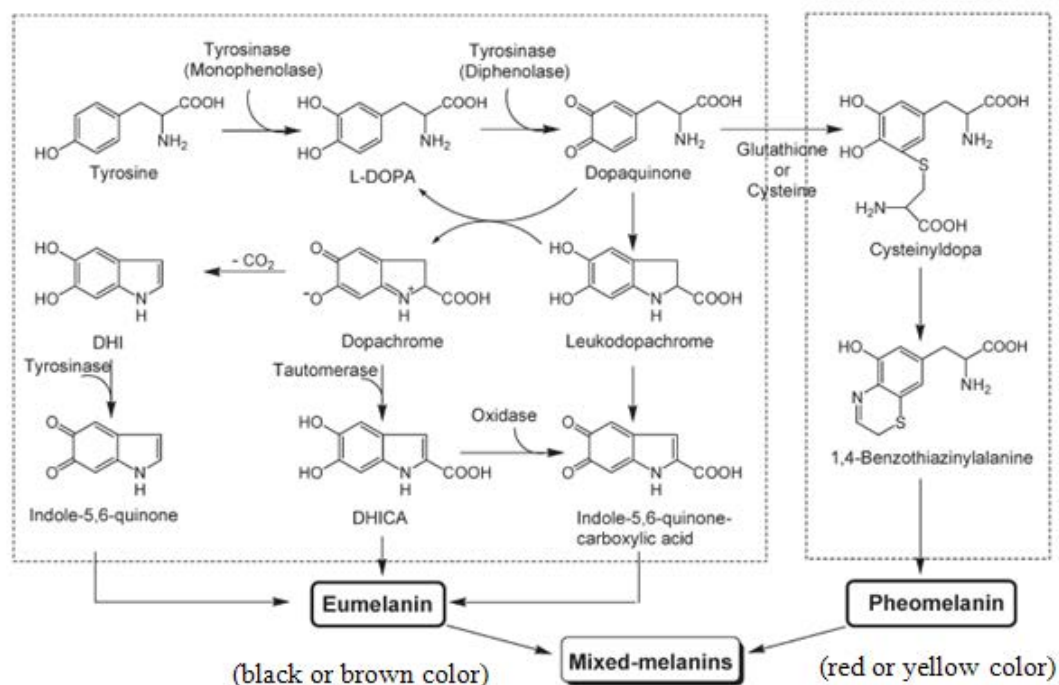


Figure 9 Biosynthetic pathway of melanin (modified from Kim and Uyama, 2005)

The development of tyrosinase inhibitors has become increasingly important for medicinal and cosmetic products that may be used to prevent or treat pigmentation disorders.

## 2. Tyrosinase inhibitors

A number of tyrosinase inhibitors from both natural and synthesis sources have been identified.

### 2.1 Plant polyphenols and derivatives of natural compounds

Plant polyphenols are usually referred to as a diverse group of compounds containing multiple phenolic functionalities. Widely distributed plants, over 4000 flavonoids, have been identified to date. Flavonoids are one of the most numerous studies such as kaempferol, quercetin and glabridin (Kim and Uyama, 2005).

Recently, some natural compounds have been modified and examined as potential tyrosinase inhibitors. Gallic acid, often by alkaline or acid hydrolysis of tannin, is used in the manufacturing of gallic acid alkyl ester such as methyl gallate, propyl gallate and dodecyl gallate. Short alkyl gallate was oxidized by tyrosinase, yield yellowish oxidation products. However, long alkyl gallate inhibited the enzyme without producing the pigment products, indicating that the carbon chain length is related to their tyrosinase inhibitory activity (Kim and Uyama, 2005).

## **2.2 Fungal metabolites**

Some compounds from fungal sources have also been identified and reported for their inhibitory activity on tyrosinase. Azelaic acid is a naturally produced by lipoperoxidation and esterified polyunsaturated fatty acids by yeast (*Pityrosporum ovale*). Kojic acid, a fungal metabolite, is a good chelator of transition metal ions and a good scavenger of free radical. Kojic acid effectively inhibited the formation of pigmented products (Kim and Uyama, 2005).

## **2.3 Peptides and proteins**

Tyrosinase inhibition by peptides may find its application in food, cosmetics or medicine. Proteins and peptides from natural resources such as milk, wheat, honey, silk, and the housefly appeared to be able to inhibit tyrosinase activity. The presence of the hydrophobic and aliphatic residues, valine, alanine or leucine, appears to be important for tyrosinase inhibition. Therefore, good tyrosinase inhibitory peptides preferably contain arginine and/or phenylalanine in combination with valine, alanine and/or leucine (Schurink, Berkel, Wichers and Boeriu, 2007).

## **2.4 Aldehydes and other compounds**

A large number of aldehydes and other compounds were also isolated and characterized as tyrosinase inhibitors, such as cinnaldehyde, anisaldehyde, cuminaldehyde and cumic acid. Their tyrosinase inhibitory mechanism presumably comes from their ability to form a Schiff base with a primary amino group in the enzyme (Kim and Uyama, 2005).

#### **D. NIOSOMES**

Niosomes, known as non-ionic surfactant vesicles, non-ionic liposomes, are the vesicular delivery systems, which are widely used to enhance drug permeation across the skin in cosmetic and dermatologic fields. These systems have attracted considerable interest because of biodegradable, non-toxic, amphiphilic in nature, and effective in the modulation of drug release properties that dependent on their physiological properties (composition, size, charge, lamellarity and application conditions). Traditionally, the main pathway for the transdermal drug delivery of active agents permeate via the intercellular and transcellular routes. However, vesicular systems use three potential pathways of active agents across the skin – through hair follicles with associated sebaceous glands, via eccrine sweat ducts or across continuous stratum corneum (SC) between these appendages. Follicular pathway is important for small or macromolecule delivery with vesicular systems (Choi and Maibach, 2005). Niosomes and liposomes are equiactive potential in drug delivery and both increase drug efficacy as compared with that of free drug. Niosomes are preferred over liposomes because they offer higher chemical stability, lower costs, great availability of surfactant classes and industrial scale production (Biswal et al., 2008).

Niosomes are formation of vesicles by hydrating mixture of cholesterol and non-ionic surfactants. They are formed by self-assembly of non-ionic surfactants in aqueous media resulting in closed bilayer structures (Figure 10) as spherical, unilamellar, multilamellar and polyhedral structures in addition to inverse structures with appear only non-aqueous solvent (Biswal et al., 2008). The assembly into closed bilayers is rarely spontaneous and usually requires some input of energy such as physical agitation, extrusion or heat, resulting that the hydrophobic parts of the molecule are shielded from the aqueous solvent and the hydrophilic head groups enjoy maximum contact with same (Uchegbu and Vyas, 1998). These structures are analogous to liposomes and are able to encapsulate aqueous solutes and serve as drug carriers such as tretinoin (Maconi et al., 2006), N-acetyl glucosamine (Shatalebi, Mostafavi and Moghaddas, 2010), propylthiouracil (Suwakul, Ongpipattanakul and Vardhanabhuti, 2006), nimesulide, insulin (Fanun, 2010).

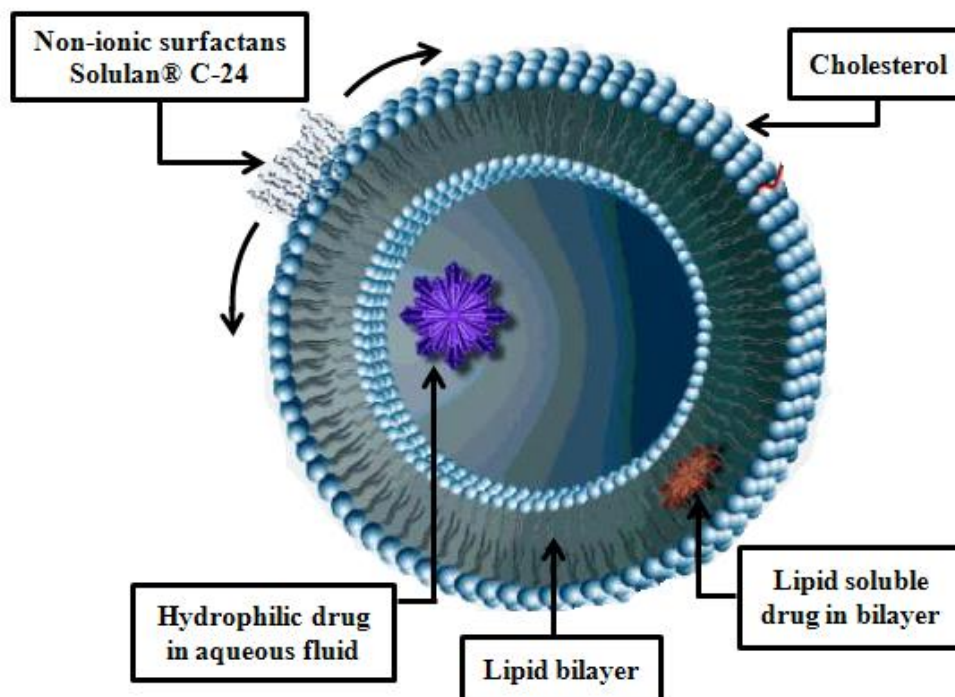


Figure 10 Structure of niosomes  
(modified from <http://www.nanopharmaceuticals.org>)

## 1. Factors affecting formation of niosomes

### 1.1 Non-ionic surfactant structure

A surfactant used for preparation of niosomes must have a hydrophilic head group and a hydrophobic tail. In certain cases cholesterol is required in the formulation and vesicle aggregation may be prevented by the inclusion of molecules that stabilize the system against the formation of aggregates by repulsive steric or electrostatic effects. An example of steric stabilization is the inclusion of Solulan<sup>®</sup> C24 and electrostatic stabilization is the inclusion of dicetyl phosphate (Balasubramaniam, Kumar and Pillai, 2002). The hydrophobic moiety may consist of one or two alkyl or perfluoroalkyl groups or a single steroidal group. The alkyl group chain length is usually from C<sub>12</sub>-C<sub>18</sub>. Hydrophilic lipophilic balance (HLB) is a good indicator of the vesicle forming ability of any surfactant. Span series surfactants, a HLB number of between 4 and 8 was found to be compatible with vesicle formation. Despite, polysorbate 20 also forms niosomes in the presence of cholesterol, the HLB



of this compound is 16.7 (Uchegbu and Vyas, 1998; Biswal et al., 2008). The chain length and hydrophilic head of non-ionic surfactants affect entrapment efficiency, such as stearyl chain  $C_{18}$  non-ionic surfactants (Brij 72, glyceryl monostearate, Span 60, Tween 61) vesicles show higher entrapment efficiency than lauryl chain  $C_{12}$  non-ionic surfactants (Brij 30, tetraglyceryl monoolaurate) vesicles (Manosroi et al., 2003). Many niosomal systems used Span series, including Span 20, Span 40, Span 60 and Span 80 (Balasubramaniam et al., 2002; Khazaeli and Pardakhty, 2007; Suwakul et al., 2006) to form vesicles. The structures of Span series are shown in Figure 11.

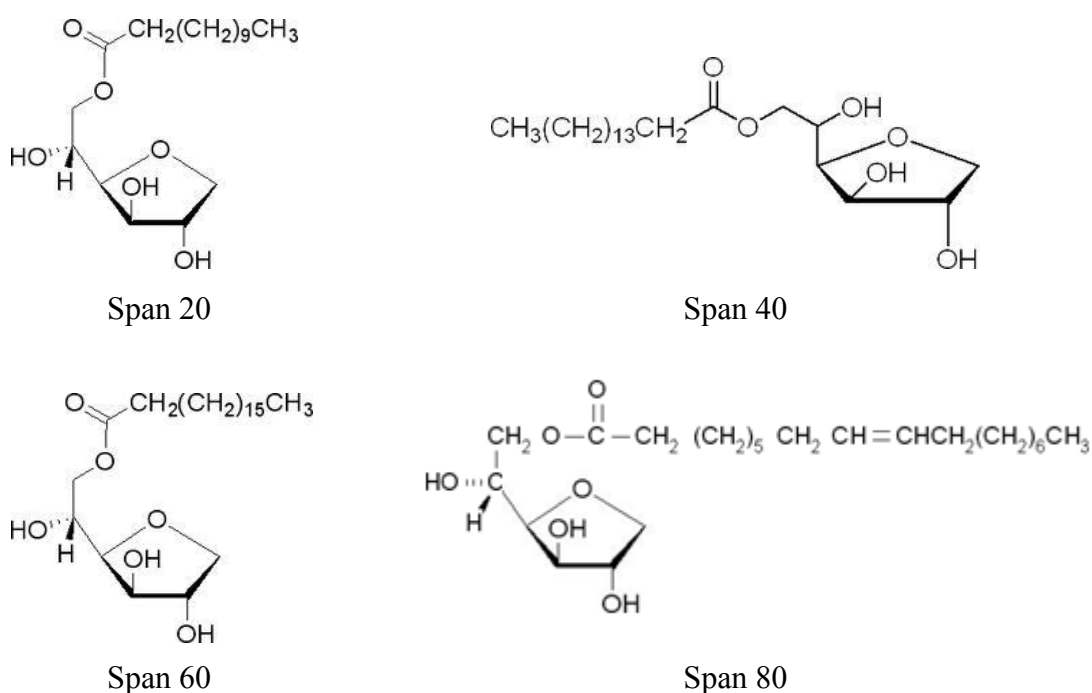
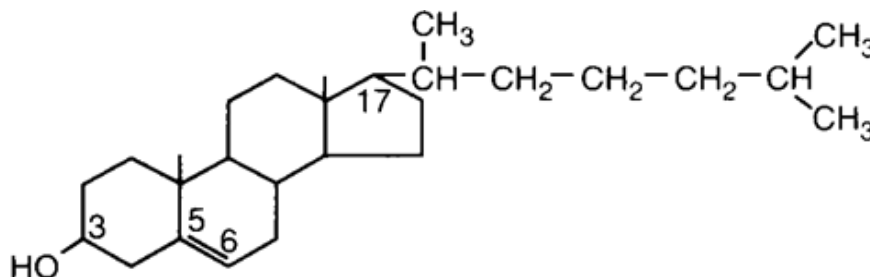


Figure 11 Chemical structures of Span series (Uchegbu and Vyas, 1998; New, 1990)

## 1.2 Membrane composition

The stable niosomes were prepared by addition of various additives with surfactants and drugs in formulation. The number of different morphologies, permeability and stability properties may be formed by manipulation of membrane forming agents. The most common additive found in niosomal systems is cholesterol that is usually included in a 1:1 molar ratio. Cholesterol is known to abolish the gel to liquid phase transition of liposome (New, 1990) and niosome systems. Span 60

niosomes prepared with cholesterol formed a homogenous niosome dispersion. Addition of cholesterol molecules to niosomal systems provides rigidity to the membrane and reduces the leakage of drug from niosomes (Uchegbu and Vyas, 1998; Biswal et al., 2008). The structure of cholesterol is shown in figure 12.



Figur 12 Chemical structure of Cholesterol (Ahmad, 1994).

### 1.3 Surfactants and lipid levels

The level of surfactants/lipid used to make niosomal dispersion is generally 10-30 mM or 100 mM (Uchegbu and Vyas, 1998; Suwakul et al., 2006). Altering the surfactant:water ratio during the hydration step may affect the system microstructure and hence the system properties. However, increasing the surfactants/lipid level also increases the total amount of drug encapsulated, highly viscous system results (Uchegbu and Vyas, 1998; Biswal et al., 2008).

### 1.4 Nature of encapsulated drug

The physicochemical properties of encapsulated drug influence charge and rigidity of the niosome bilayer. The aggregation of vesicles is prevented due to the charge development on bilayer such as dicetyl phosphate. A steric stabilizer Solulan<sup>®</sup> C24 must be added to the formulation devoid of aggregation (Uchegbu and Vyas, 1998; Biswal et al., 2008).

### 1.5 Temperature of hydration

The hydration temperature used to make niosomes should usually be above the gel to liquid phase transition temperature of the system. Temperature change of niosome system affects assembly of surfactants into vesicles and also induces vesicle shape transformation (Uchegbu and Vyas, 1998).

## **2. Niosome preparation**

Niosomes widely differ in their properties depending on the method used for production and composition of bilayer. The method of preparation of niosome is based on liposome technology (New, 1990; Torchilin and Weissig, 2003). The formulation of vesicular assembly requires the input of energy and all the experimental methods surveyed consist of the hydration of mixture of the surfactant/lipid at elevated temperature followed by size reduction to obtain a colloidal dispersion.

### **2.1 Hydration techniques**

The hydration by aqueous phase of the lipid phase which may be either a pure surfactant or a mixture of surfactant with cholesterol and dissolved in the aqueous phase/organic phase. The more commonly used laboratory methods of niosome preparation and drug loading are mentioned in the following methods (New, 1990; Uchegbu and Vyas, 1998; Torchilin and Weissig, 2003; Biswal et al., 2008; Subodh et al., 2010).

#### **2.1.1 Ether injection method**

This method was reported in 1976 by Deamer and Bangham, in which a lipid solution (surfactant or surfactant-cholesterol or surfactant-cholesterol-diacetyl phosphate or surfactant-cholesterol-drug solution mixture) dissolved in diethyl ether is slowly introduced into warm water. Typically the lipid mixture is injected into an aqueous solution of the material to be encapsulated (using syringe type infusion pump) at an elevated temperature above the boiling point of the organic solvent and under reduced pressure. Vaporization of ether leads to the formation of single layered vesicles (SLVs) depending upon the conditions used, the diameter of vesicles varies (Biswal et al., 2008; Subodh et al., 2010).

#### **2.1.2 Lipid film formation (Hand Shaking Method)**

Solution of surfactants/lipids is prepared by dissolving in organic solvent (chloroform or diethyl ether) in a round bottom flask. The organic solvent is removed by rotary evaporation under reduced pressure and leads to formation of drug surfactant/lipid film. The surfactant/lipid film is then hydrated with

aqueous solution of drug at temperature slightly above the phase transition temperature of surfactants with gentle agitation. This method produces multilamellar vesicles (MLV) with large diameter (Biswel et al., 2008; Subodh et al., 2010).

### **2.1.3 Reverse phase evaporation**

The key in this method is the removal of solvent from emulsion by evaporation. Water in oil (w/o) emulsion is formed by bath sonication of a mixture of two phases (organic solution of surfactants/lipids and an aqueous solution of the drug), and then the emulsion is dried to a semi-solid gel in a rotary evaporator under reduced pressure. The next step is to bring about the collapse of certain portion of water droplets by vigorous mechanical shaking with a vortex mixer. In these circumstances, the lipid monolayer, which encloses the collapse vesicles, is contributed to adjacent intact vesicles to form the outer leaflet of the bilayer of large unilamellar niosomes (Biswal et al., 2008; Subodh et al., 2010).

### **2.1.4 Bubble method**

It is a novel technique for the one step preparation of liposomes and niosomes without the use of organic solvents. The bubbling unit consists of round bottom flask with three necks positioned in water bath to control the temperature. Water cooled reflux and thermometer are positioned in the first and second necks and nitrogen supply through the third neck. Cholesterol and surfactant are dispersed together in this buffer (pH 7.4) at 70°C, the dispersion is mixed for 15 seconds with high shear homogenizer and immediately afterwards “bubbled” at 70°C using nitrogen gas (Biswal et al., 2008; Subodh et al., 2012).

## **2.2 Reduction of niosome size**

The size ranges of niosomes have a major effect on their fate in vivo and in vitro. Hence, size reduction stage of niosome is essential after hydration stage. The more commonly used methods for niosome size reduction are mentioned in the following methods.

### **2.2.1 Probe sonication**

Niosomes prepared by reverse phase evaporation and hand-shaking method are usually in micron size range (1.15 and 2.75  $\mu\text{m}$ ). By using probe

sonication, size of hexadecyl diglycerol ether (C<sub>16</sub>G<sub>2</sub>) niosomes formed by hand shaking method are reduced to 100-140 nm (Arunothayanun et al., 2000).

### **2.2.2 Nucleopore filter extrusion**

Size of niosomes can be reduced to nano range (140 nm) by extrusion of niosomes through nucleopore filters of pore size 100 nm.

### **2.2.3 Laser diffraction**

This method is used to reduce niosome size up to nano range. Apart from the above-state methods that the other methods are used for size reduction are microfluidization and high pressure homogenization.

## **3. Characterization of niosomes**

### **3.1 Size**

Shape of niosome vesicles assumed to be spherical. The mean diameter can be determined by using laser light scattering method, electron microscopy, photon correlation microscopy and optical microscopy (Biswal et al., 2008).

### **3.2 Bilayer formation**

Assembly of non-ionic surfactants to form bilayer vesicle is characterized by X-cross formation under light polarization microscopy (Biswal et al., 2008).

### **3.3 Entrapment efficiency**

The entrapment efficiency (EE) is expressed as the amount entrapped of drug divided by total amount added and multiplied by 100. It is determined after separation of untrapped drug, on complete vesicles were lysed by using Triton-X or sodium lauryl sulfate.

## **CHAPTER III**

### **MATERIALS AND METHODS**

#### **MATERIALS**

Silk cocoon (Nang-noi Sisaket 1) used in the experiment was purchased from the Research Institute of Silk, Sisaket Province

Acrylamide (Sigma-Aldrich, Germany, lot no. 13H0609)

Alpha-arbutin (Sigma-Aldrich, lot no. 41378101)

Ammonium persulfate (APS Finechem, Australia)

Ascorbic acid (Sigma-Aldrich, Germany, lot no. 062K0102)

Bis-acrylamide (Sigma-Aldrich, Germany, lot no. 58C-0473)

Bovine serum albumin (BSA) (Sigma-Aldrich, Inc., Germany, lot no. 045K0676)

Chloroform, AR grade (Labscan Limited, lot no. 10100111)

Cholesterol (Fluka, Japan, lot no. 423504/143804191)

Cholesteryl poly(24)oxyethylene ether (Solulan<sup>®</sup> C-24) (Noveon, lot no. CR5110900)

Coomassie brilliant blue G-250 (Fisher Scientific, UK, lot no. 025243)

2-Deoxyribose (Sigma-aldrich, Inc., Germany, lot no. 0001433976)

2,2-Diphenyl-1-picrylhydrazyl (DPPH) (Sigma-Aldrich, Germany, lot no. S4386-348)

Dimethyl sulfoxide (Riedel-de Haen, lot no. 7311A)

Ethylenediaminetetra acetic acid calcium disodium salt (Farmitalia Carlo-Erba, lot no. 2G160212G)

Glycine (Fisher Scientific, UK, lot no. 0391915)

Griess reagent (modified) (Sigma-Aldrich, Germany, lot no. 019K5020)

Guaiacol (Sigma-Aldrich, Germany, lot no. 128K1120)

Hydrochloric acid 37% (Merck, Germany, lot no.33917217443)

Hydrogen peroxide 30% w/w (Fisher Scientific, UK, lot no. 7722-84-1)

Iron(III) chloride (Merck, Germany, lot no. K26515845921)

Kojic acid (Sigma-Aldrich, Germany, lot no. 040901)

L-tyrosine (Sigma-Aldrich, Germany)

Mannitol (Merck, Germany)

Methanol (Merck, Germany, lot no. K40548609 003)

$\beta$ -nicotinamide adenine dinucleotide (NADH) (Sigma-Aldrich, Germany, lot no. 088K7003)

Nitroblue tetrazolium chloride (NBT) (Sigma-Aldrich, Germany, lot no. 97596LJ)

Octylphenol ethylene oxide condensate (Triton<sup>®</sup> X-100) (Sigma-Aldrich, Germany, lot no. 065K0122)

Peroxidase, type I from horseradish (HRP) (Sigma-Aldrich, Germany, lot no. 031K7465)

Phenazine methosulfate (PMS) (Sigma-Aldrich, Germany, 18F-5016)

Phosphoric acid 85% (Ajax Finechem, Australia, lot no. 0807333)

Potassium dihydrogen phosphate (Merck, Germany, lot no. A262673)

Quercetin dehydrate (Fluka, Japan, lot no. 39955/1 14999)

Sodium carbonate anhydrous (Ajax Finechem, Australia, lot no. AF405220)

Sodium chloride (Merck, Germany, lot no. K34243404)

Sodium dihydrogen phosphate (Merck, Germany, lot no. F1327886)

Sodium dodecyl sulfate (Merck, Germany, lot no. L57119160 741)

Sodium nitroprusside dihydrate (Fluka, Japan, lot no. 137012624308119)

Sorbitan laurate (Span<sup>®</sup> 20) (NOF CORP., Japan)

Sorbitan monopalmitate (Span<sup>®</sup> 40) (NOF CORP., Japan)

Sorbitan stearate (Span<sup>®</sup> 60) (NOF CORP., Japan)

Sorbitan oleate (Span<sup>®</sup> 80) (NOF CORP., Japan)

Tetramethylethylenediamine (TEMED) (Sigma-Aldrich, Germany)

Thiobarbituric acid (TBA) (Sigma-Aldrich, Germany, lot no. 034K0605)

Trichloroacetic acid (TCA) (Merck, Germany)

Tris (Hydroxymethyl) methylamine (Fisher Scientific, UK, lot no. 53196812-1)

Tyrosinase mushroom (Sigma-Aldrich, Germany, lot no. 24-50KUT38)

## **APPARATUSES**

Analytical balance (Model AG 285, Mettler Toledo, Switzerland)

Analytical balance (Model AX 105, Mettler Toledo, Switzerland)

Autoclave (Model HVE-25/50, Hirayama, Japan)

Centrifuge (ALC<sup>®</sup> centrifugette, Biomed group, Thailand)

Differential scanning calorimeter (DSC822e, Mettler Toledo, Switzerland)

Electrophoresis set (BioRad, USA)

Light microscope (Nikon Eclipse E200, Japan)

Magnetic stirrer (Model RCT basic, KIKA<sup>®</sup> Works Guangzhou, China)

Micropipette (Biohit, Finland)



Microplate reader (Victor<sup>®</sup>, Perkin Elmer Ltd., USA)

Modified Franz diffusion cell (Crown Glass Company, USA)

Moisture analyzer balance ( Model HB43, Mettler Toledo, Switzerland)

Particle size analyzer (Zetasizer ZS, Malvern Instruments, UK; Mastersizer 2000, Malvern Instruments, UK)

pH meter (Model 420A, Orion Research Inc., USA)

Refrigerated incubator (FOC 225I, VELP Scientifica, Italy)

Rotary evaporator (Rotavapor R-215, Buchi, Switzerland)

Scanning electron microscope (JSM-5800LV, JEOL<sup>®</sup>, Japan)

Spray dryer (SD-06, Labplant, Ltd., UK)

Transmission electron microscope (Model 1230, JOEL<sup>®</sup>, Japan)

Ultracentrifuge (L80, Beckman, USA)

Ultrasonic bath (Transsonic digitals T900/H, Elma, Germany)

UV spectrophotometer (Model UV-1601, Shimadzu, Japan)

Vortex mixer (Vortex Genie-2, Scientific Industries, USA)

Water bath (Model WB 22, Becthai Co., Ltd., Thailand)

### **ACCESSORIES**

Centrifuge bottles polycarbonate (10.4 mL) (Beckman Instruments, USA)

Quartz cell (Starna, UK)

Round bottom flask 1000 mL (Schott Duran, Germany)

Syringe needle gauge No. 23 (Nipro Corporation, Thailand)

Syringe, 3 mL (Nipro Corporation, Thailand)

Whatman filter paper No.1, diameter 150 mm (Whatman International Ltd. England)

96-well microplates (Corning, Inc., USA)

The experiments were divided into six main parts:

PART A: PREPARATION OF SILK SERICIN AND EVALUATION OF BIOLOGICAL ACTIVITIES

1. Preparation of silk cocoon
2. Silk sericin extraction methods
3. Spray drying condition
4. Evaluation of chemical and physical properties of silk sericin spray dried powder
5. Evaluation of biological activities of silk sericin spray dried powder

PART B: OPTIMIZATION OF SPRAY DRYING CONDITION

PART C: DETERMINATION OF PHYSICOCHEMICAL AND BIOLOGICAL ACTIVITIES OF OPTIMIZED SILK SERICIN POWDERS

PART D: PREPARATION AND CHARACTERIZATION OF NIOSOMES

PART E: DETERMINATION OF BIOLOGICAL ACTIVITIES OF NIOSOMES LOADED WITH SERICIN

PART F: SKIN PERMEATION STUDY OF NIOSOMES LOADED WITH SERICIN

## **METHODS**

### **A. PREPARATION OF SILK SERICIN AND EVALUATION OF BIOLOGICAL ACTIVITIES**

#### **1. Preparation of silk cocoon**

The silk cocoon used in this experiment was *Bombyx mori* Linn. (Nang-Noi Srisaket 1) from the Research Institute of Silk, Sisaket Province. Silk cocoons were cut into small pieces, approximately 1 cm<sup>2</sup>.

#### **2. Silk sericin extraction methods**

Two extraction methods for silk sericin were designed. The silk sericin products obtained from both methods were collected and compared of their physicochemical and biological properties.

##### **2.1 Method I (High temperature and pressure degumming technique)**

Silk cocoons were extracted using a high temperature and pressure degumming technique (Lee et al., 2003 and Aramwit et al., 2009). Silk cocoons in small pieces were mixed with purified water (3 g of dry silk cocoon: 100 mL of water) and the samples were boiled under pressure at 120°C for 20 min. After removing insoluble fibers by paper membrane filtration, the clear filtrate was immediately dialyzed against water for 24 h using 3,500 molecular cutoff cellulose tubing. The clear dialyzate was kept at 4°C overnight to eliminate of silk fibroin precipitate (Datta et al., 2001). The supernatant liquid was collected for spray drying.

##### **2.2 Method II (Catalyzed by Na<sub>2</sub>CO<sub>3</sub> technique)**

This method was modified from Yamada et al. (2001). Silk cocoons in small pieces were mixed with 0.05% Na<sub>2</sub>CO<sub>3</sub> solution (3 g of dry silk cocoon: 100 mL of 0.05% Na<sub>2</sub>CO<sub>3</sub> solution) and the samples were boiled at 100°C for 30 min. After removing insoluble fibers by paper membrane filtration, the clear dialyzate was immediately dialyzed against water for 24 h using 3,500 molecular cutoff cellulose tubing in order to completely remove Na<sub>2</sub>CO<sub>3</sub>. The clear filtrate was kept at 4°C

overnight to eliminate silk fibroin precipitate (Datta et al., 2001). The supernatant liquid was collected for spray drying.

### **3. Spray drying condition**

Silk sericin was prepared by spray drying of the supernatant solution using spray dryer (SD-06, Labplant, Ltd., UK). The operating parameters were set from the result of the preliminary study with the fast deblock, fan speed level of 50 (300 m<sup>3</sup>/hr.), nozzle size of 0.5 mm. The flow rate was fixed at level of 5 (4.67 mL/min) and inlet temperature of 120°C (Hino et al., 2003). The powders were collected from the collector, weighed and stored in a desiccator and kept at 4°C until use.



Figure 13. Spray dryer (SD-06, Labplant, Ltd., UK)

### **4. Evaluation of chemical and physical properties of silk sericin spray dried powder**

To determine the appropriate method for the silk sericin extraction, the silk sericin spray dried powders obtained from two different methods (Method I and II) were studied.

#### 4.1 Percentage yield

The percentage yield (w/w) was calculated from the weight of spray dried powder collected of each condition divided by the total weight of silk cocoons (dried cocoon) and multiplied with 100. The spray dried product was both collected from the collector and the cyclone of the apparatus.

$$\% \text{ yield} = \frac{\text{Weight of spray dried powder (g)} \times 100}{\text{Weight of total silk cocoons (g)}}$$

$$\% \text{ yield} = \frac{\text{Weight of spray dried powder (g)} \times 100}{\text{Weight of total silk cocoons (g)} - \text{weight of degummed cocoons (g)}}$$

#### 4.2 Moisture Content

A sample of silk sericin spray dried powder was accurately weighed on the aluminum pan of moisture analyzer balance. The temperature was set at 105°C and the maintainable constant weight for 30 seconds was detected. The sample was exposed to a halogen lamp until a constant weight was obtained. The percentage moisture content was calculated automatically.

#### 4.3 Total protein content

The determination of protein content of silk sericin spray dried powder obtained from two extraction methods was performed by Bradford assay. The Bradford assay is based on the absorbance shift observed in an acidic solution of dye Coomassie Brilliant Blue G-250. When added to a solution of protein, the dye binds to the protein resulting in a colour change from a reddish brown to blue. The binding has been assumed via electrostatic attraction of the dye's sulfonic groups to the protein. The bound points are primarily arginine residual, but the dye also binds to a lesser degree to histidine, lysine, tyrosine, tryptophan and phenylalanine. The peak absorbance of the acidic dye solution changes from 465 to 595 nm when binding to protein occurs. Therefore, measuring absorbance of the protein-dye complex at 595 nm allows an accurate quantification of the protein content of a sample (Reigosa Roger, 2001). A bovine serum albumin (BSA) was used as positive control (standard protein). To 5 µL of sample, 195 µL of Bradford reagent was added and shaken. The

reaction was maintained for 15 min at room temperature (25°C) and protected from light. The absorbance was measured at 595 nm by microplate reader. Each study corresponds to three experiments, performed in triplicate.

#### 4.3.1 Standard solution

A stock solution of BSA was prepared at the concentration of 2 mg/mL in ultrapure water. Aliquots of the stock solution can be stored at -20 °C. The dilution to volume with ultrapure water gave final concentrations of 62.5, 100, 250, 375, 500, 750, 1000 µg/mL of BSA, respectively.

Sericin solution concentrations ranging from 0.5 to 4 mg/mL were prepared and analyzed.

#### 4.3.2 Bradford reagent

To prepare 1 L of protein reagent, Coomassie Brilliant Blue G-250 (100 mg) was dissolved in 50 mL 95% methanol. To this solution 100 mL 85% (w/v) phosphoric acid was added.

### **4.4 Estimated molecular mass of silk sericin using sodium dodecyl sulfate polyacrylamide gel electrophoresis (SDS-PAGE)**

SDS-PAGE is a method used to separate proteins according to their molecular size. Since different proteins with similar molecular weights may migrate differently due to their differences in secondary, tertiary or quaternary structure, SDS, an anionic detergent, is used in SDS-PAGE to reduce proteins to their primary (linearized) structure surrounded by uniform negative charges of SDS.

Firstly, silk sericin and BSA were dissolved in ultrapure water to be solutions at 2 mg/mL and then diluted for desired concentrations, 20-30 µg protein and 5 µg protein per lane, respectively.

Secondly, stock solutions were prepared as bellowed section:

- a) 4 x sample buffer was prepared by 1.6 g of SDS, 4 mL of 2-mercaptoethanol, 5 mL of 500 mM Tris (pH 6.8), 4 mg of bromophenol blue, 8 mL of glycerol and ultrapure water qs to 20 mL.

- b) Stock solution of 50% acrylamide solution was prepared by weighing 49.2 g of acrylamide mixed with 0.8 g of N,N'-methylene bisacrylamide and ultrapure water qs. to 100 mL.
- c) 4 x stacking buffer solution was prepared by 25 mL of 2 M Tris base mixed with 4 mL of 10% SDS and ultrapure water qs. to 100 mL. (adjust to pH 6.8)
- d) 4 x separating buffer solution was prepared by 75 mL of 2 M Tris base mixed with 4 mL of 10% SDS and ultrapure water qs. to 100 mL. (adjust to pH 8.8)
- e) 1 x laemmli SDS electrophoresis buffer was prepared by 100 mL of 10 x laemmli SDS electrophoresis buffer mixed with 900 mL of ultrapure water (10 x laemmli SDS electrophoresis buffer was prepared by 30.3 g of Tris base, 144.2 g of glycine, 10 g of SDS and ultrapure water qs to 100 mL).
- f) Colloidal Coomassie Blue G-250 working solution was prepared by 400 mL of colloidal coomassie blue G-250 dye stock solution mixed with 100 mL of methanol ( colloidal coomassie blue G-250 dye stock solution was prepared by 50 g of ammonium sulfate, 6 mL of phosphoric acid 85% (w/w), 10 mL of 5% coomassie blue G-250 stock and ultrapure water qs to 500 mL.
- g) Fixing solution was prepared by 10 mL of acetic acid, 40 mL of ethanol and ultrapure water 50 mL.

Thirdly, setting up gel cassettes was demonstrated in Figure 14.

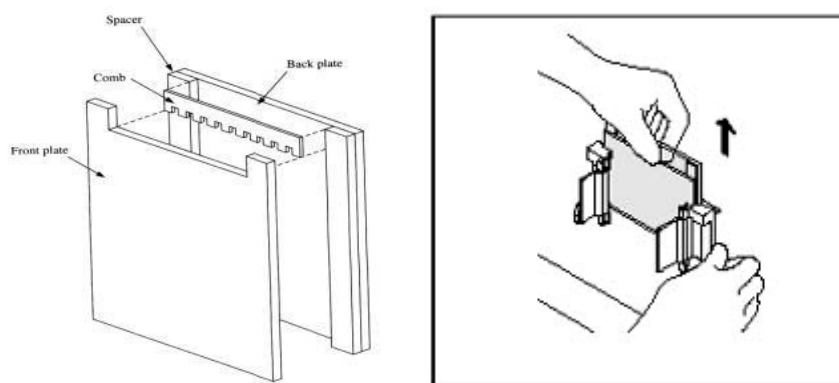


Figure 14 Procedure of setting up gel cassettes.

Separating gel was freshly prepared at 6, 8 and 10% acrylamide by adding and mixing ingredients in the order shown in Table 3. The separating gel was rapidly loaded into gel cassettes for 4 in 5 parts and then the mixture was added by ultrapure water above the gel for preventing it from contacting with air and bubbles, and waiting for about 30 minutes for the gel to polymerize completely.

The stacking gel was freshly prepared at 4% acrylamide by adding and mixing ingredients in the order (Table 3). Before adding stacking gel, excess ultrapure water was removed. The stacking gel was rapidly added upside the separating gel until reaching the front, suddenly inserted combs and allowed another about 30 min for complete polymerization. When gel had already formed, the gel was clamped to the electrophoresis apparatus. The electrophoresis buffer was added all over the electrophoresis set and the comb was removed.

Sample was prepared by mixing sample 4:1 with 4 x sample buffer. The mixture was heated in water bath at 95°C for 5 min and it was cooled in room temperature. Carefully loading 4x sample buffer, marker and each sample into each lane, slowly added for preventing blown it out.

Next, the conditions during running electrophoresis were 90 V, about 1.5 h and monitored color of bromophenol blue (4 x sample buffer). When the color reached the front, the current was turned off.



Carefully removed the gel from gel cassettes, fixed protein into the gel by fixing solution about 10 min. The gel was stained by Colloidal Coomassie Blue G-250 working solution at room temperature over night and then washed by ultrapure water for many times with gently shaken. When the edge of the gel was clear, it meant completely destaining so kept the gel in plastic at 8°C.

Table 3 Component of separating gel and stacking gel.

	Stacking gel	Separating gel			
		6%	8%	10%	
Ultrapure water	2.6	6.3	5.9	5.5	mL
4 x stacking buffer solution	1	-	-	-	mL
4 x separating buffer solution	-	2.5	2.5	2.5	mL
50% acrylamide solution	0.4	1.2	1.6	2	mL
10% ammonium persulfate	30	50	50	50	μL
TEMED	5	10	10	10	μL

## 5. Evaluation of biological activities of silk sericin spray dried powder

### 5.1 Anti-oxidant activities of silk sericin

#### 5.1.1 DPPH free radical scavenging activity assay

The free radical scavenging activity using DPPH reagent was measured by a method described by Wu, Wang and Xu (2007). To 0.5 mL of sericin dissolved in distilled water at gradually increasing concentrations of 1.25, 2.50, 5.00, 10, 20 and 40 mg/mL, 3.5 mL of freshly prepared DPPH reagent in a methanol solution (0.1 mM) was added and vortexed. The reaction was maintained for 25 min at room temperature (25°C) and protected from light. After that reaction mixtures were centrifuged at 6,000 rpm for 5 min. The decolorizing result of the supernatant was assayed at 517 nm and compared with a blank control containing the sericin solution and pure methanol instead of DPPH. In addition, a blind control containing DPPH and distilled water instead of sericin solution was also assayed. Ascorbic acid at the concentrations ranging from 1.00 to 20.0 μg/mL) was used as positive control and

methanol as a negative control. Each assay was performed in three different experiments and each experiment was run in triplicate. The ability of free radical scavenging activity was calculated using the following equation.

$$\% \text{ Scavenging activity} = \frac{(\text{Absorbance of control} - \text{Absorbance of sample}) \times 100}{\text{Absorbance of control}}$$

Absorbance of control: The absorbance of mixture containing 0.5 mL of distilled water without test sample and 3.5 mL of 0.1 mM DPPH solution

Absorbance of sample: The absorbance of mixture containing 0.5 mL of test sample and 3.5 mL of 0.1 mM DPPH solution

Calculation of half maximum effective concentration (EC<sub>50</sub>): after calculation of % scavenging activity for each concentration of the test sample, a relationship between % scavenging activity and concentration was plotted. The EC<sub>50</sub> of each test sample was calculated from the linear regression equation of the initial linear portion of the graph.

### 5.1.2 Superoxide radical scavenging assay (Choi et al., 2007)

Superoxide radicals were generated by the NADH/PMS system and the O<sub>2</sub><sup>•-</sup> scavenging activity was determined spectrophotometrically in a microplate reader by monitoring the effect of the tested compound on the O<sub>2</sub><sup>•-</sup> induced reduction of NBT at 560 nm for 8 min.

The assay was performed at room temperature. The reaction mixtures in the sample wells contained, in a final volume of 200 µL, the following reagents: 60 µL of NADH (0.553 mM), 60 µL NBT (0.143 mM), 60 µL of PMS (9µM), and 20 µL of tested compounds were dissolved in distilled water (0.625, 1.250, 2.500, 5.000, 10.00, 20.00 and 40.00 mg/mL). All other components were dissolved in 0.1 M phosphate buffer, pH 7.4. The effects are expressed as the percentage inhibition of the NBT reduction to diformazan. Quercetin at the concentrations ranging from 6.25 to 400 mM was used as a positive control. Each assay was performed in three different experiments and each experiment was run in

triplicate. The ability of superoxide radical scavenging activity was calculated using the follow equation.

$$\% \text{ Scavenging activity} = \frac{(\text{Absorbance of control} - \text{Absorbance of sample}) \times 100}{\text{Absorbance of control}}$$

Absorbance of control: The absorbance of reaction mixtures containing distilled water without test sample

Absorbance of sample: The absorbance of reaction mixtures containing test sample

Calculation of EC<sub>50</sub>: after calculation of % scavenging activity for each concentration of the test sample, a relationship between % scavenging activity and concentration was plotted. The EC<sub>50</sub> of each test sample was calculated from the linear regression equation of the initial linear portion of the graph.

### **5.1.3 Hydrogen peroxide scavenging assay (Choi et al., 2007)**

H<sub>2</sub>O<sub>2</sub> scavenging was measured using the guaiacol method. The reaction mixtures in the sample wells contained, in a final volume of 200 µL, the following reagents: 20 µL of tested compounds were dissolved in distilled water (0, 0.625, 1.250, 2.500, 5.000, 10.00, 20.00 and 40.00 mg/mL), 30 µL of 0.1 M potassium phosphate buffer, 25 µL of 4 mM H<sub>2</sub>O<sub>2</sub>, 25 µL of 0.08% guaiacol solution and 100 µL of 14.5 U/mL of horseradish peroxidase. This solution was incubated for 30 min at room temperature. The absorbance was measured at 450 nm by microplate reader. Quercetin at the concentrations ranging from 6.25 to 400 µM was used as positive controls. Each study corresponding to three experiments was performed in triplicate. The ability of superoxide radical scavenging activity was calculated using the follow equation

$$\% \text{ Scavenging activity} = \frac{(\text{Absorbance of control} - \text{Absorbance of sample}) \times 100}{\text{Absorbance of control}}$$

Absorbance of control: The absorbance of reaction mixtures containing distilled water without test sample

Absorbance of sample: The absorbance of reaction mixtures containing test sample

Calculation of EC<sub>50</sub>: after calculation of % scavenging activity for each concentration of the test sample, a relationship between % scavenging activity and concentration was plotted. The EC<sub>50</sub> of each test sample was calculated from the linear regression equation of the initial linear portion of the graph.

#### **5.1.4 Hydroxyl radical scavenging assay** (Fernandes et al., 2004)

The scavenging effect against hydroxyl radicals was determined using a deoxyribose method. When deoxyribose exposed to hydroxyl radicals generated by a Fenton system (ascorbic acid/FeCl<sub>3</sub>-EDTA/H<sub>2</sub>O<sub>2</sub>), it is degraded to malonaldehyde, which generates a pink chromogen on heating with TBA, at low pH. Reaction mixtures contained, in a final volume of 1 mL, the following reagents: 100 µL of 28 mM deoxyribose, 250 µL of 0.1 M potassium phosphate buffer (pH 7.4), 250 µL of tested compounds were dissolved in distilled water (5, 1.0, 2.0, 4.0, 8.0 and 16.0 mg/mL), 100 µL of FeCl<sub>3</sub>-EDTA (100 µM FeCl<sub>3</sub>+104 µM EDTA (1:1)), 100 µL of 1 mM H<sub>2</sub>O<sub>2</sub> and 100 µL of 1 mM ascorbic acid. The iron salt was premixed with the chelator dissolved in water before addition to the reaction mixture. All other components were dissolved in 10 mM potassium phosphate buffer, pH 7.4. After incubation at 37°C for 1 h, 1 mL of 1 % (w/v) TBA and 1 mL of 2.8% (w/v) trichloroacetic acid were added, and the mixture was heated in a water bath at 100°C for 15 min. The absorbance of the resulting solution was measured by UV spectrophotometer at 532 nm. This assay was also performed without ascorbic acid or EDTA to evaluate a possible pro-oxidant and/or iron chelation activity. Mannitol was used as a positive control (concentration: 0.5-16 mg/mL). Each assay was performed in three different experiments and each experiment was run in triplicate. The ability of hydroxyl radical scavenging activity was calculated using the follow equation.

$$\% \text{ Scavenging activity} = \frac{(\text{Absorbance of control} - \text{Absorbance of sample}) \times 100}{\text{Absorbance of control}}$$

Absorbance of control: The absorbance of reaction mixtures containing distilled water without test sample

Absorbance of sample: The absorbance of reaction mixtures containing test sample

Calculation of EC<sub>50</sub>: after calculation of % scavenging activity for each concentration of the test sample, a relationship between % scavenging activity and concentration was plotted. The EC<sub>50</sub> of each test sample was calculated from the linear regression equation of the initial linear portion of the graph.

### **5.1.5 Nitric oxide radical scavenging assay** (Ebrahimzadeh et al., 2009 and Mandal et al., 2009)

At physiological pH, sodium nitroprusside (SNP) in aqueous solution spontaneously generates nitric oxide which interacts with oxygen to produce nitrite ions that can be estimated using Griess reagent. The reaction mixtures in the sample wells contained, in a final volume of 200 µL, the following reagents: 20 µL of tested compounds dissolved in ultrapure water (0, 0.625, 1.250, 2.500, 5.000, 10.00, 20.00 and 40.00 mg/mL), 80 µL of 2.5 mM SNP in phosphate buffer saline. This solution was mixed and light incubated for 2.5 h at room temperature. After incubation, 1 µL of Griess reagent was added and the mixture was protected from light incubation for 15 min. The pink chromophore formed during diazotization of nitrite ions with sulphanilamide and subsequent coupling with NED was measured spectrophotometrically against blank sample. The absorbance was measured at 560 nm by microplate reader. Quercetin 6.25-400 mM was used as positive control. Each study corresponding to three experiments was performed in triplicate. Assay of the mixture at each concentration was performed in triplicate. The ability of nitric oxide scavenging activity was calculated using the follow equation.

$$\% \text{ Scavenging activity} = \frac{(\text{Absorbance of control} - \text{Absorbance of sample}) \times 100}{\text{Absorbance of control}}$$

Absorbance of control: The absorbance of reaction mixtures containing distilled water without test sample

Absorbance of sample: The absorbance of reaction mixtures containing test sample

Calculation of EC<sub>50</sub>: after calculation of % scavenging activity for each concentration of the test sample, a relationship between % scavenging activity and concentration was plotted. The EC<sub>50</sub> of each test sample was calculated from the linear regression equation of the initial linear portion of the graph.

### 5.2 Anti-tyrosinase activities of silk sericin ( Piao et al., 2002)

Tyrosinase-inhibition activity was determined by the minor modified method from Piao et al (2002) using L-tyrosine as a substrate. The reaction mixtures in the sample wells contained, in a final volume of 200 µL, the following reagents: 40 µL of mushroom tyrosinase solution (100 units/mL) and 80 µL of 0.1 M potassium phosphate buffer (pH 6.8) were mixed with the 40 µL of tested compounds (sericin powders dissolved in distilled water (0.125, 0.250, 0.500, 1.000, 2.000, 4.000 and 8.000 mg/mL). The mixture was then pre-incubated at 37°C for 10 min before adding 40 µL of 2 mM L-tyrosine solution. The assay mixture was after-incubated at 37°C for 30 min. Instead of a sample in distilled water, distilled water was added to a blank solution. Before and after incubation, the amount of dopachrome produced in the reaction mixture was measured at 490 nm in a microplate reader. The percentage of inhibition of tyrosinase activity was calculated as follows:

$$\% \text{ Inhibition} = \frac{(A-B)-(C-D)}{A-B} \times 100$$

A: absorbance of blank solution after incubation

B: absorbance of blank solution before incubation

C: absorbance of sample solution after incubation

D: absorbance of sample solution before incubation

Calculation of EC<sub>50</sub>: after calculation of % inhibition of tyrosinase activity for each concentration of the test sample, a relationship between % inhibition of tyrosinase activity and concentration was plotted. The EC<sub>50</sub> of each test sample was calculated from the linear regression equation of the initial linear portion of the graph.

## B. OPTIMIZATION OF SPRAY DRYING CONDITION

From the investigation of silk sericin extraction methods, the extraction by boiling at high temperature and pressure (method I) was selected. The spray drying solution was prepared from 3, 6.5 and 10% of silk cocoons. The silk solutions were prepared and kept at 4°C and thawed at room temperature before spray drying process.

### 1. Preparation of spray drying solution

A spray dryer was used for the preparation of spray dried powder (Figure 14). The operating parameters were set with the fast deblock, fan speed of level 50 (300 m<sup>3</sup>/hr.) and nozzle size of 0.5 mm. The inlet temperature was established at 100, 120 and 140°C; the outlet temperature depended on the inlet temperature and the flow rate was fixed at level 5 (4.67 mL/min). The powders were collected and stored in dessicator and kept 4°C until further investigations.

### 2. Optimization design: Face-centered composite design (FCCD)

A face-centered composite design is a central composite design with  $\alpha = 1$ . For this purpose, a face-centered composite design with two factors at two levels was used to study the response surface and to determine the combination of variables that would produce the maximal yield and the minimal moisture content. According to the model, it contains four full factorial design points, four axial points and five center points. Higher and lower levels of each factor were coded as +1 and -1 respectively, and the mean value as 0. The selected factor levels are summarized in Table 4.

Table 4 Factors and levels of studied variables

Independent Variables		
Coded values	Cocoon concentration (%)	Inlet Temperature (°C)
-1	3	100
0	6.5	120
1	10	140

The center points were repeated 5 times to estimate the pure experimental uncertainty at the factor levels. The combination effect of cocoon concentration and inlet temperature was studied by response surface methodology. The response surface plots indicated the effects of factors on the percentage yield and percentage moisture content responses at each level of the factors. The face-centered composite design in this study was 13 runs. The design matrix with responses was given in Table 5.

Table 5 A face-centered composite design with observed responses

Code	Factors	
	Cocoon concentration (%)	Inlet Temperature (°C)
F1	3 (-)	100 (-)
F2	3 (-)	140 (+)
F3	3 (-)	120 (0)
F4	10 (+)	100 (-)
F5	10 (+)	140 (+)
F6	10 (+)	120 (0)
F7	6.5 (0)	100 (-)
F8	6.5 (0)	140 (+)
F9	6.5 (0)	120 (0)
F10	6.5 (0)	120 (0)
F11	6.5 (0)	120 (0)
F12	6.5 (0)	120 (0)
F13	6.5 (0)	120 (0)

Statistical analysis and a graphical optimization were performed using Design-Expert version 8.0.4 statistical software. The method basically consisted of overlaying the curves of the models according to the criteria imposed. The selection of conditions to overlay plot were ranged from 3-10% of cocoon concentration and 100-140°C of inlet temperature. The main objective was to maximize %yield and minimize %moisture content.



### **3. Characterization of silk sericin spray dried powder**

The silk sericin spray dried powders prepared from the 13 designed conditions in Table 5 were evaluated for percentage yield (Topic A4.1) and moisture content (Topic A4.2). Additionally, morphology, size and size distribution of these powders were also studied by the procedure mentioned below.

#### **3.1 Scanning electron microscopy**

The morphological features of 13 spray-dried silk sericin powders were examined under a scanning electron microscope (JSM-5800LV, JEOL, Japan). Powder samples were stuck on the adhesive tape on the aluminum stubs and coated with a thin layer of gold before examination. The magnifications of the photomicrographs of powder were x500, x1,000 and x3,000.

#### **3.2 Particle size and size distribution**

The particle size and size distribution of spray-dried powders were determined with a laser granulometer Mastersizer 2000 (Malvern Instruments) by dry dispersion using 4-bar pressure.

## **C. DETERMINATION OF PHYSICOCHEMICAL AND BIOLOGICAL ACTIVITIES OF OPTIMIZED SILK SERICIN POWDERS**

### **1. Moisture Content**

The moisture content of silk sericin spray-dried powder was determined by the same method as described in Topic A4.2.

### **2. Total protein content**

The total protein content of silk sericin spray-dried powder was determined by the same method as described in Topic A4.3.

### **3. Molecular mass of silk sericin by sodium dodecyl sulfate polyacrylamide gel electrophoresis (SDS-PAGE)**

The molecular mass of silk sericin spray-dried powder was determined by the same method as described in Topic A4.4.

#### **4. Thermal analysis by differential scanning calorimetric method**

The differential scanning calorimetric (DSC) thermogram was determined by using differential scanning calorimeter (DSC822<sup>o</sup>, Mettler Toledo, Switzerland). The sample was accurately weighed (3-5 mg) into an aluminum pan (40  $\mu$ l) and pierced lid. The DSC was operated on the temperature range 0-270  $^{\circ}$ C at heating rate 10  $^{\circ}$ C/min, under nitrogen gas atmosphere at flow rate 200 mL/min.

#### **5. Powder X-ray diffraction study**

The diffractogram of silk sericin spray-dried powder was examined by powder x-ray diffractometry (JDX-3530, Jeol, Japan). The data was investigated over an angular range 5 $^{\circ}$ -50 $^{\circ}$  in continuous mode, using a step angle of 0.0188 $^{\circ}$  and step time: 96.2 seconds.

#### **6. Morphology**

The morphology of spray-dried powder was determined by the same method as described in Topic B3.1.

#### **7. Determination of size and size distribution**

The particle size and size distribution of spray-dried powder was determined by the same method as described in Topic B3.2.

#### **8. Anti-oxidant activities of silk sericin**

##### **8.1 Free radical scavenging activity (DPPH assay)**

Free radical scavenging activity of silk sericin spray-dried powder was determined by the same method as described in Topic A5.11.

##### **8.2 Superoxide radical scavenging assay**

Superoxide radical scavenging activity of silk sericin spray-dried powder was determined by the same method as described in Topic A5.12.

#### **9. Anti-tyrosinase activities of silk sericin**

Anti-tyrosinase activity of silk sericin spray-dried powder was determined by the same method as described in Topic A5.2.

## D. PREPARATION AND CHARACTERIZATION OF NIOSOMES

### 1. Preparation of niosomes (New, 1990; Puangmalai, 2007; Torchilin and Weissig, 2003)

Niosomes were prepared by reverse phase evaporation with varied types of surfactant. The reverse phase evaporation technique was used due to the ability to entrap a large percentage of the aqueous material presented, and LUVs were proposed from this technique. Silk sericin prepared from the optimized spray drying condition was used for loading niosomes.

The total lipid concentration used was 100  $\mu\text{mol/mL}$  of aqueous phase. Cholesterol, surfactant and Solulan<sup>®</sup> C-24 were calculated to get final lipid concentration in 30 mL of final volume of niosome preparation.

Firstly, amounts of cholesterol, surfactant and Solulan<sup>®</sup> C-24 (Table 6) were accurately weighed and dissolved with chloroform in a 500 mL pear-shaped flask. A portion of 15 mL of distilled water was introduced into the lipid solution by rapidly injecting through a needle gauge No. 23 from a 10 mL syringe followed by closing the system and sonication in bath sonicator at 4 °C for 10 min. Then, the flask was transferred to the rotary evaporator, which was swirled gently at 60 °C and vacuum (450 mbar) about 10 min until gel forming. The flask was vigorously agitated by vortex mixer until gel collapsed and was transformed into viscous fluid or niosome dispersion. Afterwards, 15 mL of 20 mg/mL or 2% silk sericin was added to hydrate lipid at the same temperature without reduce pressure until a homogeneous niosome suspension obtained (New, 1990). Finally, the niosome was further sonicated for 60 min for size reduction.

Table 6 Composition of lipid in formulations in various ratios of cholesterol and surfactant\*.

Surfactant	Surfactant : cholesterol : Solulan <sup>®</sup> C-24* (molar ratio)
Span 20	47.5 : 47.5 : 5
Span 40	47.5 : 47.5 : 5
Span 60	47.5 : 47.5 : 5
Span 80	47.5 : 47.5 : 5

\*Each formulation was fixed with ratio surfactant: cholesterol (1:1), 5% mole of Solulan C-24, loaded with 2% silk sericin and prepared in triplicate.

## 2. Characterization of niosomes

The characteristics of niosomes such as appearance, morphology, size and size distribution and the percentage of entrapment efficiency of each formulation were investigated.

### 2.1 Microscopic appearances

The appearances of niosomes were observed in shape, size, aggregation and X-cross bilayer formation under polarized light microscopy. They were observed and photographed under the microscope with magnification of 10x100.

### 2.2 Particle size and size distribution

Particle size and size distribution of niosomes were estimated with a photon correlation spectroscopy (Zetasizer ZS, Malvern Instruments, UK) at 25 °C.

### 2.3 Transmission electron microscopy (TEM)

Niosomes were characterized for their shape using transmission electron microscopy (TEM). Samples were examined by negative staining technique and observed the results in photographs.

## 2.4 Entrapment efficiency

The niosome suspensions were weighed into balanced centrifuge polycarbonate bottles. The encapsulated protein was separated by ultracentrifugation (Ultracentrifuge, L80, Beckman, USA) at 65,000 rpm at 4 °C for 8 hours. The sediments containing with sericin niosome vesicles were lyzed by adding 0.5% Triton X-100. After sonicated, the clear solution was assayed for protein content by Bradford assay. The absorbances were monitored at 595 nm and compared with the standard curve of silk sericin solution. The supernatants were also analyzed by Bradford assay. All analyses were determined in triplicate and calculated the percentage of recovery. The entrapment efficiency was calculated by the equation below (Puangmalai, 2007; Manosroi et al., 2002).

$$\% \text{ Entrapment efficiency} = \frac{\text{Total protein content in vesicles} \times 100}{\text{Initial protein content added}}$$

$$\% \text{ Recovery} = \frac{(A+B)}{\text{Initial protein content added}} \times 100$$

Where A is total protein content in vesicles, B is total protein content in supernatant.

Statistical analysis of differences in the entrapment efficiency was performed by using Analysis of Variance (ANOVA). A *P*-value of 0.5 was taken as the level of significance.

#### **E. DETERMINATION OF BIOLOGICAL ACTIVITIES OF NIOSOMES LOADED WITH SERICIN**

Samples of niosomes loaded with silk sericin were determined for anti-oxidant activity (superoxide radical scavenging activity) by modified superoxide radical assay as described in Topic A5.12.

Samples were determined for anti-tyrosinase activity by modified anti-tyrosinase assay as described in Topic A5.2.

#### **F. SKIN PERMEATION STUDY OF NIOSOMES LOADED WITH SERICIN**

The experiments were carried out with carefully prepared back skin of selected pigs (about 100 kg weight, obtained from a local butcher according to our specifications, Colipa, 1997). Skin discs were prepared about 0.6-1 mm thickness containing stratum corneum, epidermis and some part of dermis (Schmook, Meingassner and Billich, 2001). The full-thickness abdominal skin membrane of a new born pig was prepared by the following step. Firstly, the abdominal skin was excised and inspected for any defects. The fat layer was removed from the stratum corneum by using sharp butcher knife and forcep. Finally, residues of fat were carefully scraped off with forcep and the bristles were cut with scissors. And then, the skin was rinsed with purified water. The skin discs were wrapped with aluminium foil, put into plastic bags, and stored in freezer at -20 °C until used (Colipa, 1997).

In vitro skin permeation was determined by using modified Franz vertical diffusion cell (Manconi et al., 2006). The frozen skin discs had been thawed at room temperature and soaked with PBS (pH 7.4) for 1 h before equilibrated. The skin membrane was fixed in the diffusion chamber where the dermis side was in contact with the receptor fluid, and the horny layer was exposed to air. The receptor fluid was PBS (pH 7.4), and maintained at  $37 \pm 1$  °C by a thermostatic water bath and was stirred with magnetic bar at 600 rpm. The skin was equilibrated for 1 h and the cell was gently rocked for repelling any air bubbles. After equilibration, 1 mL sample of

nanosomes loaded with silk sericin was applied into donor compartment without occlusion. The silk sericin solution of 0.5% w/w was also investigated and compared. An aliquot of 1 mL sample from the receptor compartment at certain time intervals of 0.5, 1, 1.5, 2, 4, 6, 8, 10, 12, 14, 16, 18, 20, 22 and 24 h. The receptor compartments were replaced with PBS to keep constant volume during the experiment. Samples were analyzed for amount of silk sericin which permeated through pig skin by Bradford assay.

## CHAPTER IV

### RESULTS AND DISCUSSION

#### A. COMPARISON OF EXTRACTION METHODS FOR SILK SERICIN

##### 1. Characteristics of silk sericin spray dried powder

The percentage yield, percent moisture content, pH value and physical appearance of silk sericin spray dried powders prepared by two different methods are displayed in Table 7. Figure 15 show the physical appearances of silk sericin spray dried powders obtained from two different methods. From both methods, silk sericin spray dried powders were obtained as yellow bulky fine powder. The percentage yield was calculated on total silk cocoon basis and on degumming water basis of silk cocoons. The percentages yield of silk sericin spray dried powders (collected from both collecting chamber and cyclone) from method I was higher than that obtained from method II. The percent moisture content of sericin spray dried powder prepared from method I were lower than the powder obtained from method II. However, pH values of both spray dried powder were similar at 6.84-6.87. This result showed that the dialysis of the degumming water in method II could effectively remove  $\text{Na}_2\text{CO}_3$  from the solution. สุพนิตา วินิจฉัย และพิลาณี ไวกนอมสัจช์ (2553) reported that %yield of sericin extraction using autoclaving and basic hydrolysis were 26.9 and 16.3% (w/w), respectively. Wu et al (2007) have also reported that %yield extraction of sericin with 75% (v/v) ethanol from silk waste water was 46.1-71.3 % (w/w).

The particle sizes of silk sericin spray dried powder from method I and II determined by laser scattering technique were  $6.825 \pm 0.085 \mu\text{m}$  with span values of  $1.651 \pm 0.076$  and  $5.725 \pm 0.164 \mu\text{m}$  with span values of  $1.408 \pm 0.072$ . The particle sizes of silk sericin spray dried powder from method I were larger than those from method II because degumming solution from method I was obtained as gel-like liquid



and viscous. It was demonstrated that higher viscous liquid resulted in larger particle sizes of spray dried powder.

The particle topography from scanning electron microscopy of all spray-dried silk sericin showed spherical particles with smooth shrinking surface (Figure 16).

Table 7 Comparison of percentage yield, percentage moisture content and physical appearances of silk sericin spray dried powders from two different methods (Mean  $\pm$  SD, n = 3)

Method	% Yield		Moisture content (%)	pH	Particle size ( $\mu\text{m}$ )	Span values
	%yield (compared with total silk cocoon)	%yield (compared with degumming water)				
I	13.69 $\pm$ 1.00	54.17 $\pm$ 4.68	7.31 $\pm$ 0.95	6.87 $\pm$ 0.17	6.825 $\pm$ 0.085	1.651 $\pm$ 0.076
II	11.14 $\pm$ 0.77	51.55 $\pm$ 2.17	8.59 $\pm$ 0.60	6.84 $\pm$ 0.16	5.725 $\pm$ 0.164	1.408 $\pm$ 0.072

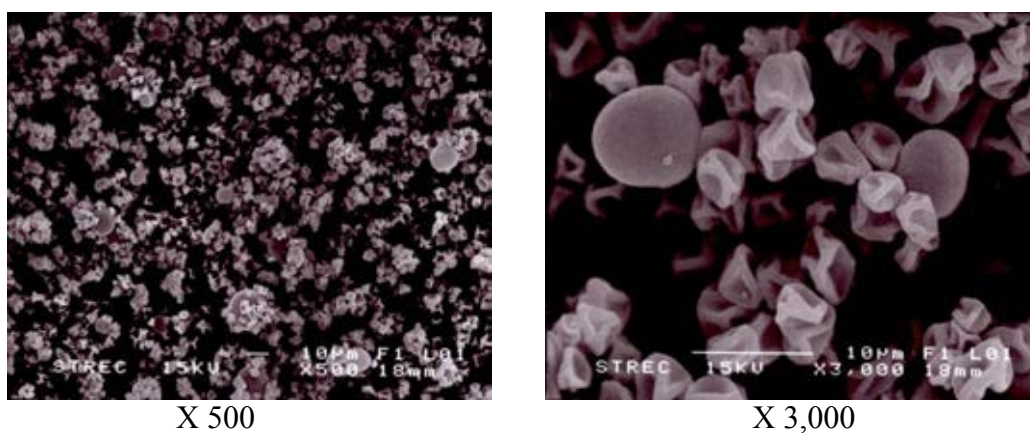


Method I

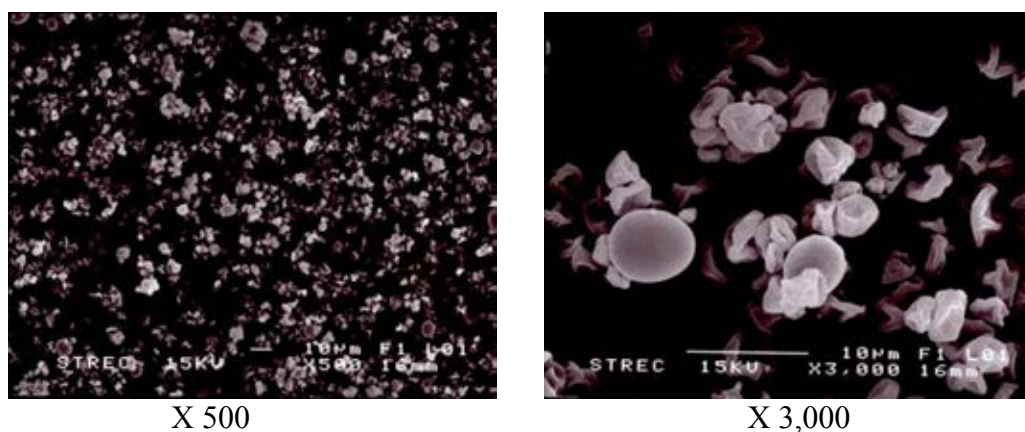


Method II

Figure 15 Silk sericin spray dried powder from two different methods.



### Method I



### Method II

Figure 16 Morphology of particles of spray dried products from method I and II.

## 2. Quantification of total protein by Bradford assay

The Bradford assay has several advantages such as greater sensitivity, greater speed, decreased susceptibility to interferences, requirement for a single reagent and lower cost (Owusu-Apenten, 2002). BSA and sericin (method I and method II) were analyzed for protein content by Bradford assay of seven concentrations ranging from 0.06-1.00 mg/mL and 0.50-4.00 mg/mL. Linear regression analysis of the absorbances of BSA at 595 nm versus the corresponding concentrations is depicted in Figure 17. The coefficients of determination ( $R^2$ ) of standard curve of BSA were calculated as 0.9909. The calibration data were found to be linear with good  $R^2$ . The

amounts of protein in sericin (method I) and sericin (method II) were  $22.97 \pm 0.86$  and  $17.92 \pm 0.29\%$  (w/w) of BSA (n=5). The results showed that the extraction at high temperature and pressure by autoclaving gave sericin powder with higher total protein content than the extraction catalyzed by  $\text{Na}_2\text{CO}_3$ . Lamoolphak et al (2008) reported that the total protein content of sericin obtained by hydrothermal treatment was 26.39-29.98% (w/w) of raw silk waste (Lowry method). สรัลรัตน์ พ่วงบริสุทธิ์ และคณะ (2553) have also reported that percentage protein of sericin using autoclaving and basic hydrolysis were 23.08 and 18.72% (w/w), respectively.

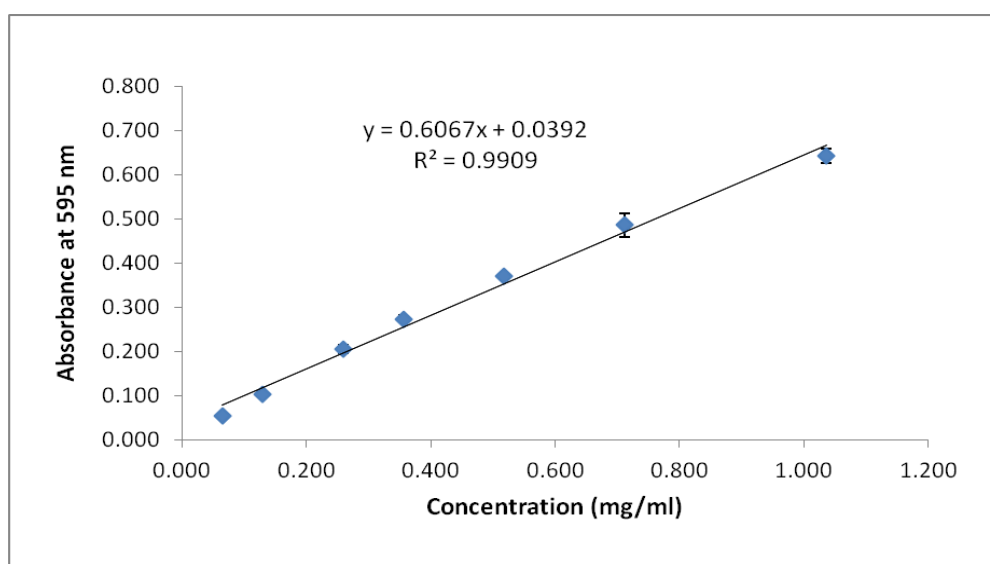


Figure 17 Standard curve of BSA, n=5.

### 3. Molecular mass of silk sericin by sodium dodecyl sulfate polyacrylamide gel electrophoresis (SDS-PAGE)

The electrophoresis was run by using 5  $\mu\text{g}$  BSA, 20-30  $\mu\text{g}$  protein of sericin per lane, respectively. BSA was used to evaluate method reliability and compare molecular masses from the marker. The results shown in Figures 18-20 were performed in 6-10% acrylamide. Molecular mass of BSA (66 kDa) was truly run electrophoresis between 50-75 kDa. This result suggested that the method for running SDS-PAGE was reliable.

Sericin from both methods were run in gel, showing the molecular mass ranging from 10 to 250 kDa. The result was close to the previous studies that SDS-PAGE of silk sericin protein demonstrated in range widely from 10 to 300 kDa (Zhang, 2002). An accurate determination of the molecular weight distribution of sericin is not reported to date because of the complex components of peptides obtained from different extraction and process condition (Wu et al., 2007). Although sericin were in range 10-250 kDa, their patterns were clearly different. The molecular weight distribution range of sericin (method I) was 75-250 kDa (Figures 19 and 20), but the main of sericin (method II) were in lower part (below 20 kDa, Figure 18) and higher part (250 kDa) (Figure 19).

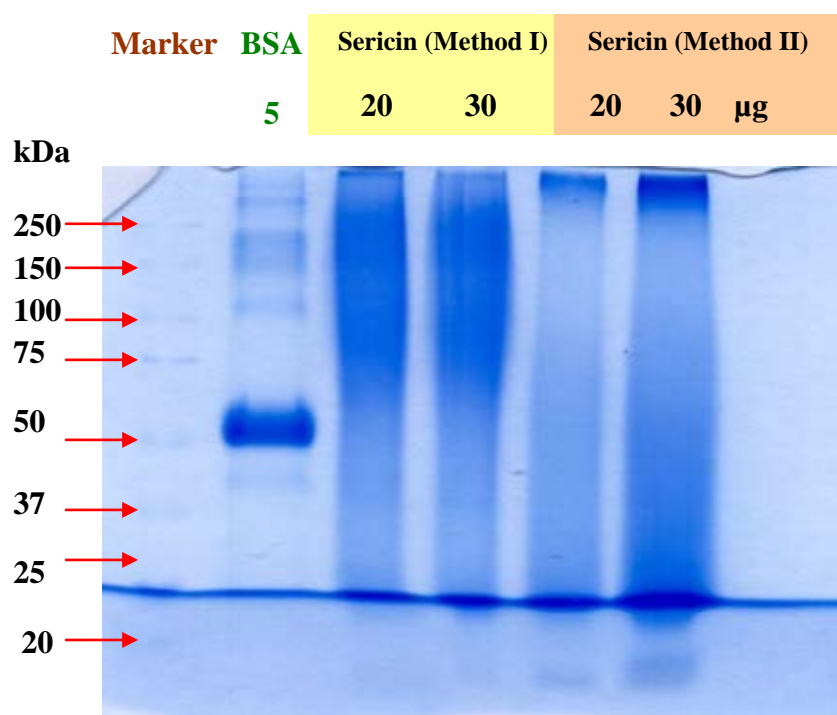


Figure 18 SDS-PAGE (10% ) analysis of BSA, sericin (method I) and sericin (methodII), compared with the rainbow marker.

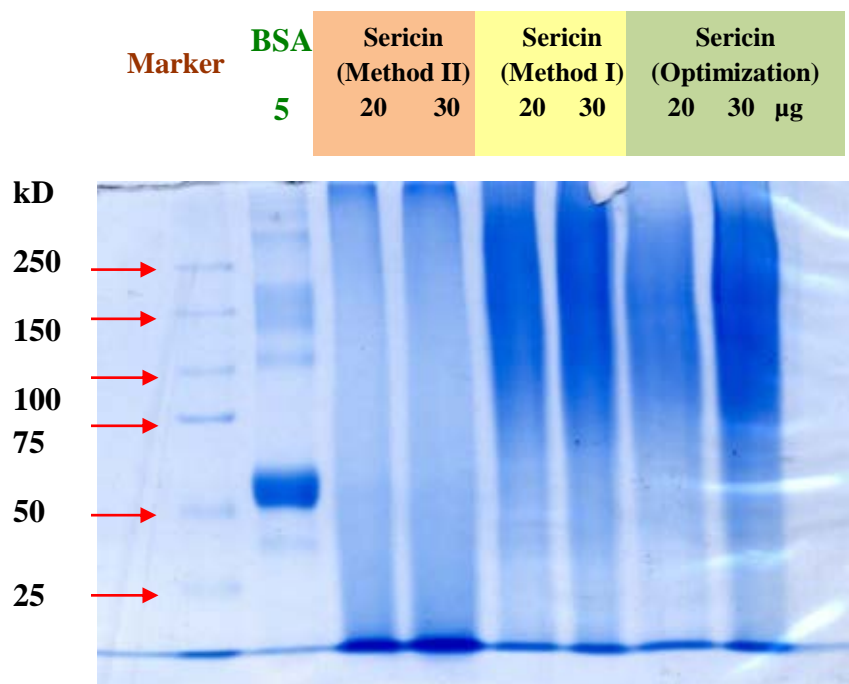


Figure 19 SDS-PAGE (8%) analysis of BSA, (method I), sericin (method II) and sericin (optimization), compared with the rainbow marker.

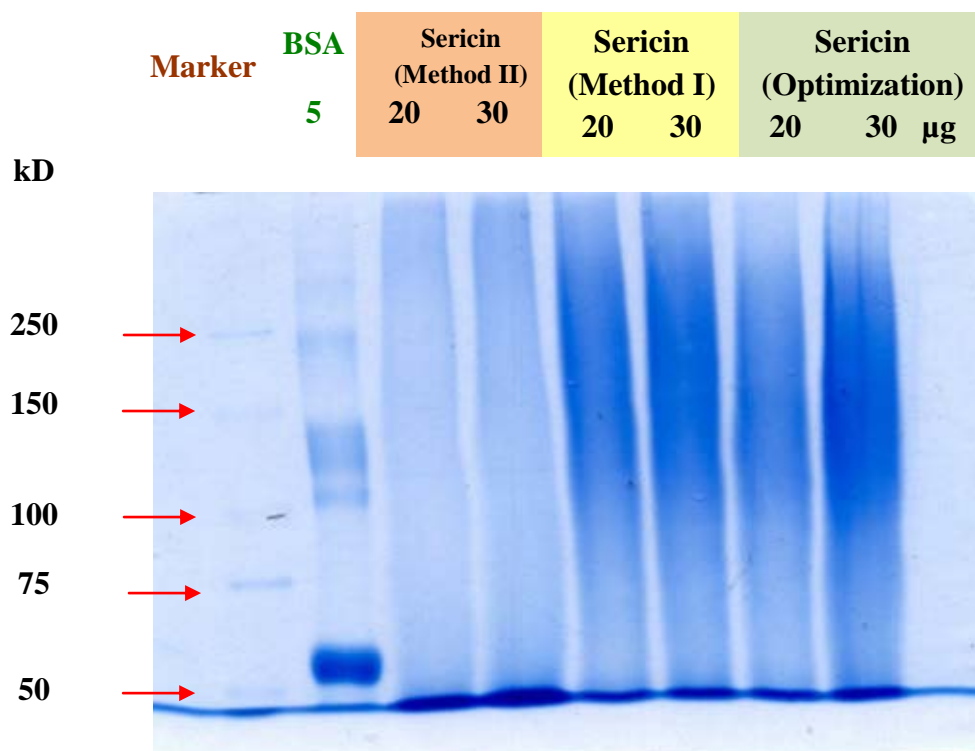


Figure 20 SDS-PAGE (6%) analysis of BSA, (method I), sericin (method II) and sericin (optimization), compared with the rainbow marker.

#### 4. Evaluation of biological activities of silk sericin spray dried powder

##### 4.1 Anti-oxidant activities of silk sericin

##### 4.1.1 DPPH scavenging activity

The DPPH assay is used worldwide in the quantification of free radical scavenging activity. DPPH is a stable free radical that shows maximum absorbance at 517 nm in methanol. When DPPH radicals encounter a proton-donating substance such as an antioxidant, the DPPH radicals would be scavenged and the absorbance is reduced. Based on this principle, the antioxidant activity of the substance can be expressed as its ability in scavenging the DPPH radicals. In this study, ascorbic acid was used as a positive control. The 50% Scavenging activity ( $EC_{50}$ ) of ascorbic acid was 2.4  $\mu\text{g}/\text{mL}$ . It was observed that 1.30 mg/mL of silk sericin powder (method I) and 2.59 mg/mL of silk sericin powder (method II) scavenged 50% of DPPH radicals (Figure 21). The free radical scavenging activity of silk sericin powders prepared by method I and method II were non-significantly different ( $p > 0.05$ ). The  $EC_{50}$  values of silk sericin from both methods were lower than those obtained by heating at 95°C for 120 min (Wu et al., 2007) or by autoclaving and basic hydrolysis (Manosroi et al., 2010), which were in the range of 31-55 mg/mL.

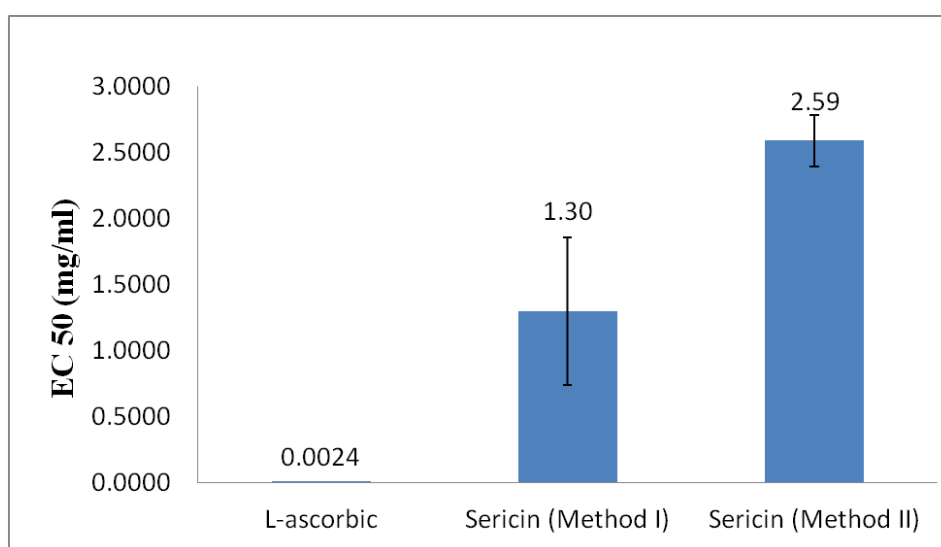


Figure 21 DPPH scavenging activity of silk sericin obtained from method I and II. L-ascorbic acid was used as a positive control (n=3).

#### 4.1.2 Superoxide radical scavenging activity

The non-enzymatic generation of superoxide anions was detected by reduction of NBT in a PMS/NADH system. The  $EC_{50}$  (mg/mL) values of superoxide radical scavenging activity of silk sericin obtained by method I and were  $0.43 \pm 0.05$  and  $0.81 \pm 0.08$ , respectively (Figure 22). Fan et al. (2007) reported that 2.5 mg/ml of silk sericin leading suppressed 58.13% superoxide radical scavenging activity. This study indicated that the silk sericin prepared by method I gave significantly higher superoxide radical scavenging activity than that prepared by method II ( $p < 0.05$ ). Quercetin was used as a positive control, exhibiting an  $EC_{50}$  value of  $0.02 \pm 0.00$  mg/mL (50.22 mM).

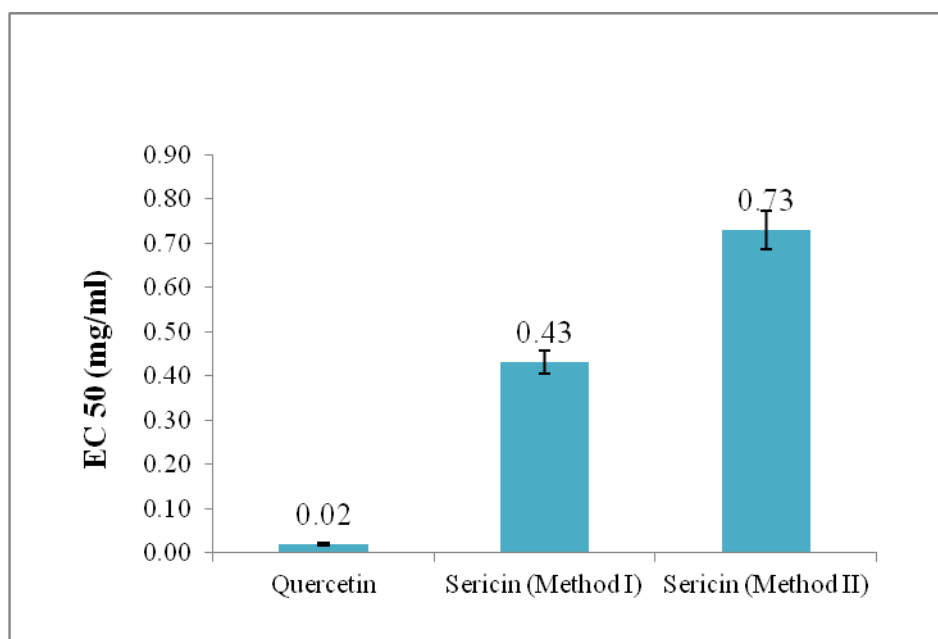


Figure 22 Superoxide radical scavenging activity of silk sericin obtained from method I and II. Quercetin was used as a positive control (n=3).



### 4.1.3 Hydrogen peroxide scavenging activity

The ability of silk sericin to effectively scavenge hydrogen peroxide was determined according to the modified method of Aruoma (Choi et al., 2007). The EC<sub>50</sub> (mg/mL) values of silk sericin obtained by method I and II were 1.63±0.51 and 1.77±0.49, respectively. The EC<sub>50</sub> value for quercetin, used as a positive control, was 0.015±0.003 mg/mL (Figure 23). The hydrogen peroxide scavenging activity of both silk sericin powders were non-significantly different ( $p > 0.05$ ).

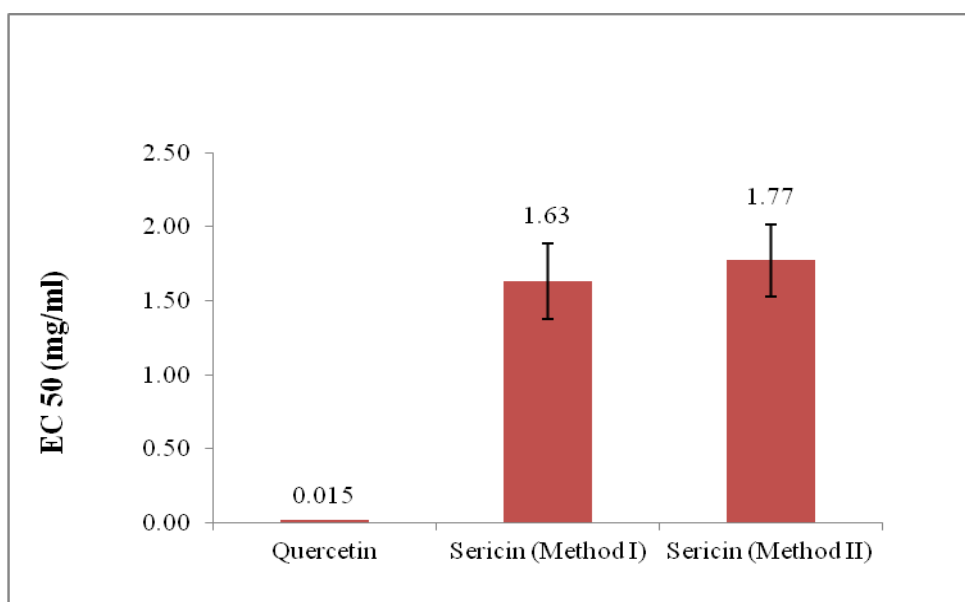


Figure 23 Hydrogen peroxide scavenging activity of silk sericin obtained from method I and II. Quercetin was used as a positive control (n=4).

### 4.1.4 Hydroxyl radical scavenging assay

Hydroxyl radical generated in a Fenton system (ascorbic acid/FeCl<sub>3</sub>-EDTA/H<sub>2</sub>O<sub>2</sub>), the hydroxyl radical reacted to the sugar 2-deoxy-D-ribose. The products reacts with thiobarbituric acid to generate a chromogen. Any added scavenger of hydroxyl radical will compete with deoxyribose for the hydroxyl radical generated and decrease chromogen formation (Fernandes et al., 2004). Although mannitol is not anti-free radical substance, it was generally employed as a positive control. Silk sericin extraction from autoclaving (method I) and basic hydrolysis



(method II) were tested in this method. The  $EC_{50}$  (mg/mL) values of hydroxyl radical scavenging activity of silk sericin obtained from method I and II including mannitol were  $0.94 \pm 0.11$ ,  $0.96 \pm 0.10$  and  $0.54 \pm 0.11$ , respectively (Figure 24). The hydroxyl radical scavenging activity of both silk sericin powders were non-significantly different ( $p > 0.05$ ).

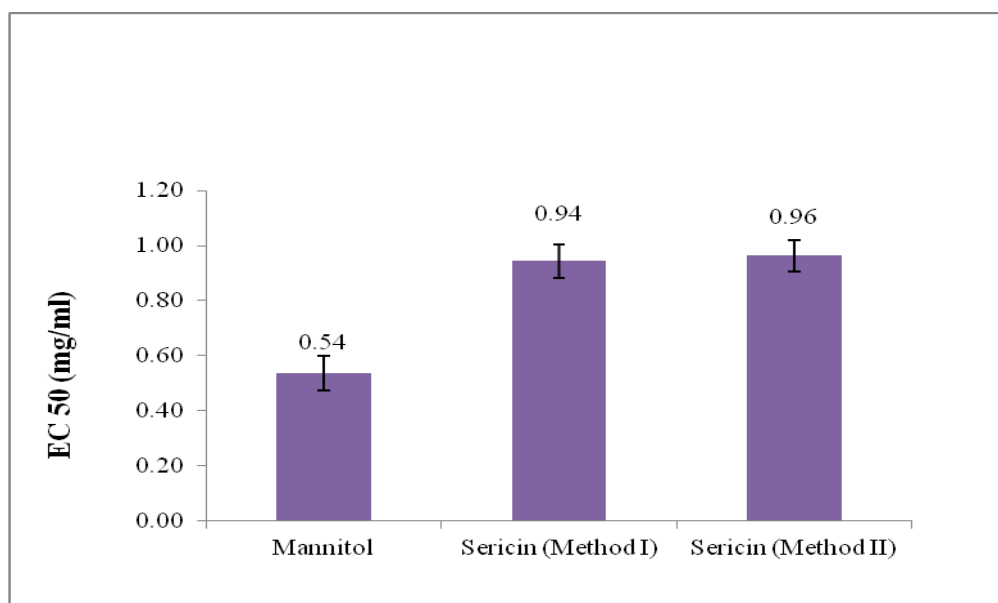


Figure 24 Hydroxyl radicals scavenging activity of silk sericin obtained from method I and II. Mannitol was used as a positive control (n=3).

#### 4.1.5 Nitric oxide radical scavenging assay

The  $EC_{50}$  (mg/ml) values of nitric oxide scavenging activity of silk sericin from autoclaving (method I) and basic hydrolysis (method II) processes were  $2.02 \pm 0.28$  and  $1.67 \pm 0.47$  mg/mL, respectively (Figure 25). The  $EC_{50}$  value of quercetin (positive control) was  $0.01 \pm 0.00$  mg/mL. The nitric oxide scavenging activity of both silk sericin powders were non-significantly different ( $p > 0.05$ ).

The scavenging activities against hydrogen peroxide and nitric oxide radicals of silk sericin have not been reported elsewhere.

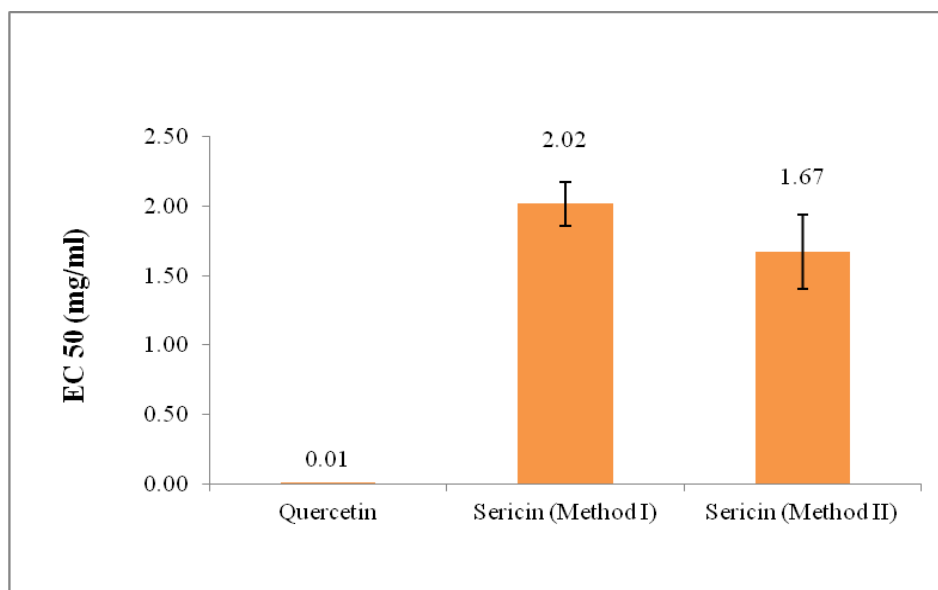


Figure 25 Nitric oxide radical scavenging activity of silk sericin obtained from method I and II. Quercetin was used as a positive control (n=3).

#### 4.2 Anti-tyrosinase activities of silk sericin

Tyrosinase is a copper-containing monooxygenase enzyme widely distributed in nature. It catalyzes the conversion of tyrosine to dopa, dopaquinone, and subsequent autopolymerization to melanin. Tyrosinase inhibitor has been used as a whitening agent or antihyperpigment agent because of its ability to suppress dermal-melanin production (Piao et al., 2001). The inhibitory effect on tyrosinase activity was examined by the dopachrome enzymatic method using L-tyrosine as the substrate (Piao et al., 2001 and Manosroi et al., 2010). The EC<sub>50</sub> (mg/mL) values of silk sericins were shown in Figure 26. Silk sericin extraction from autoclaving (method I), basic hydrolysis processes (method II), alpha-arbutin and kojic acid gave the EC<sub>50</sub> values of 0.26±0.05, 2.54±0.62, 0.21±0.03 and 0.005±0.000 mg/mL, respectively. This study indicated that the silk sericin extraction by the autoclaving gave significantly higher anti-tyrosinase activity than basic hydrolysis (0.05% Na<sub>2</sub>CO<sub>3</sub>) ( $p < 0.05$ ). However, the inhibition of mushroom tyrosinase activity of silk sericin extraction by the autoclaving was non-significantly different from standard alpha-arbutin and kojic acid ( $p > 0.05$ ). Wu et al (2007) reported that the EC<sub>50</sub> (mg/mL) values for the inhibition of mushroom tyrosinase activity by sericin prepared from silk industry wastewater was

10 mg/mL. Manosroi et al (2010) have also reported that the  $EC_{50}$  (mg/mL) values for the inhibition of mushroom tyrosinase activity by sericin prepared from Nangnoi-Srisaket 1 by autoclaving method was 18.76 mg/mL.

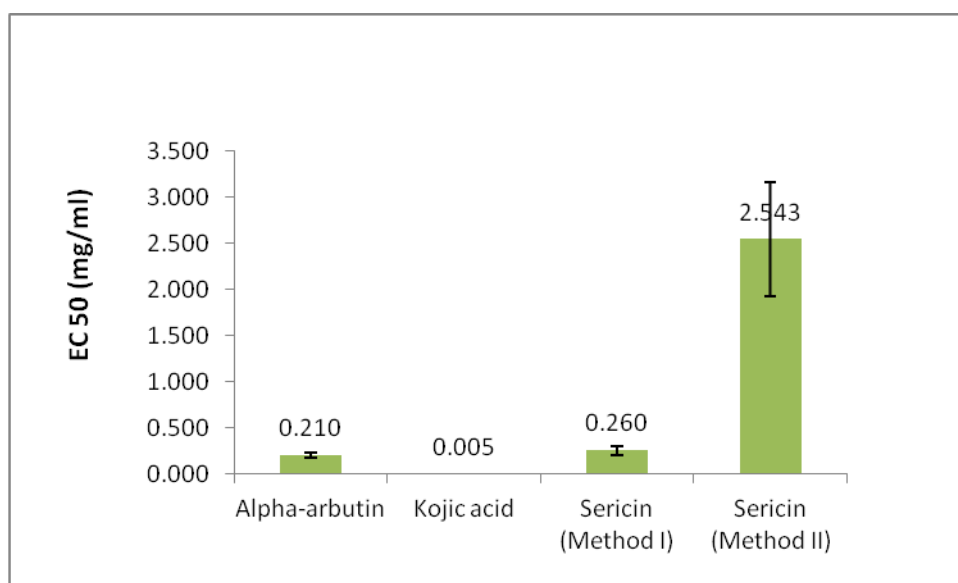


Figure 26 Anti-tyrosinase activity of silk sericin obtained from method I and II. Alpha-arbutin and kojic acid were used as a positive control (n=3).

The results could be explained that method of silk sericin extraction had effect on the physical appearances, protein content, molecular weight and biological activities. However, silk sericin that prepared by method I (autoclaving method) gave higher protein content and biological activities than method II (basic hydrolysis). This study has suggested that silk sericin from Nangnoi-Sisaket 1 extracted by autoclaving, gave the higher tyrosinase inhibition, free radical scavenging activity, and superoxide scavenging activity, than silk sericin from method II. Consequently, method I (autoclaving method) was the appropriate method for silk sericin extraction and chosen to prepare silk sericin in the further study.

## B. OPTIMIZATION OF SPRAY DRYING CONDITION

### 1. Optimization of spray drying condition on production yield and moisture

There were many factors in spray drying process effected on yield and powder properties such as sample concentration, inlet and outlet air temperatures, air flow rate and feed flow rate. In this report, the effect of sample concentration and inlet temperature on the yield and moisture content of spray dried powder were investigated, whereas feed flow rate was fixed at level 5 (4.67 ml/min).

To explore the region of the response surface in the neighborhood of the optimum, a second order approximation to the response surface could be developed. A face-centered composite design was used for this purpose. The design matrix with responses is given in Table 8.

Table 8 A face-centered composite design with observed responses

Code	Factors		Responses	
	Cocoon concentration (%)	Inlet Temperature (°C)	%Yield	%Moisture content
F1	3 (-)	100 (-)	15.05	8.52
F2	3 (-)	140 (+)	14.10	7.09
F3	3 (-)	120 (0)	14.74	8.37
F4	10 (+)	100 (-)	6.91	7.71
F5	10 (+)	140 (+)	8.43	5.68
F6	10 (+)	120 (0)	9.31	8.56
F7	6.5 (0)	100 (-)	10.17	7.15
F8	6.5 (0)	140 (+)	11.9	6.44
F9	6.5 (0)	120 (0)	10.34	8.65
F10	6.5 (0)	120 (0)	11.98	7.71
F11	6.5 (0)	120 (0)	12.17	7.18
F12	6.5 (0)	120 (0)	10.76	7.5
F13	6.5 (0)	120 (0)	10.43	8.09

The percentage yield and moisture content varied from 8.43-15.05% and 5.68-8.65%, respectively. The results of the second order, response surface linear model fitting in the form of analysis of variance for %yield and the quadratic model for %moisture content are given in Table 9 and Table 10, respectively.

The analysis of variance of the regression model states that the model of %yield and %moisture content was significant ( $P < 0.05$ ). The response surface linear model was an adequate model for %yield and the quadratic model for %moisture content, as were evident from the  $F$ -test ( $F_{\%yield} = 42.14$  and  $F_{\%moisture\ content} = 4.535$ ) and a very low probability values (%yield:  $P_{model} > F < 0.0001$  and %moisture content:  $P_{model} > F = 0.0365$ ) (Table 9 and Table 10). Values of “Prob  $> F$ ” were less than 0.05 indicated that model terms were significant ( $P > 0.05$ ) (Montgomery, 2005). Lack of fit for both models was not significant ( $P > 0.05$ ). Non significant lack of fit was good.

The goodness of fit of the models was checked by the determination coefficient ( $R^2$ ). The  $R^2$  value is always between 0 and 1. The closer  $R^2$  value is to 1, the stronger model is, and the better it predicted the response (Montgomery, 2005). In this study, the values of  $R^2 = 0.8939$  and  $0.7641$ , indicated that 89.39% and 76.41% of variability in the response could be explained by the model for %yield and %moisture content, respectively (Table 11).

The application of  $P$ -values is to check the significance of each of the coefficients which were necessary to understand the pattern of the mutual interactions between the test variables (Montgomery, 2005). This implied that, %yield, was mainly affected by %cocoon concentration (A), referring from the  $P$ -value  $< 0.0001$ . Consequently, it was the most significant effect ( $P < 0.05$ ) (Table 9). For moisture content, the first order main effect of inlet temperature (B) and second order main effect of inlet temperature ( $B^2$ ) were a significant effect by referring from its  $P$ -value  $= 0.0193$  and  $P$ -value  $= 0.0130$  ( $P < 0.05$ ), respectively (Table 10).

By applying multiple regression analysis on the experimental data, the experiment results of the face-centered composite design were fitted with a linear equation of %yield and second-order quadratic equation of %moisture content. The

coefficients of regression equation associated to the responses to the experimental variables and interaction are represented in Table 12.

Table 9 ANOVA for response surface linear model of %yield

<b>Source</b>	<b>Sum of Squares</b>	<b>df</b>	<b>Mean Square</b>	<b>F Value</b>	<b>p-value Probability &gt; F</b>
Model	62.58	2	31.29	42.14	< 0.0001*
A-%concentration	61.70	1	61.70	83.09	< 0.0001*
B-inlet temp	0.8817	1	0.8817	1.187	0.3014
Residual	7.425	10	0.7425		
Lack of Fit	4.370	6	0.7283	0.9537	0.5445**
Pure Error	3.055	4	0.7637		
Corrected Total	70.00	12			

\* Significant at  $P$  value = 0.05

\*\* Not significant at  $P$  value = 0.05

Table 10 ANOVA for response surface quadratic model of %moisture content

<b>Source</b>	<b>Sum of Squares</b>	<b>df</b>	<b>Mean Square</b>	<b>F Value</b>	<b>p-value Prob &gt; F</b>
Model	7.188	5	1.4376	4.535	0.0365*
A-concentration	0.6868	1	0.6868	2.166	0.1845
B-inlet temp	2.898	1	2.8982	9.14	0.0193*
AB	0.0900	1	0.0900	0.2839	0.6107
A <sup>2</sup>	0.8360	1	0.8360	2.637	0.1484
B <sup>2</sup>	3.464	1	3.4635	10.93	0.0130*
Residual	2.219	7	0.3170		
Lack of Fit	0.9335	3	0.3112	0.9681	0.4901**
Pure Error	1.286	4	0.3214		
Corrected Total	9.407	12			

\* Significant at  $P$  value = 0.05

\*\* Not significant at  $P$  value = 0.05

Table 11 Model Summary Statistics of %yield and %moisture

Responses	Std.	R-Squared	Adjusted	Predicted	PRESS
	Dev.		R-Squared	R-Squared	
<b>%Yield</b>					
Linear	0.86	0.8939	0.8727	0.8069	13.51
<b>%Moisture content</b>					
Quadratic	0.56	0.7641	0.5956	0.2016	11.3

Table 12 Coefficients of the regression equation linking the response to the experimental factors and major interactions (coded units)

Responses	Factor	Coefficients
<b>%Yield</b>	Intercept	11.25
	A-concentration	-3.21
	B-inlet temp	0.38
<b>%Moisture content</b>	Intercept	7.8514
	A-concentration	-0.34
	B-inlet temp	-0.70
	AB	-0.15
	A <sup>2</sup>	0.55
	B <sup>2</sup>	-1.12

Thus, the mathematical regression model for %yield and %moisture content fitted in the coded factors were given as following:

$$\%Yield = 11.25 - 3.21A + 0.38B \dots\dots\dots (1)$$

$$\%Moisture\ content = 7.85 - 0.34A - 0.70B - 0.15AB + 0.55A^2 - 1.12B^2 \dots (2)$$

Where, A and B were the coded values of the test variables;

A: %Cocoon concentration

B: Inlet temperature

According to the final equation in terms of coded parameters, it may be shown in the equation (1) that decreasing of %cocoon concentration (A) enhanced the %yield while the inlet temperature (B) has not significantly affected on %yield (Table 9). However, the equation (1) concluded the inlet temperature (B) because the experimental data (Table 8) shown the inlet temperature may be affected on %yield. The reason might be attributed to the compositions of spray drying solution such as sericin solution gelatin-like characteristics (Zhu, Arai and Hirayashi, 1994). The %yield of different value of the variables could be predicted from linear regression plot (linear model).

For %moisture content, the main factor was inlet temperature (B) while the %cocoon concentration (A) was not a significant factor. It was suggested that an increase in inlet temperature (B) was a direct decrease in residual moisture in the products. However, the equation (2) concluded the cocoon concentration (A), interaction of cocoon concentration and inlet temperature (AB) and second order main effect of cocoon concentration ( $A^2$ ) because the experimental data (Table 8) shown the cocoon concentration, the interaction of cocoon concentration and inlet temperature and second order main effect of cocoon concentration may be affected on %moisture content. The moisture content was possibly forecasted from the response surface plot (quadratic model). Figure 27 and Figure 28 show the linear regression plot for %yield and response surface plot for %moisture content, and contour plots of the %yield and %moisture content, respectively.

The normal probability plot of the residuals is a vital diagnostic tool for the detection and explanation of the systematic departures from the assumptions to support errors normally distributed and no affected to each other whose variances are homogeneous (Montgomery, 2005). Figure 29 are the plots of normal probability of experiment results. The normal probability plot of the “Studentised” residuals indicates almost no violation of the assumptions outlying the analyses.

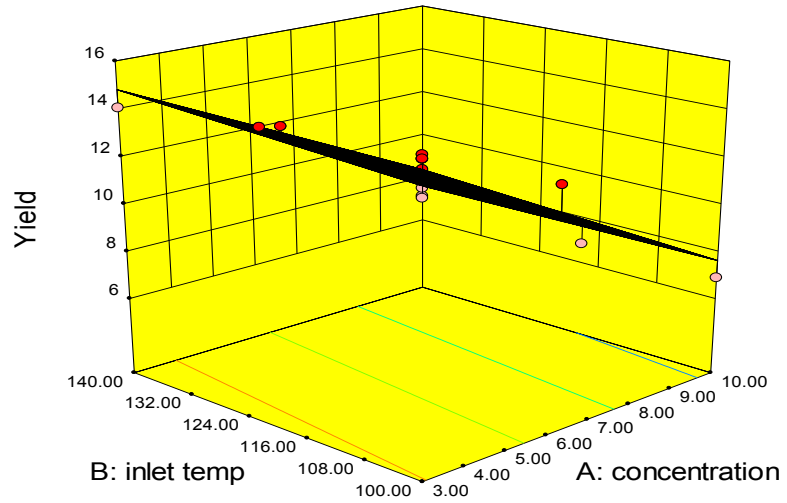


(a)

Design-Expert® Software  
Factor Coding: Actual  
Yield

● Design points above predicted value  
○ Design points below predicted value  
15.05  
6.91

X1 = A: concentration  
X2 = B: inlet temp



(b)

Design-Expert® Software  
Factor Coding: Actual  
Moisture content

● Design points above predicted value  
○ Design points below predicted value  
8.65  
5.68

X1 = A: concentration  
X2 = B: inlet temp

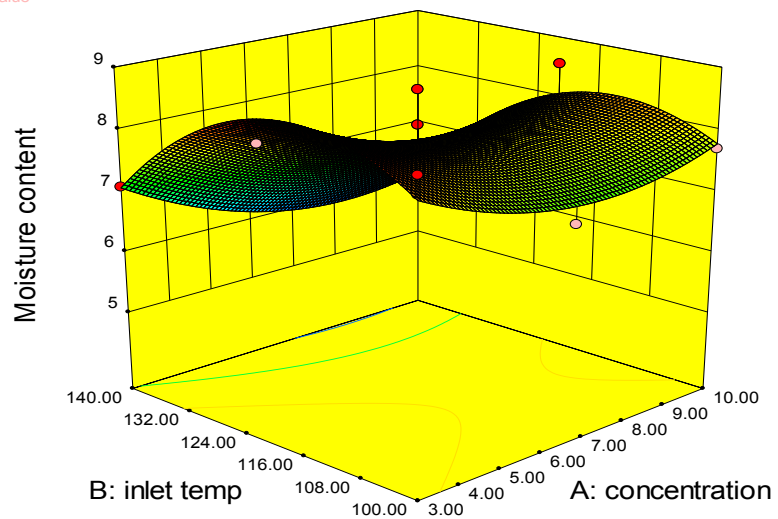


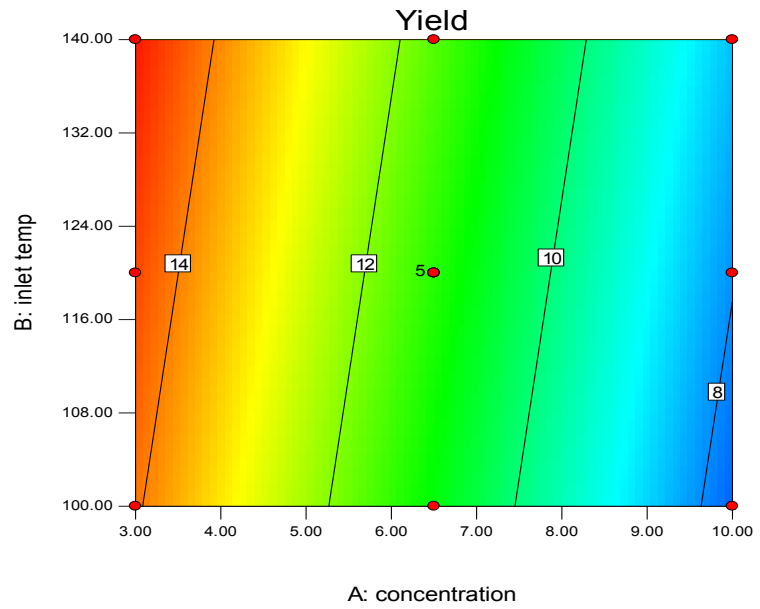
Figure 27 Linear regression plot of %yield and response surface plot of the %moisture content

(a) Linear regression plot of the %yield

(b) Response surface plot of the %moisture content

(a)

Design-Expert® Software  
 Factor Coding: Actual  
 Yield  
 • Design Points  
 15.05  
 6.91  
 X1 = A: concentration  
 X2 = B: inlet temp



(b)

Design-Expert® Software  
 Factor Coding: Actual  
 Moisture content  
 • Design Points  
 8.65  
 5.68  
 X1 = A: concentration  
 X2 = B: inlet temp

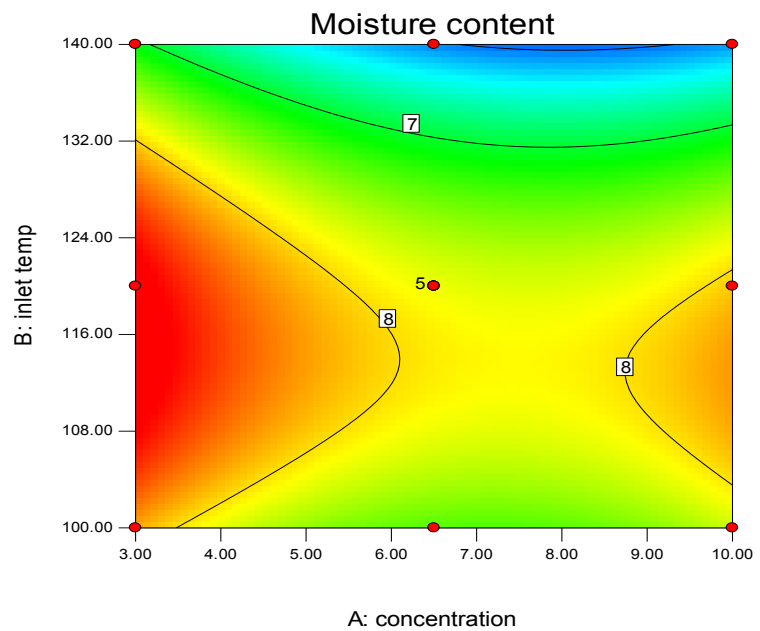
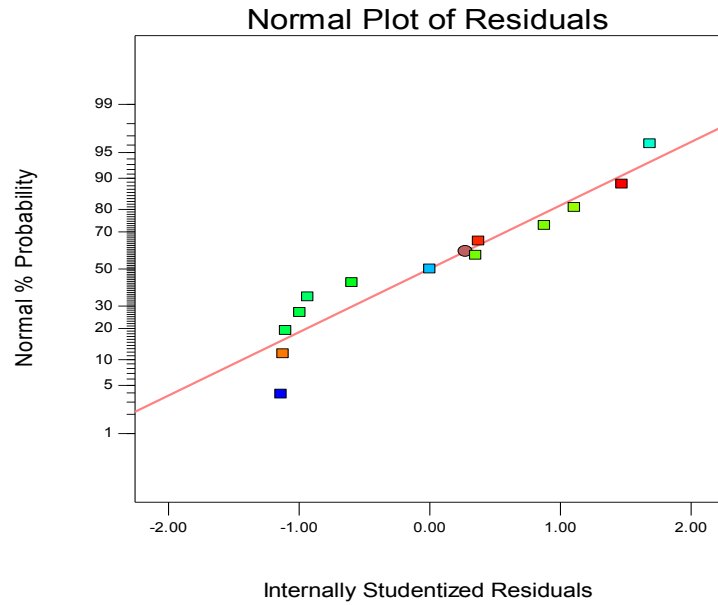


Figure 28 Contour plots of the %yield and %moisture content

(a) The contour plot of the %yield

(b) The contour plot of the %moisture content

(a)

Design-Expert® Software  
YieldColor points by value of  
Yield:  
15.05  
6.91

(b)

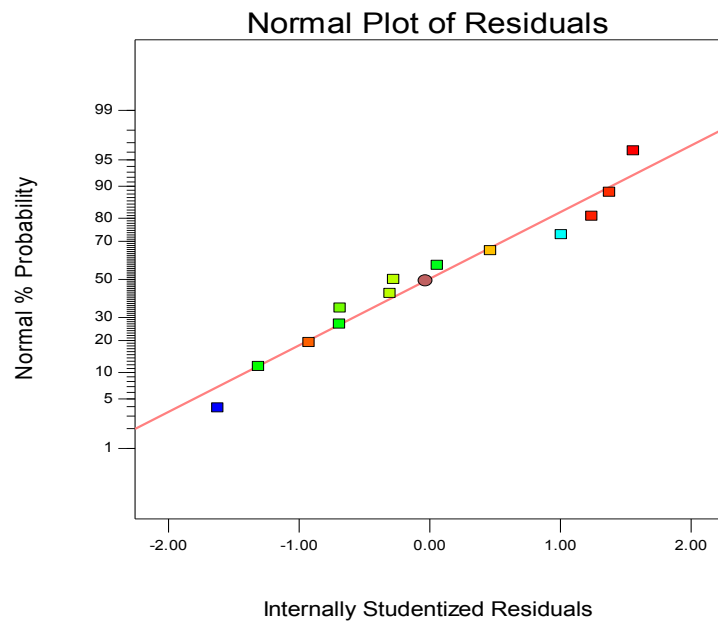
Design-Expert® Software  
Moisture contentColor points by value of  
Moisture content:  
8.65  
5.68

Figure 29 The normal probability plots of the %yield and %moisture content

(a) The normal probability plot of the %yield results

(b) The normal probability plot of the %moisture content results

Based on the two models obtained, a graphical optimization was also conducted using the Design-Expert version 8.0.4 statistical software. Recall, the main objective was the maximization of %yield and the minimization of %moisture content. The selection of conditions to overlay plot ranged from 3-10% and 100-140°C for % and inlet temperature, respectively. The method basically consisted of overlaying the curves of the models according to the criteria imposed that was to increase %yield and decrease %moisture content as much as possible.

By considering the inverse relationship between %yield and %moisture content, the attained overlaying plot displayed a non-shaded area (white area) where both criterias imposed were satisfied (Figure 30). Hence, a point was selected on the graph (marked by the square). This point was assigned as optimal point and corresponded to 140°C of inlet temperature and 4.64% of cocoon concentration. Under such conditions, the model predicted 13.38 %yield (a variation of = 11.19-15.56% being possible) and 6.46 %moisture content (a variation of = 4.83-8.10% being possible) in the confidence range of 95%.

The statistical interpretation of the results concerning both yield and moisture content using the response surface methodology led us to choice of optimal operating condition. These parameters had to maximize yields while reducing moisture contents.

To confirm the result, three batches were produced using the optimal conditions to validate the fabrication process (Table 13).

According to Table 14, the observed means and standard deviations of the responded obtained for yield and moisture content were found to be  $11.64 \pm 0.62\%$  and  $6.38 \pm 0.23\%$ , respectively. They were in range of the prediction intervals at 95% confidence level. From these results, it may be concluded that the model fitted the experimental data well and described the region studied well. Figure 31 displays silk sericin spray dried powder from the optimal spray drying condition, obtained as fine yellow color, and bulky powder.

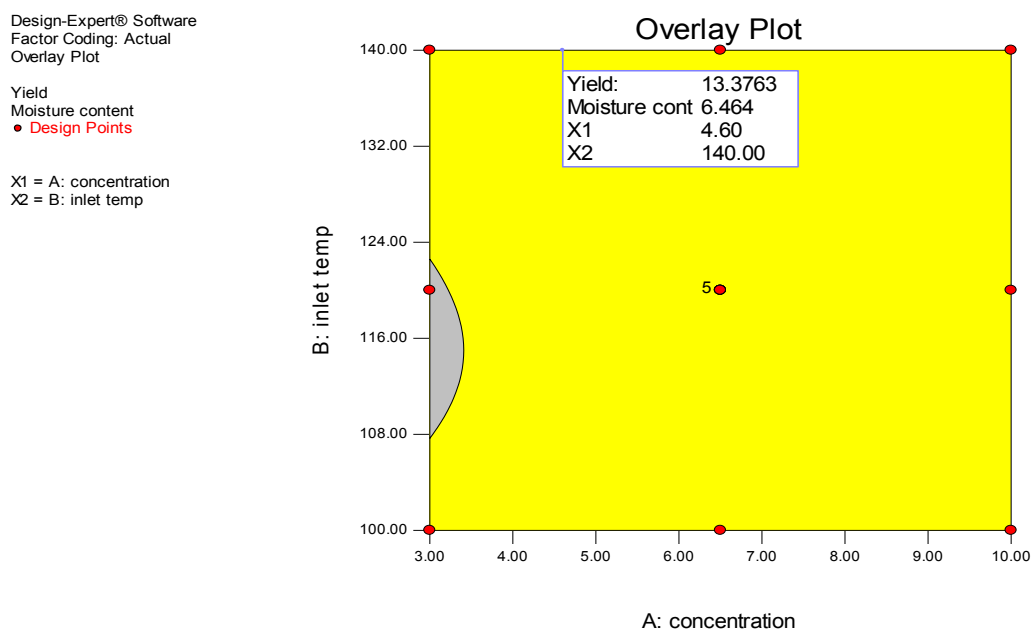


Figure 30 The optimum region by overlay plot of two responses (%yield and %moisture content) evaluated as a function of inlet temperature and %cocoon concentration

Table 13. The optimum region by overlay plot of two parameters and the observed responses

Code	Factor		Responses	
	%Cocoon concentration	Inlet temperature (°C)	%yield	%moisture
1	4.64	140	11.22	6.12
2	4.64	140	11.35	6.44
3	4.64	140	12.347	6.57

Table 14. Observed responses and 95% CI (confidence interval) of optimization spray dried condition

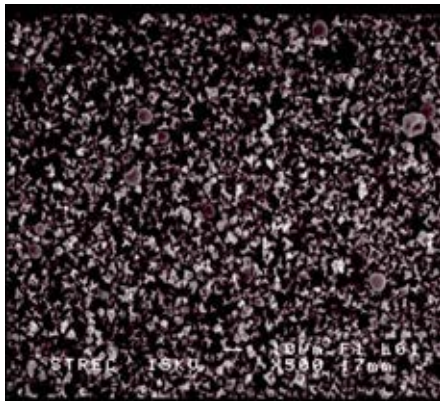
Responses	Values		
	%Observed	%Predicted	95% Confidence intervals
Total yield (%)	11.64±0.62	13.38	11.19-15.56
Moisture content (%)	6.38±0.23	6.46	4.83-8.10



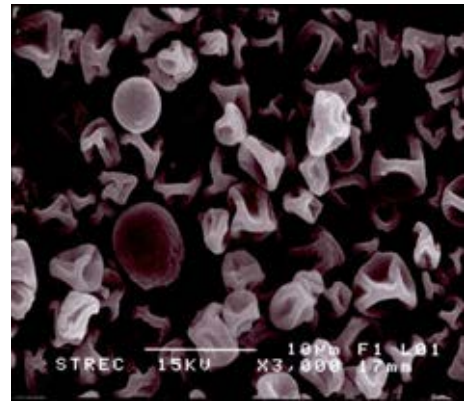
Figure 31 Silk sericin spray dried powder from the optimal spray dried condition

## **2. Morphology of silk sericin spray dried powder**

The shape and surface topography of the silk sericin spray dried particles were found to be affected by the spray drying condition. The observation of size, shape and surface topography were performed by scanning electron microscopy (SEM). Figure 32-34 showed the scanning electron photomicrographs of silk sericin spray dried particles obtained from varied conditions. The particle topography from all conditions were very small spheres, smooth surface and shrunk particles. It was observed that at higher temperature, the shrinkage of particles surfaces was found increased which might be the result of water loss from the drying droplets at the early stage of processing. The size of particles was found smaller when lowered the concentration of the feed solution. These results were consistent with a previous study by Genc, Narin and Bayraktar (2008).

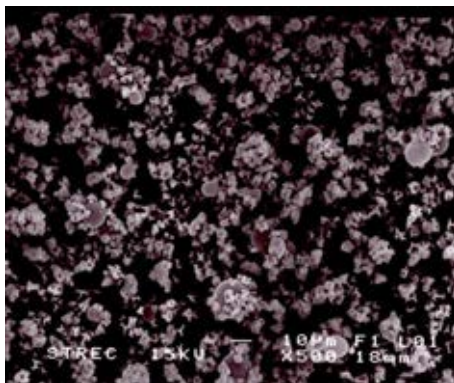


X 500

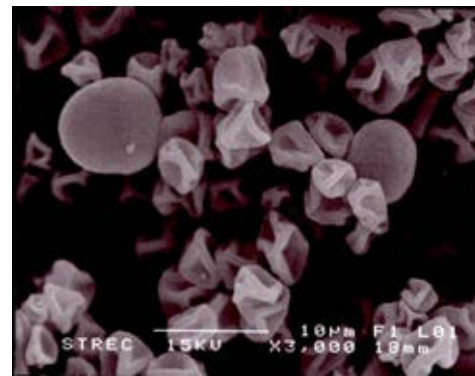


X 3,000

Inlet temperature 100°C

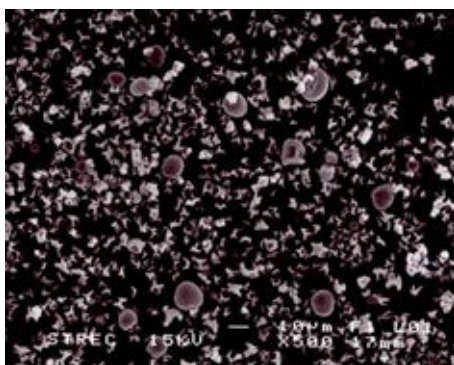


X 500

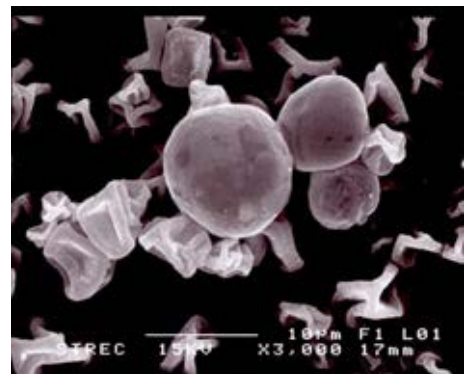


X 3,000

Inlet temperature 120°C



X 500

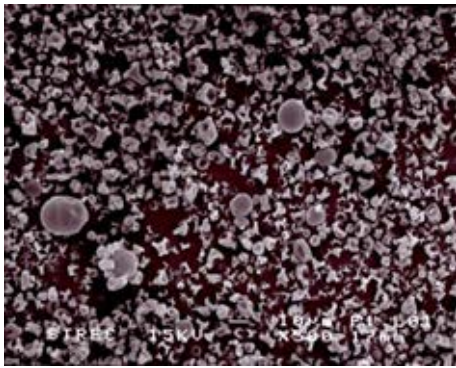


X 3,000

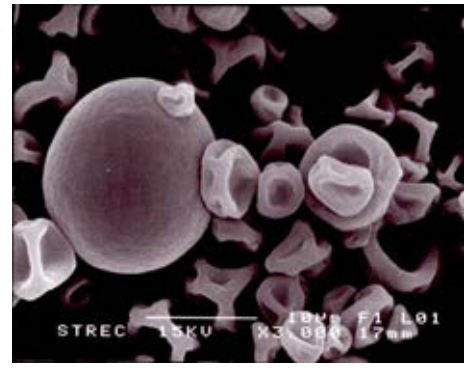
Inlet temperature 140°C

Figure 32 The morphology of particles of spray dried products under 3% cocoon concentration and three levels of inlet temperature, 100, 120 and 140°C.



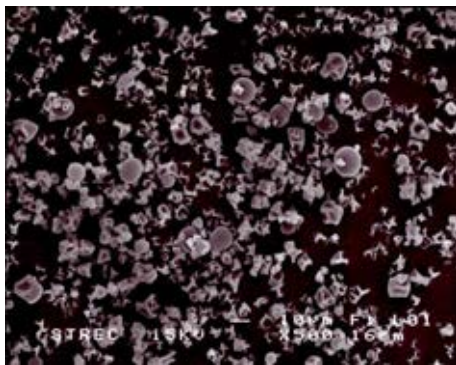


X 500

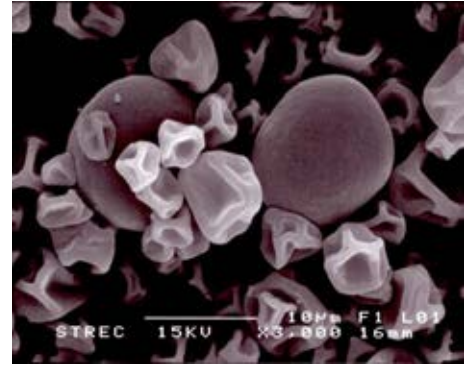


X 3,000

Inlet temperature 100°C

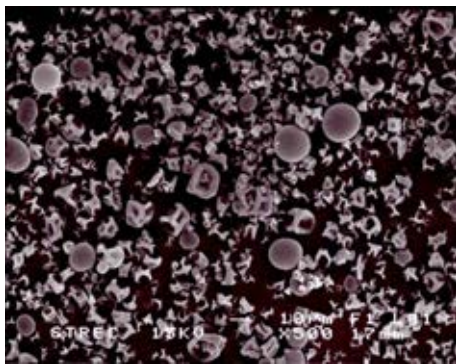


X 500

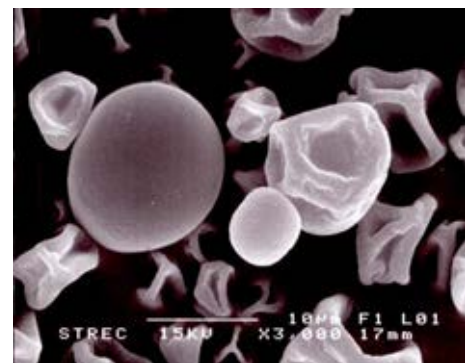


X 3,000

Inlet temperature 120°C



X 500

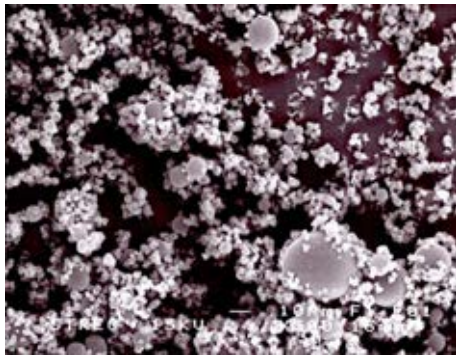


X 3,000

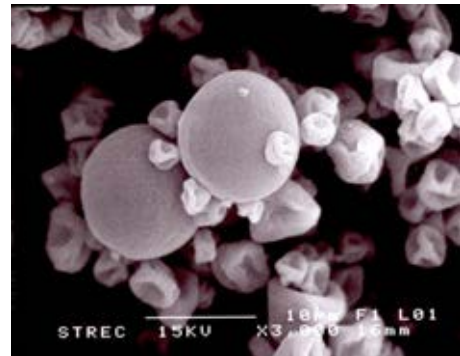
Inlet temperature 140°C

Figure 33 The morphology of particles of spray dried products under 6.5% cocoon concentration and three levels of inlet temperature, 100, 120 and 140°C.



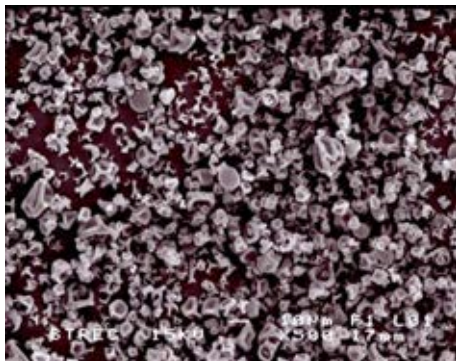


X 500

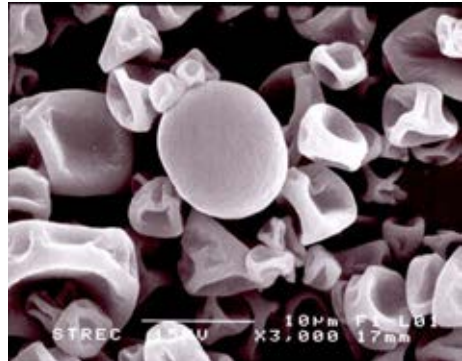


X 3,000

Inlet temperature 100°C

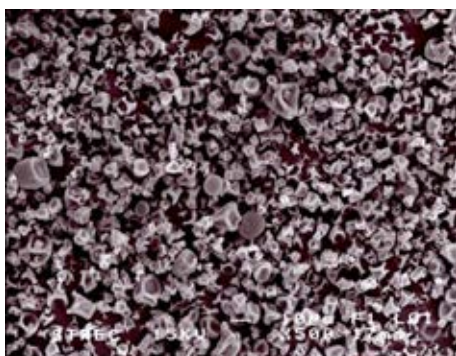


X 500

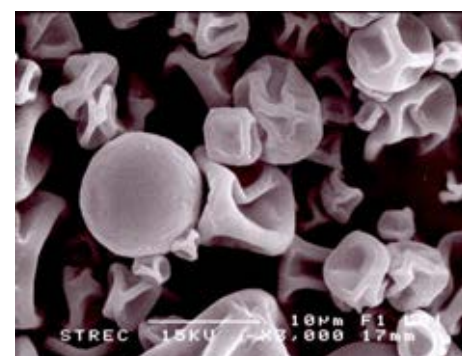


X 3,000

Inlet temperature 120°C



X 500



X 3,000

Inlet temperature 140°C

Figure 34. The morphology of particles of spray dried products under 10% cocoon concentration and three levels of inlet temperature, 100, 120 and 140°C.

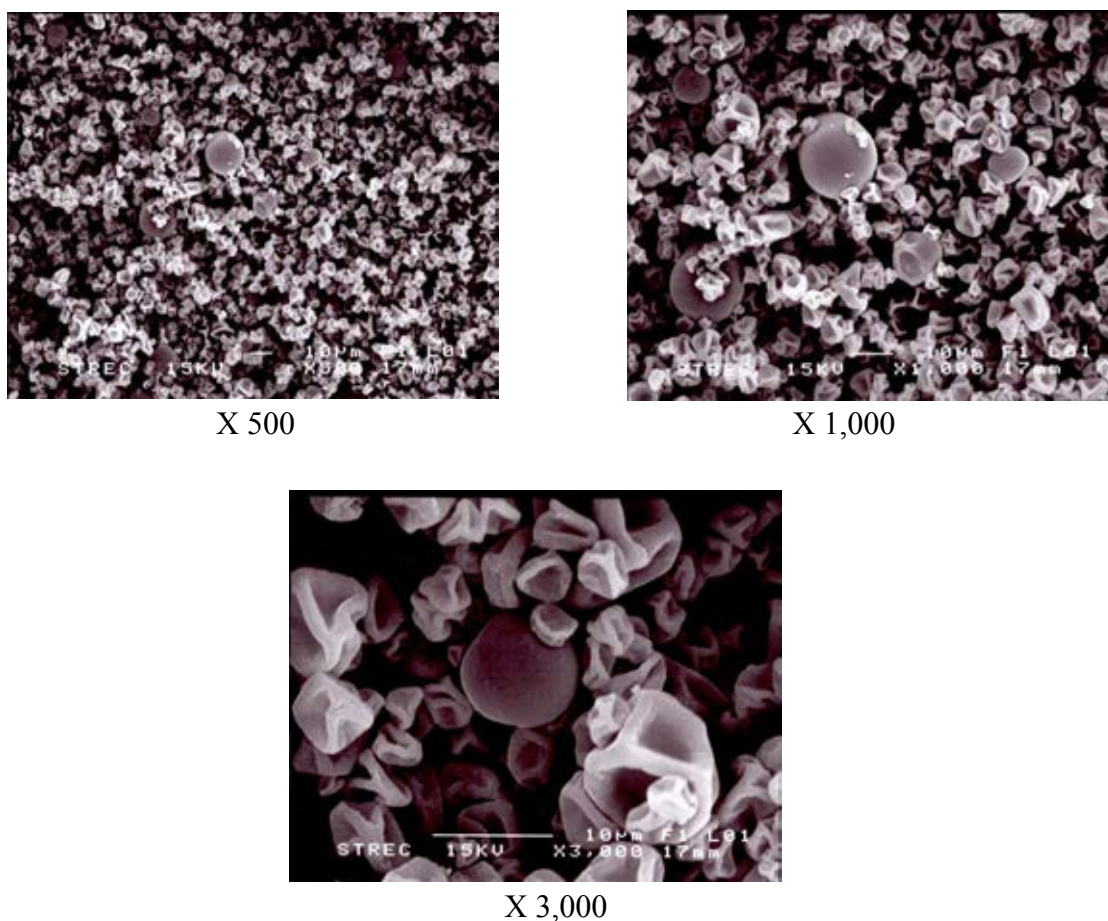


Figure 35 The morphology of particles of spray dried products under 4.6% cocoon concentration and 140°C of inlet temperature (the optimal condition).

### 3. Particle size and size distribution

In this study, the average particle size ( $D_{[4,3]}$ ) and particle size distribution (Span value) of silk sericin spray dried powders prepared from varied conditions were determined and compared. The particle sizes ranged from 6.325 to 9.180  $\mu\text{m}$  and span values ranged from 1.121 to 1.961 (Table 15). It was noticed that the measurement by light scattering method provided the values in the same range as observed from the SEM. As it has been shown, an increase in inlet temperature trended to increase the particle size and an increase of % cocoon concentration also increased the particle size. The correlation between the particle size and the inlet temperature was in

agreement with the previous study that used spray drying as a method of producing silk sericin powder (Genc et al., 2009).

Table 15 The particle size distributions of silk sericin spray dried particles (mean  $\pm$  SD; n=3)

Factor		Average particle size	
%Cocoon concentration	Inlet temperature (°C)	D[4, 3 ] $\pm$ SD ( $\mu\text{m}$ )	Span $\pm$ SD
3	100	7.649 $\pm$ 0.086	1.961 $\pm$ 0.008
3	120	6.325 $\pm$ 0.085	1.651 $\pm$ 0.076
3	140	7.213 $\pm$ 0.226	1.543 $\pm$ 0.040
6.5	100	6.494 $\pm$ 0.108	1.121 $\pm$ 0.068
6.5	120	6.974 $\pm$ 0.106	1.305 $\pm$ 0.065
6.5	140	7.419 $\pm$ 0.274	1.273 $\pm$ 0.024
10	100	7.312 $\pm$ 0.106	1.261 $\pm$ 0.050
10	120	8.353 $\pm$ 0.281	1.345 $\pm$ 0.100
10	140	9.180 $\pm$ 0.035	1.392 $\pm$ 0.001
4.6	140	7.114 $\pm$ 0.299	1.317 $\pm$ 0.033

Optimization of the spray drying process for Thai silk sericin powder by a face-centered composite design resulted a linear equation of %yield and a second-order quadratic equation of %moisture content. The optimal silk sericin spray-dried powders obtained have 11.64 $\pm$ 0.62% yield and 6.38 $\pm$ 0.23% moisture contents, where were in the predicted rang by the optimization at 95% interval.

### **C. DETERMINATION OF PHYSICOCHEMICAL AND BIOLOGICAL ACTIVITIES OF SILK SERICIN POWDER (FROM THE OPTIMIZED CONDITION)**

The silk sericin spray-dried powder prepared from the optimized condition was fine bulky yellow powders. The particle topography were spherical particles with smooth shrinking surfaces (Figure 35). The particle sizes were  $7.114 \pm 0.299 \mu\text{m}$  with span value of  $1.317 \pm 0.033$ . The amount of protein of silk sericin was found to be  $21.83 \pm 1.71\%$ . The molecular weight of silk sericin spray-dried powder from optimization was shown in Figures 19-20. The main molecular weight distribution ranged between 75-250 kDa.

#### **1. Differential scanning calorimetric thermograms**

The DSC thermogram of silk sericin spray-dried powders is shown in Figure 36. The thermograms of silk sericin powders demonstrated a sharp endothermic peak at about 145-148 °C and a small board peak at about 240 °C. As reported by Lee et al (2003) sericin showed a water evaporation peak around 100°C and board peaks around 216 and 313 °C due to thermal degradation of sericin. They explained that aggregation of protein polymers accompanied conformation changes, the conformation of sericin in solution was changed from random coil to  $\beta$ -sheet structure by dehydration process. Similar results were reported from the preparation of freeze-dried particles of silk sericin (Lee et al., 2003; Tao, Li, and Xie, 2005). Drummy et al (2005) have also reported that the structure of thin films cast from solutions of *Bombyx mori* cocoon silk occurred thermally induced to  $\beta$ -sheet structure at a temperature of approximately 140 °C. Many investigations reported that spray drying or freeze drying process promoted the appearance of silk sericin powders and might be generated amorphous form. However, in this study, it was surprising that the endothermic peak at about 145-148 °C did not consist to water evaporation. It was thermally induced to  $\beta$ -sheet structure.

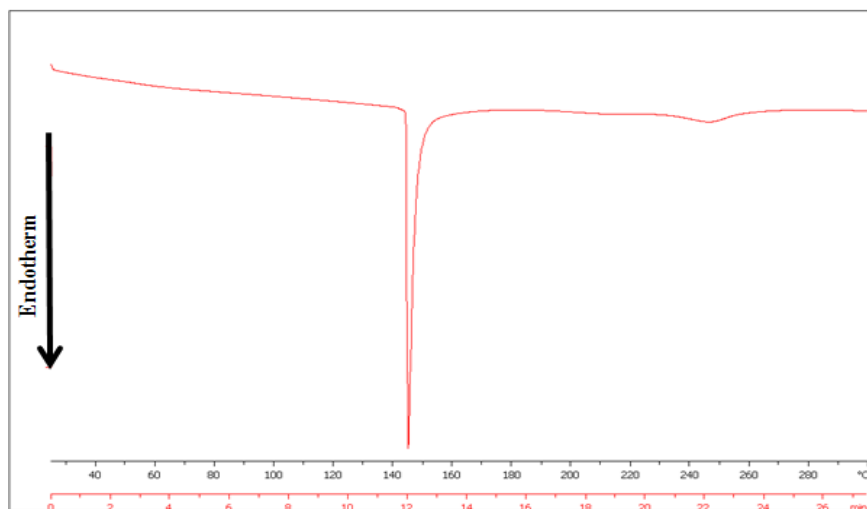


Figure 36 DSC thermogram of optimized silk sericin spray-dried powder.

## 2. Powder X-ray diffraction

Powder X-ray diffractometry may be used to detect crystallinity in the solid state. Figure 37 shows the x-ray diffractogram of silk sericin spray-dried powder. It presented an absence of intense diffraction peak, that revealed that silk sericin powder existed in an amorphous state. This was in agreement with many previous studies (Lee et al., 2003; Tao, Li, and Xie, 2005) that producing silk sericin powder by spray drying resulted to silk sericin in amorphous form.

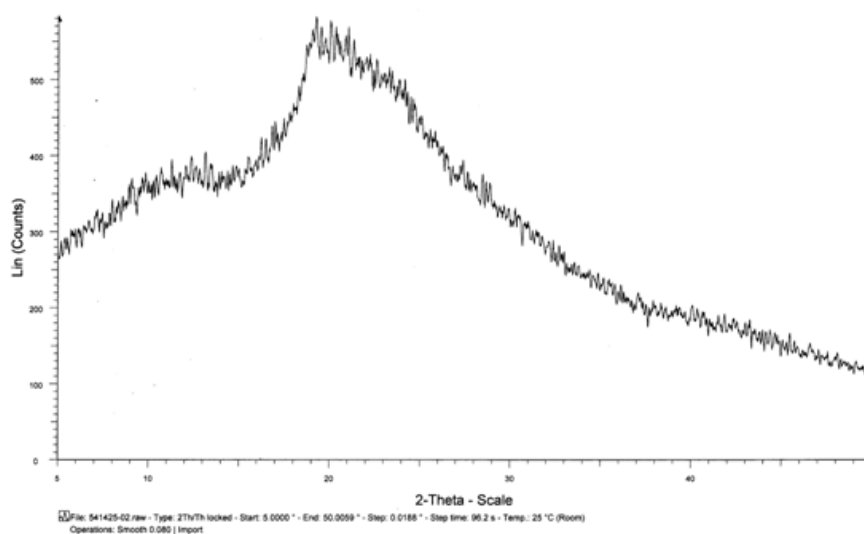


Figure 37 X-ray diffractograms of silk sericin spray-dried powder (optimization).

### 3. Anti-oxidant activities of silk sericin

#### 3.1 DPPH Free radical scavenging activity assay

The EC<sub>50</sub> (mg/mL) values of free radical scavenging activity of silk sericin from Nangnoi-Sisaket 1 by optimization was 0.82 mg/mL (Figure 38). Wu et al. (2007) reported that the 50% scavenging activity by DPPH assay of silk sericin prepared from silk industry wastewater was 31 mg/mL. Manosroi et al. (2010) have also reported that the 50% scavenging activity by DPPH assay of silk sericin from Nangnoi by autoclaving method was 32.33 mg/mL.

Recently, antioxidant activity index (AAI) was found to be appropriate to compare the antioxidant strength of plant extracts. The AAI calculated as follows:  $AAI = \text{final DPPH}^{\bullet} \text{ concentration } (\mu\text{g/mL}) / EC_{50} (\mu\text{g/mL})$  (Scherer and Godoy, 2009). In this study, the AAI values of silk sericin from some investigation were calculated for comparison. The AAI values of silk sericin powder from this study, from Wu et al (2007), and from Manosroi et al (2010) were 0.035, 0.001 and 0.010, respectively. This result showed that silk sericin from this study had higher free radical scavenging activity than silk sericin from Wu et al. (2007) and Manosroi et al. (2010). However, due to the low AAI value (AAI value < 0.5), it might say that silk sericin did not present a potential antioxidant activity.

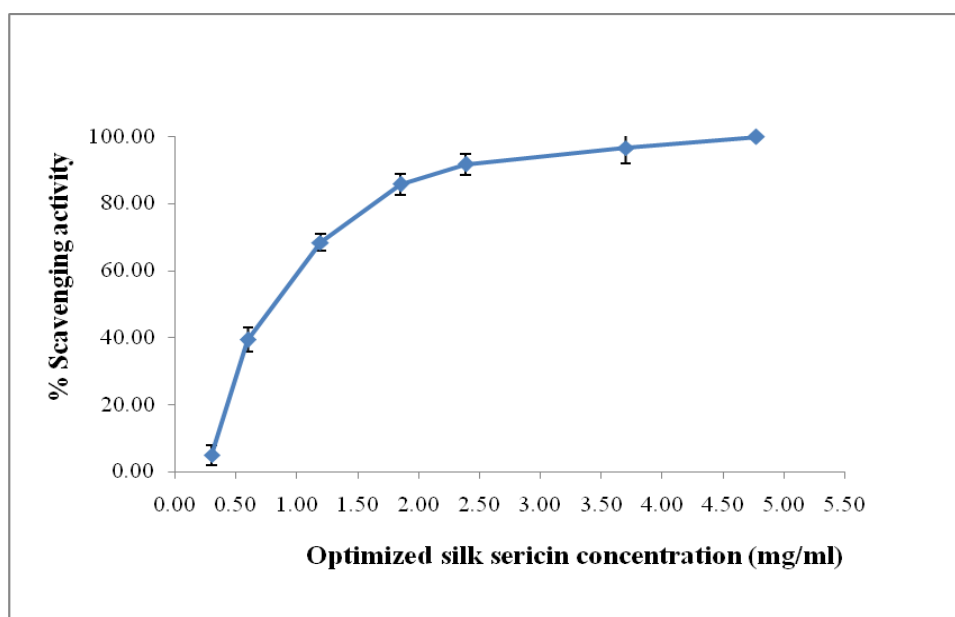


Figure 38 DPPH scavenging activity of silk sericin (optimization) (n=3).



### 3.2 Superoxide radical scavenging assay

The EC<sub>50</sub> (mg/mL) values of superoxide radical scavenging activity of silk sericin from Nangnoi-Sisaket 1 by optimization was 0.43 mg/ml (Figure 39). Fan et al. (2009) reported that silk sericin showed not only DPPH radical scavenging activity, but also many antioxidant activities, such as hydroxyl radical and superoxide radical scavenging, lipid peroxidation of linoleic acid, reducing power, and ferrous ion chelating activity.

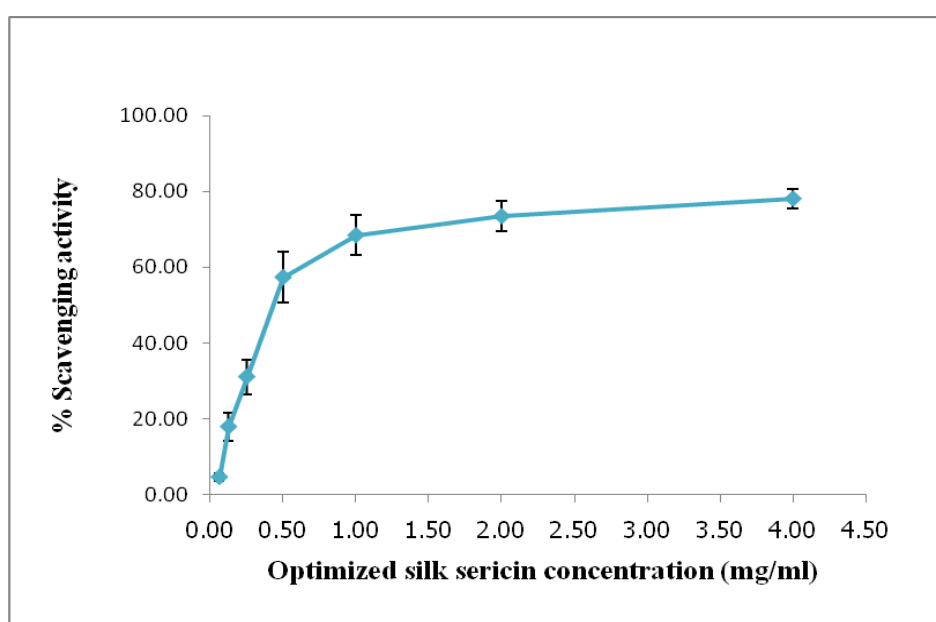


Figure 39 Superoxide radical scavenging activity of silk sericin (optimization) (n=3).

### 4. Anti-tyrosinase activity

The EC<sub>50</sub> (mg/ml) values for the inhibition of mushroom tyrosinase activity by silk sericin prepared from Nangnoi-Sisaket 1 by optimization condition was 0.40 mg/mL (Figure 40). In this study, the standard alpha-arbutin and kojic acid gave the EC<sub>50</sub> values of, 0.21±0.03 and 0.005±0.000 mg/mL, respectively. This indicated that the optimized silk sericin was non-significantly different from standard alpha-arbutin and kojic acid ( $p > 0.05$ ).

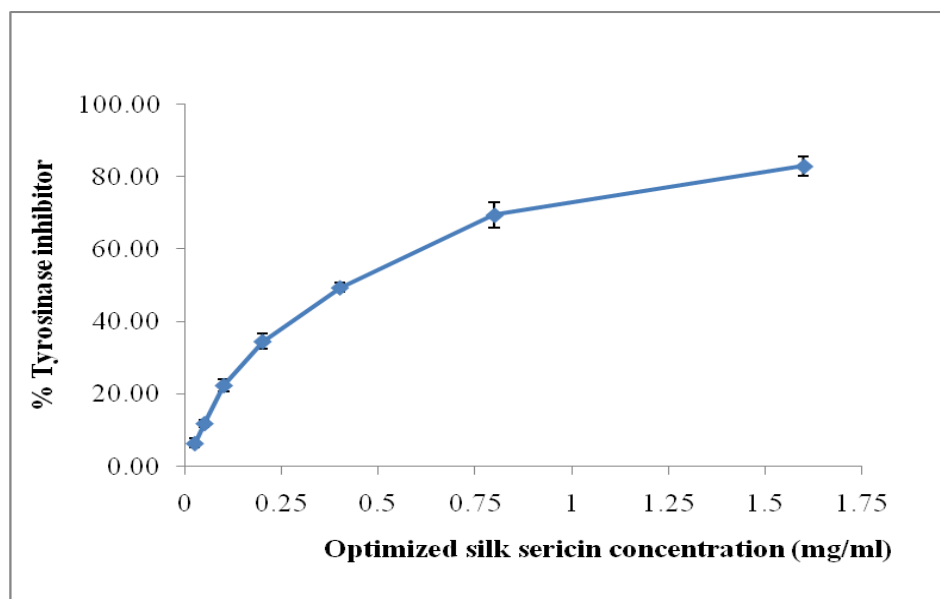


Figure 40 Anti-tyrosinase activity of optimized silk sericin (n=3).



## **D. PREPARATION AND EVALUATION OF NIOSOMES VERIFIED IN COMPOSITIONS**

### **1. Preparation of niosomes**

In this study, niosomes were prepared by reverse-phase evaporation methods (New, 1990; Puangmalai, 2007; Torchilin and Weissig, 2003) because the highest skin penetrating and bioactive carrying capability is frequently associated with such nanoparticles. Further, this preparation method is also associated with relatively higher encapsulation efficiency of macromolecules such as antigens and peptides (Gupta et al., 2005; New, 1990). Conditions for forming w/o emulsion were the ratio of oil in solvent to aqueous phase at 3:1 and sonication time 10 min in the bath sonicator. Evaporation conditions were 60 °C, 450 mbar for 10 min. After w/o emulsion was evaporated about 5 min, it would dry down to be gel attached to the round bottom glass. Gel collapse would be occurred about 10 min after starting evaporation. The vesicles occurred when water was added to hydrate them. It might occur because the concentration of lipid employed was increased, it should be add water at the gel state (New, 1990). Afterthat, reduced pressure evaporation was done to remove trace of solvent and further size reduction was done by sonication for 60 min. It was found that niosome formulations at 100 mM of lipid concentration and 1:1 ratio of surfactant:cholesterol could be successfully prepared. The varied four niosome formulations with silk sericin loaded could be prepared, and showed bilayer vesicles under cross light polarization microscopy in Figure 41.

After gel collapsed, it was hydrated at the same temperature without reducing pressure for 150 min. Sericin could be entrapped in the niosomes. The conditions of preparation of niosomes were crucial for characteristic of vesicles. The reproducibility of vesicles would be another topic, which should be examined. The study of reproducibility of niosomes was done triplicate in each niosome formulation that prepared by Span<sup>®</sup>20, Span<sup>®</sup>40, Span<sup>®</sup>60, and Span<sup>®</sup>80 without sericin loading. The niosomes formulations at 100 mM of lipid concentration were determined of their sizes by photon correlation spectroscopy. It was found that vesicular sizes of three batches were 246.87±14.85, 181.20±13.45, 183.87±3.11, and 341.17±35.69 nm,

respectively. This finding demonstrated the good reproducibility of formulation and the preparation method.

## 2. Evaluation of niosomes

This study investigated the effect of formulation, that was type of surfactant. All formulations were investigated in many properties that the results were shown as follows:

### 2.5 Microscopic appearances

Physical examination by light microscopy of all vesicles revealed that they were smaller than 1  $\mu\text{m}$  diameter, thus vesicles could not depict the accurate sizes. Assembly of non-ionic surfactants to form bilayer vesicles was characterized by X-cross light polarization microscopy. Figure 41 shows the bilayer vesicles of niosomes loaded with silk sericin.

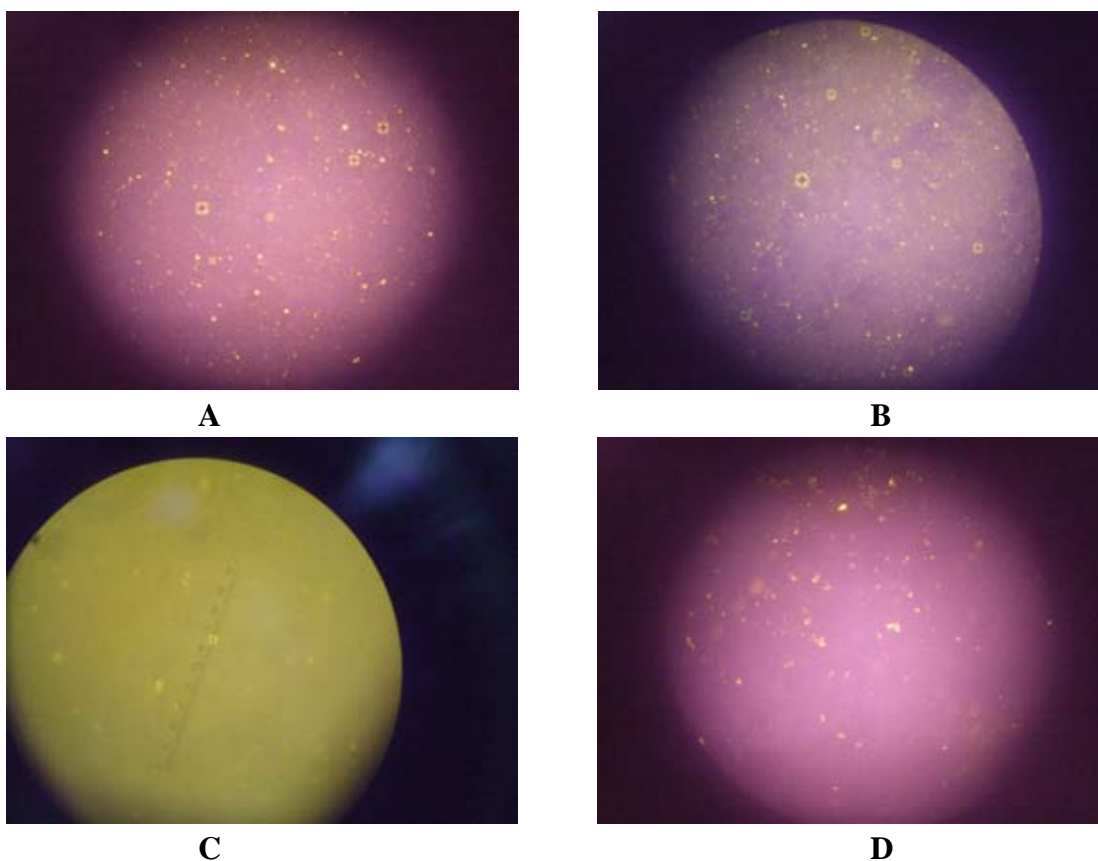


Figure 41 X-cross bilayer formation of niosomes loaded silk sericin by X-cross light polarization microscopy with magnification 10X100. Silk sericin loaded in niosome prepared by Span<sup>®</sup>20 (A), Span<sup>®</sup>40 (B), Span<sup>®</sup>60 (C), and Span<sup>®</sup>80 (D).

## 2.6 Particle size and size distribution

The particle size determined by photon correlation spectroscopy of noisome and silk sericin loaded niosomes using Span<sup>®</sup>20, Span<sup>®</sup>40, Span<sup>®</sup>60, and Span<sup>®</sup>80 as surfactant are shown in Table 16. The mean diameter of all preparations of blank niosomes and silk sericin loaded niosomes were in nanometer range as 181.20-341.17 and 217.67-397.44 nm, respectively. The size distributions as indicated by polydispersity index were between 0.248-0.494 and 0.391-0.494. The particle sizes of all loaded niosomes with silk sericin were larger than their corresponding blank niosomes. The aqueous solution of silk sericin was presumed to be entrapped inside the niosomes and interaction with lipid membrane that resulted in the enlargement of the vesicular size (Gupta et al., 2005).

The results showed that size of vesicles were influenced by type of surfactant. The vesicle size of the formulation that composed of Span<sup>®</sup>80 was larger than those of the formulations that composed of Span<sup>®</sup>20, Span<sup>®</sup>40 and Span<sup>®</sup>60. The ranking of sizes from varied types of surfactant might be as follows: Span<sup>®</sup>80 > Span<sup>®</sup>20 > Span<sup>®</sup>60 > Span<sup>®</sup>40. The vesicle size of the formulations might be related to the nature of alkyl chain of surfactant. Span<sup>®</sup>80 has a long (C18) unsaturated alkyl chain that is different from Span<sup>®</sup>20, Span<sup>®</sup>40 and Span<sup>®</sup>60 which have saturated alkyl chain. This was consistent to the previous report by Singh, Jain and Kumar, (2011) that the niosomes prepared using Span<sup>®</sup>80 were larger in size than niosomes prepared using Span<sup>®</sup>40. Span 80 had a long (C18) unsaturated alkyl chain whereas Span 20, Span 40 and Span 60 which had saturated alkyl chains with C12, C16 and C18, respectively. The corresponding HLB values of surfactants: Span<sup>®</sup>20, Span<sup>®</sup>40 and Span<sup>®</sup>60 are 8.6, 6.7 and 4.7, respectively. The mean size of the niosomes increased with progressive increase in the HLB value or surfactant hydrophilicity from Span<sup>®</sup>60 (HLB 4.7) and Span<sup>®</sup>40 (HLB 6.7) to Span<sup>®</sup>20 (8.6) because surface free energy decrease on increasing hydrophobicity of surfactant (Khazaeli and Pardakhty, 2007; Ruckmani, Jayakar and Ghosal, 2000).

The results (Table 16) showed that polydispersity indices of the formulation were rather high. This might be due to in the stage of adding water phase

for hydrating vesicles, the higher lipid phase was hardly completely hydrated. Thus the heterogeneous size might occur during hydrating the vesicles.

The results showed that polydispersity indices of the formulation were rather high. This might be due to in the stage of adding water phase for hydrating vesicles, the higher lipid phase was hardly completely hydrated. Thus the heterogeneous size might occur during hydrating the vesicles.

Table 16 Particle sizes and polydispersity index (mean $\pm$ SD) of silk sericin loaded niosome formulations under storage in refrigerator (4 °C) (n=3).

Formulation	Blank niosomes		Silk sericin loaded in niosomes	
	Size (nm)	Pdi	Size (nm)	Pdi
<b>Span<sup>®</sup> 20</b>	246.87 $\pm$ 14.85	0.307 $\pm$ 0.233	250.64 $\pm$ 67.50	0.428 $\pm$ 0.213
<b>Span<sup>®</sup> 40</b>	181.20 $\pm$ 13.45	0.273 $\pm$ 0.05	217.67 $\pm$ 32.99	0.391 $\pm$ 0.042
<b>Span<sup>®</sup> 60</b>	183.87 $\pm$ 3.11	0.248 $\pm$ 0.025	252.07 $\pm$ 23.40	0.440 $\pm$ 0.085
<b>Span<sup>®</sup> 80</b>	341.17 $\pm$ 35.69	0.494 $\pm$ 0.114	397.44 $\pm$ 88.42	0.494 $\pm$ 0.149

## 2.7 Transmission electron microscopy (TEM)

The results showed that TEM could visualize the images of niosomes. All formulations appeared spherical shaped. No agglomerated vesicles was not observed. It was noticed that approximate size of silk sericin loaded niosomes prepared by Span<sup>®</sup>20, Span<sup>®</sup>40, Span<sup>®</sup>60, and Span<sup>®</sup>80 were close to the size determined by photon correlation spectroscopy. Figure 42 showed the electron micrograph of all silk sericin loaded niosome formulations.

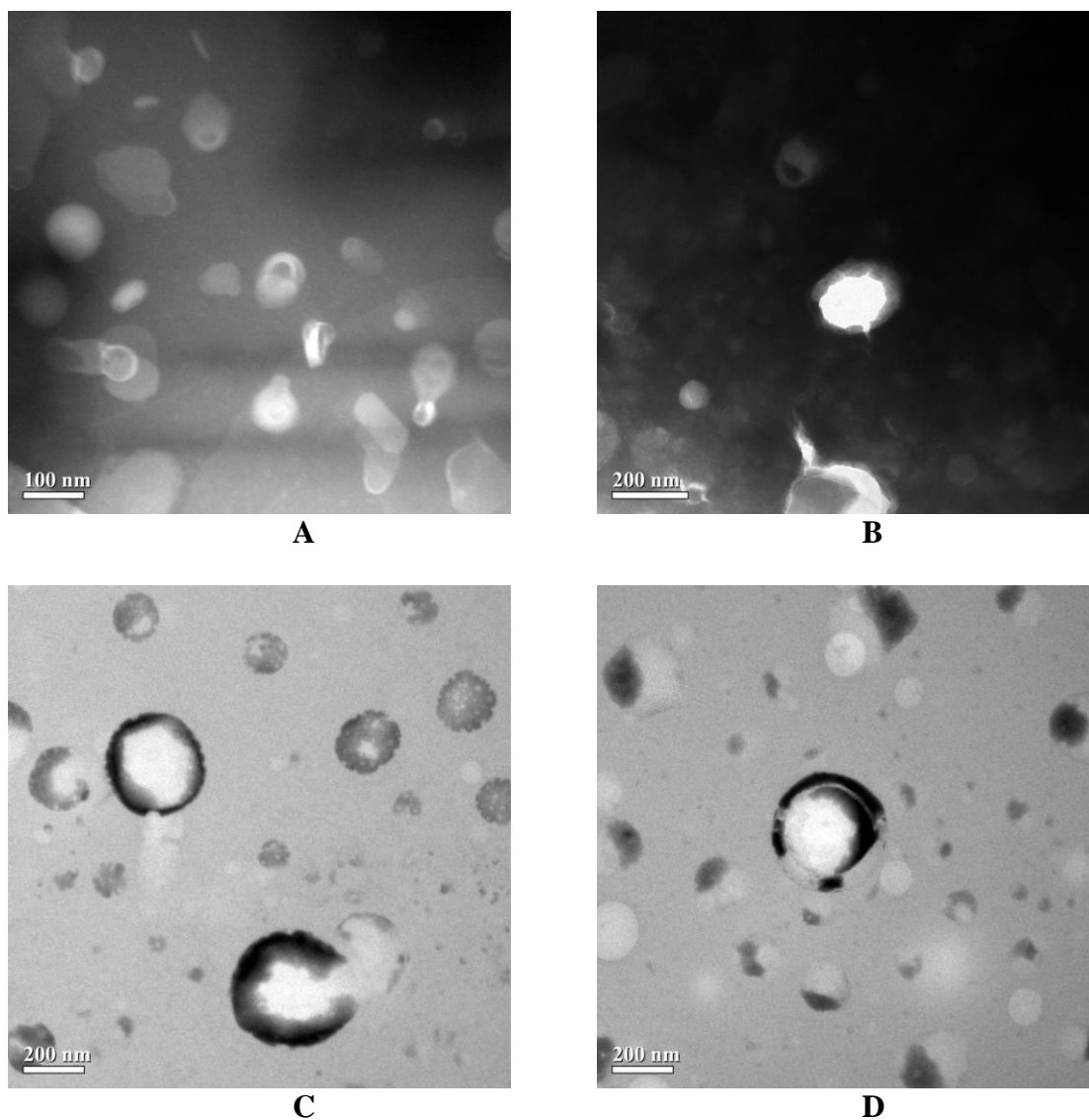


Figure 42 Transmission electron microscope (TEM) photomicrograph of silk sericin loaded niosomes prepared by Span<sup>®</sup>20 (A), Span<sup>®</sup>40 (B), Span<sup>®</sup>60 (C), and Span<sup>®</sup>80 (D).

### 2.8 Entrapment efficiency

The entrapment efficiencies of all silk sericin loaded niosomes formulations were in range 84.22-93.88% (Table 17). The results showed that the preparation by reverse phase evaporation gave high entrapment efficiency of silk sericin. The finding was consistent with previous studies that claimed for higher encapsulation efficiency of macromolecules such as antigens and peptides by the same method (New, 1990; Gupta et al., 2005; Puangmalai, 2007).

Type of surfactants influences encapsulation and stability of niosomes. Span series surfactants, a HLB number of between 4 and 8 was found to be compatible with vesicle formation (Uchegbu and Vyas, 1998; Biswal et al., 2008). The effect of type of surfactant on entrapment efficiency was evaluated. The result showed the formulation that composed of Span<sup>®</sup>60 had entrapment efficiency higher than the formulations that composed of Span<sup>®</sup>80, Span<sup>®</sup>20 and Span<sup>®</sup>40. One possible explanation to the result might involve the chemical structure of niosomes. Span series surfactants have the same hydrophilic head group but alkyl chain in different lengths. Span<sup>®</sup>20, Span<sup>®</sup>40 and Span<sup>®</sup>60 are monolaurate (C12), monopalmitate (C16) and monostearate (C18), respectively. Whereas Span<sup>®</sup>80 is monooleate (C18) with unsaturated double bonds. Several studies reported that increase of the alkyl chain length led to a higher entrapment efficiency, and Span<sup>®</sup>60 (C18) vesicles show higher entrapment efficiency of hydrophilic drugs than Span<sup>®</sup>20 (C12) and Span<sup>®</sup>40 (C16) vesicles which the length of alkyl chain is a crucial factor that should be considered in niosomes system with high efficiency (Uchegbu and Vyas, 1998; Manosroi et al., 2003). Whereas, Span<sup>®</sup>60 and Span<sup>®</sup>80 have the same head groups and same length of alkyl chain but Span<sup>®</sup>80 has an unsaturated double bonds that caused a marked explaining the lower entrapment than Span<sup>®</sup>60.

After statistic analysis with one-way ANOVA and Turkey's Honesty Significant Difference test at 5% significant level, there were significant differences between varied compositions of niosomes as dispersion in Table C2 (Appendix C). The silk sericin loaded in niosomes prepared from Span<sup>®</sup>60 had significantly higher entrapment efficiency ( $P < 0.05$ ). This result was similar to Guinedi et al (2005) that entrapment efficiency of acetazolamide that composed of Span<sup>®</sup>60 had higher entrapment efficiency than the formulation that composed of Span<sup>®</sup>40. This can be explained by many facts: Span<sup>®</sup>60 has the highest phase transition temperature. The length of alkyl chain of surfactant is a crucial factor in permeability that long chain surfactant produces high entrapment. Span<sup>®</sup>60 has a longer saturated alkyl chain (C18) composed to Span<sup>®</sup>40 (C16) or Span<sup>®</sup>20 (C12), so it produces niosomes with higher entrapment efficiency. The longer alkyl chain influences the HLB values of the surfactant mixture which by it turn directly influences the drug entrapment efficiency.

The lower the HLB of the surfactant the higher will be the drug entrapment efficiency and stability as in the case of niosomes prepared from Span<sup>®</sup>60.

Table 17 Entrapment efficiency of silk sericin loaded niosome when storage in refrigerator (4 °C) for 8 weeks.

Type of surfactant in formulations	%EE (mean ± SD)				
	Day 0	Week 1	Week 2	Week 4	Week 8
Span <sup>®</sup> 20	84.46±1.15	81.35±2.58	83.01±2.57	78.52±2.32	76.48±2.53*
Span <sup>®</sup> 40	84.22±2.02	84.33±3.47	81.68±3.29	81.58±3.05	83.55±0.55
Span <sup>®</sup> 60	93.88±1.78	94.10±1.33	90.87±2.71	90.56±2.56	88.32±2.86
Span <sup>®</sup> 80	89.66±0.36	80.29±6.85	72.06±11.05	71.71±7.36	69.34±2.83*

\* Significant at *P value* = 0.05

### 2.9 Physical and chemical stabilities of silk sericin loaded niosomes

For physical stability study, particle size analysis and the leaching of silk sericin from formulations of developed formulations was monitoring during 8 weeks under storage in refrigerator (4 °C).

The particle size and polydispersity index of silk sericin loaded in niosome formulations are illustrated in Table 18. The results showed that the vesicle sizes of nearly all formulations had no appreciable change (Figure 43). This could be due to decreased mobility of the bilayer at low temperature, thus offering no change of particle size. It might be seen that nearly all niosome formulations were rather physical stable at refrigerator temperature during the period study.

Unfortunately, the fluctuations of the particle size was noted, thus the conclusion can be hardly stated. It might occur from the variation during sampling for determining the particle size by photon correlation spectroscopy.

Table 18 Particle size\* and polydispersity index\* of silk sericin loaded niosome formulations under storage in refrigerator (4 °C) for 8 weeks.

Formulation	Day 0		Week 1		Week 2		Week 4		Week 8	
	Size (nm)	Pdi	Size (nm)	Pdi	Size (nm)	Pdi	Size (nm)	Pdi	Size (nm)	Pdi
<b>Span®20</b>	250.6 (67.5)	0.428 (0.213)	224.5 (8.7)	0.352 (0.018)	307.1 (2.6)	0.45 (0.02)	279.2 (31.0)	0.464 (0.071)	225.7 (10.2)	0.359 (0.062)
<b>Span®40</b>	217.7 (33.0)	0.391 (0.042)	232.2 (7.9)	0.400 (0.036)	391.7 (82.5)	0.60 (0.08)	332.4 (40.4)	0.482 (0.069)	330.4 (23.3)	0.532 (0.062)
<b>Span®60</b>	252.1 (23.4)	0.440 (0.085)	225.2 (5.4)	0.351 (0.012)	280.1 (17.4)	0.42 (0.04)	322.2 (10.2)	0.479 (0.034)	304.7 (5.4)	0.436 (0.027)
<b>Span®80</b>	397.4 (88.4)	0.494 (0.149)	297.5 (27.9)	0.535 (0.047)	365.0 (15.5)	0.60 (0.08)	420.5 (20.0)	0.577 (0.022)	390.6 (58.5)	0.512 (0.018)

\*Mean of nine measurements (SD)

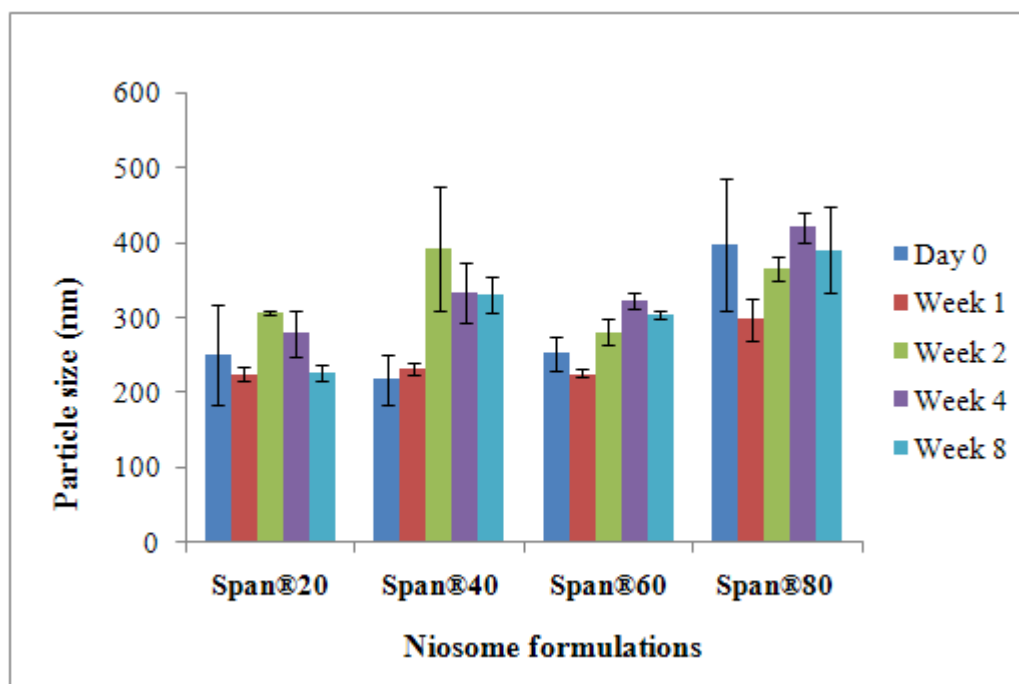


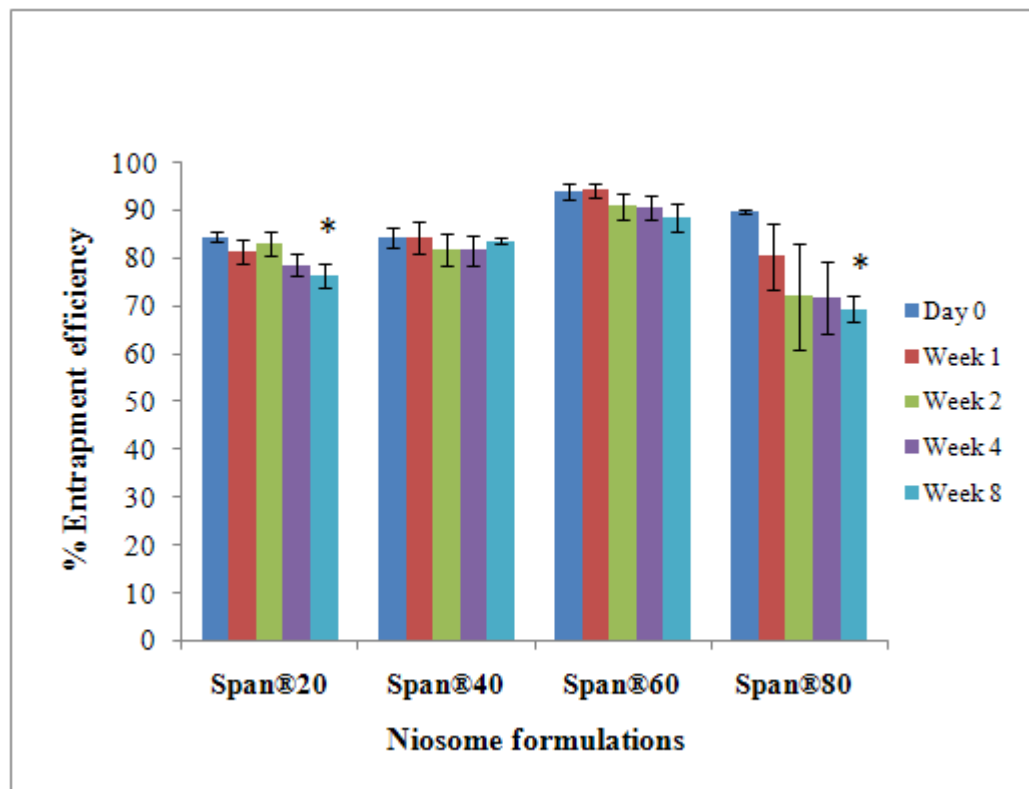
Figure 43 Plots of particle size of silk sericin loaded niosome formulations under storage in refrigerator (4 °C) for 8 weeks.



The leakage study of niosome formulations, which correlated with the ability of entrapment of silk sericin. The leakage assumed from the ability of retaining the entrapped silk sericin. The leakage of entrapped silk sericin might be due to the degradation of the niosomal bilayers. The degradation of surfactants in the bilayers resulting in defects in membrane packing making them leaky (Agarwal, Katare and Vyas, 2001). The percentages entrapment efficiencies were monitored at refrigerator (4 °C) for 8 weeks. The entrapment efficiency data are shown in Table 17 and Figure 44.

The percentage entrapment efficiency of all formulations decreased with an increasing storage duration. The decrease of entrapment efficiency were ranged from 0.67-20.32. After statistic analysis with one-way ANOVA and Turkey's Honesty Significant Difference test at 5% significant level, there were significant differences between time for storage for 8 weeks condition as dispersion in Table 17. The formulation composed of Span<sup>®</sup>20 and Span<sup>®</sup>80 showed a significant decrease of entrapment efficiency at 8 weeks ( $p < 0.5$ ) from initial time. However, the results indicate that all of formulations showed no significant decrease of entrapment efficiency at 4 weeks. Similar results were obtained by Shahiwala and Misra (2002) and Ruckmani et al. (2002).

The leakage of vesicles might be due to phase transition temperature of surfactant. The phase transition temperature of the vesicle systems indicated the thermodynamic state of the bilayers. Molecule of Span<sup>®</sup>80 ( $T_c = -12$  °C) are in the liquid crystalline state, whereas molecules of Span<sup>®</sup>20 ( $T_c = 16$  °C), Span<sup>®</sup>40 ( $T_c = 42$  °C) and Span<sup>®</sup>60 ( $T_c = 53$  °C) are in the ordered gel state, which the hydrocarbon chain are fully extended and closely packed. This would make the niosomal membrane more rigid and resisting to drug leakage (Suwakul et al., 2006). Therefore, the formulations that composed of Span<sup>®</sup>20, Span<sup>®</sup>40 and Span<sup>®</sup>60 had more stability than the formulations that composed of Span<sup>®</sup>80, which has double bond making the packing membrane as close as saturated alkyl chain.



\* Significant at  $P$  value = 0.05

Figure 44 %Entrapment efficiency of silk sericin loaded niosome formulations under storage in refrigerator (4 °C) for 8 weeks.

### E. DETERMINATION OF BIOLOGICAL ACTIVITIES OF NIOSOMES LOADED WITH SERICIN

Niosomes loaded with 1% silk sericin that composed of Span<sup>®</sup>20, Span<sup>®</sup>40, Span<sup>®</sup>60 and Span<sup>®</sup>80 were evaluated for their biological activities. Superoxide radical scavenging activity and anti-tyrosinase activity were focused in the study.

The values of superoxide radical scavenging activity of silk sericin loaded niosome formulations that composed of Span<sup>®</sup>20, Span<sup>®</sup>40, Span<sup>®</sup>60 and Span<sup>®</sup>80 (1.0 mg/mL) were 65.11±7.98, 67.28±9.89, 70.45±3.99, 65.94±5.67%, respectively (Figure 45). The superoxide radical scavenging activity of optimized silk sericin concentration 1.0 mg/mL was about 70% (Figure 39). The results indicated that silk sericins from niosome formulations shows antioxidant activity and revealed that the preparation method and the organic solvent in niosome preparation did not affect silk sericin.

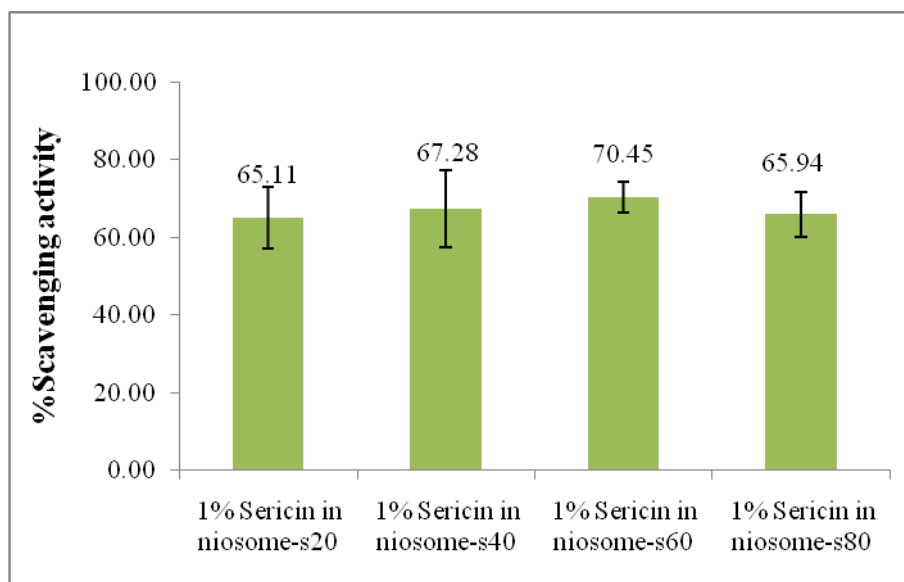


Figure 45 Superoxide radicals scavenging activity of silk sericin loaded niosome formulations 1 mg/mL. (n=4).

The anti-tyrosinase activity was used to evaluate silk sericin loaded niosome formulations. The inhibition of mushroom tyrosinase activity of formulations that composed of Span<sup>®</sup>20, Span<sup>®</sup>40, Span<sup>®</sup>60 and Span<sup>®</sup>80 (1.5 mg/mL) were 74.17±9.14, 87.59±4.24, 82.90±7.53, 68.62±7.01%, respectively (Figure 46). The inhibition of mushroom tyrosinase activity of optimized silk sericin concentration 1.5 mg/mL was about 80% (Figure 40). The results indicated that all of formulations could demonstrate biological activity of silk sericin and the chloroform in preparation method did not effect silk sericin. From these results, silk sericin could be prepared by reverse phase evaporation method and demonstrate biological activities.

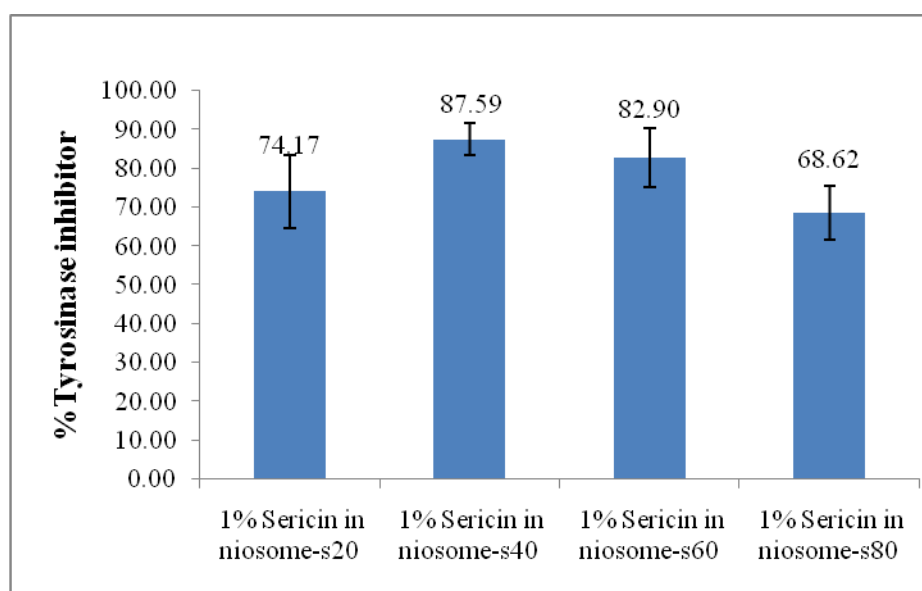


Figure 46 Anti-tyrosinase activity of silk sericin loaded niosome formulations (n=3).

## F. SKIN PERMEATION STUDY OF NIOSOMES LOADED WITH SERICIN

In vitro percutaneous absorption methods have been used for measuring the absorption of compounds that come in contact with skin. In this study, the in vitro skin permeation study of different component of formulations was performed using modified Franz diffusion cell through newborn pig skin. Newborn pig skin was used because it gave similar permeation characteristics to human skin (COLIPA, 1997).

Typically, cumulative amounts (M) of silk sericin permeated through newborn pig skin were plotted as function of time. The permeation rate constant (Flux, J,  $\text{mg}/\text{cm}^2\text{h}$ ) of silk sericin at steady state was calculated from the slope of linear portion of the plot between cumulative amount permeated per unit area versus time. The permeation profiles of silk sericin incorporated in niosome formulations are depicted in Figures 47 and 48. The plot showed the relation between cumulative amounts of sericin permeated through abdominal skin of newborn pig versus time for 24 h. As expected, silk sericin solution could permeate through skin in a negligible extent. The result from the present study was consistent to the previous study reported by Gupta et al. (2005). It concerned about molecular mass of bioactive molecules which normally could not permeate across the skin if it was larger than 500 Da. From the figure 47, the cumulative amount of silk sericin solution could be detected about  $0.17 \text{ mg cm}^{-2}$ .

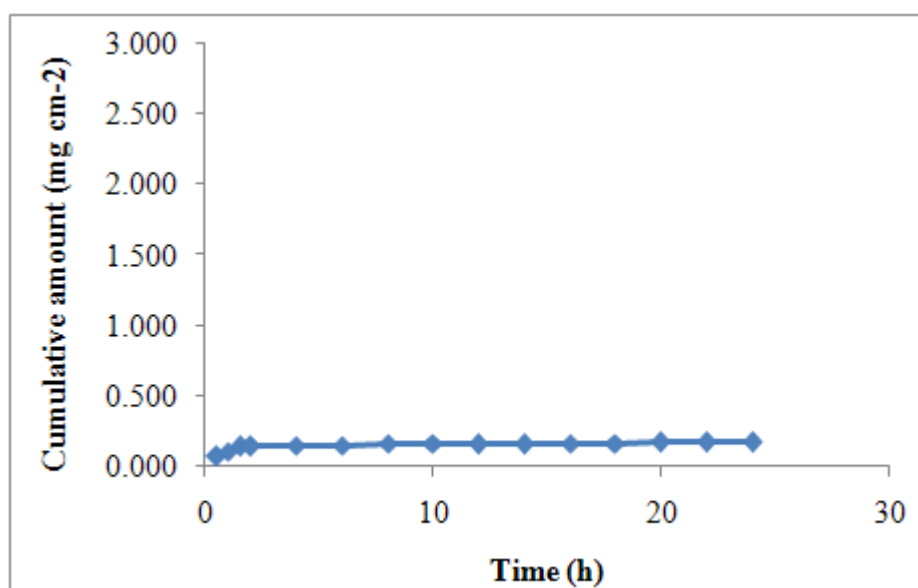


Figure 47 Cumulative amount of silk sericin from silk sericin solution in permeation study in vitro.

The comparative results of all silk sericin loaded in niosomes are exhibited in Figure 48. The finding demonstrated that the cumulative amount profiles of silk sericin from all niosomes that composed of Span<sup>®</sup>20, Span<sup>®</sup>40, Span<sup>®</sup>60 and Span<sup>®</sup>80 had a linear profile. It was noticed that permeability of silk sericin from all niosomes that composed of Span<sup>®</sup>20, Span<sup>®</sup>40, Span<sup>®</sup>60 and Span<sup>®</sup>80 were close. This finding

demonstrated that niosomes could clearly enhance the permeation of silk sericin through the skin. In the permeation process, the niosomes had a desirable interaction with human skin when applied in a topical preparation. They improved the characteristics of the horny layer of skin, both by reducing transepidermal water loss and by increasing skin smoothness by replenish lost lipids (Sagar, Arunagirinathan and Bellare, 2007). Choi and Maibach (2005) reported that in the permeation process, niosomes were adsorbed and fused with the skin surface, which led to a high thermodynamic activity gradient of a drug at the interface.

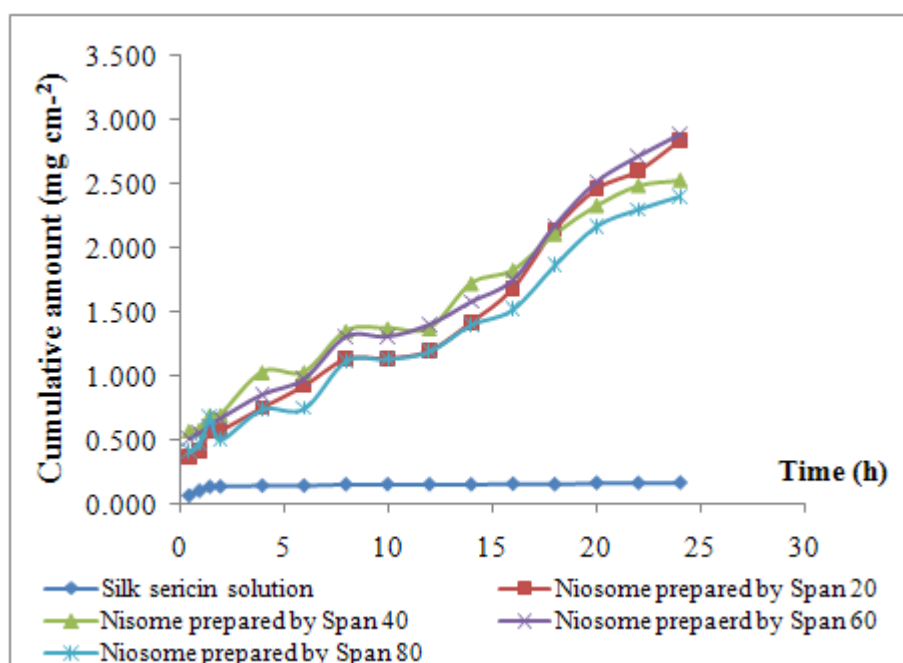


Figure 48 Cumulative amount of silk sericin from silk sericin loaded niosomes that compose of Span<sup>®</sup>20, Span<sup>®</sup>40, Span<sup>®</sup>60 and Span<sup>®</sup>80 in permeation study in vitro (n = 3-4).

For further comparing and understanding the membrane permeability of these formulations, the membrane permeability coefficients ( $P_{app}$ , cm/h) were calculated from the cumulative amount profiles. These coefficients were calculated from the slope, which obtained from the linear plot as in Figure 49. The slopes were divided by the concentration in the donor phase ( $C_d$ , mg/ml) as shown below. Notably,  $P$  was determined in the term of the diffusion coefficient ( $D$ ), the partition coefficient ( $K$ ) and thickness of membrane ( $h$ ) which influenced to the permeability (Reichiling et al., 2006; Sinko, 2006).

$$M = PSC_{dt}$$

$$P = \frac{DK}{h}$$

Where:

$M$  = Cumulative amount of silk sericin (mg)

$P$  = permeability coefficient (cm/h)

$S$  = surface area (cm<sup>2</sup>)

$C_d$  = concentration of drug in donor (mg/ml)

$t$  = time (h)

$D$  = diffusion coefficient

$K$  = partition coefficient

$H$  = thickness of membrane

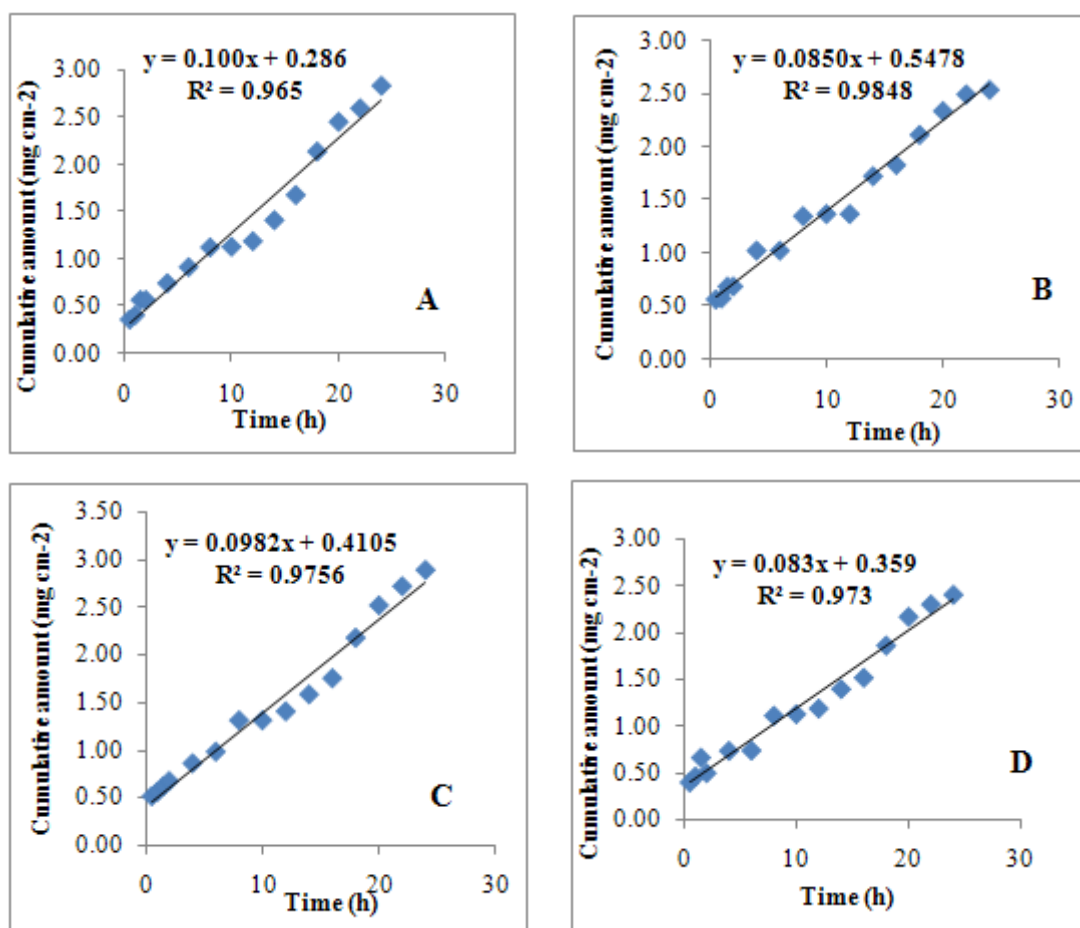


Figure 49 Cumulative amount of silk sericin loaded niosomes in permeation study in vitro for obtained slope (A, B, C and D: silk sericin loaded in niosomes that compose of Span<sup>®</sup> 20, Span<sup>®</sup> 40, Span<sup>®</sup> 60 and Span<sup>®</sup> 80, respectively).

Table 19 shows the membrane permeability coefficients (P) of various formulations. From the results, the permeability of all niosome formulations were non-significantly different ( $p > 0.05$ ). The flux and the permeability coefficient of silk sericin were in range of 0.083-0.100 mg/cm<sup>2</sup>/h and 0.0043-0.0051 cm/h, respectively. The permeability coefficients of all niosome formulations were very close. However, the formulation that composed of Span<sup>®</sup>20 had the non-significantly higher flux which was 0.100±0.014 mg/cm<sup>2</sup>/h and permeability coefficient was 0.0049±0.0005 cm/h. Whereas, the permeability coefficients of formulation that composed of Span<sup>®</sup>40, Span<sup>®</sup>60 and Span<sup>®</sup>80 were 0.0047±0.0006, 0.0051±0.0004 and 0.0043±0.0027 cm/h. This finding agreed with Ibrahim et al. (2008) that the steady state transdermal fluxes of flurbiprofen loaded in proniosomal liquids of Span<sup>®</sup>20 was more than those of Span<sup>®</sup>40 and Span<sup>®</sup>60. It might be occurred from phase transition temperature (Mokhtar, et al., 2008; Balakrishnan et al., 2009). The phase transition temperature of the vesicle systems indicated the thermodynamic state of the bilayers. At the temperature in the study ( $T = 37 \pm 0.1^\circ\text{C}$ ), molecules of Span<sup>®</sup>20 ( $T_c = 16^\circ\text{C}$ ), are in the liquid crystalline state, whereas molecules of Span<sup>®</sup>40 ( $T_c = 42^\circ\text{C}$ ) and Span<sup>®</sup>60 ( $T_c = 53^\circ\text{C}$ ) are in the ordered gel state, which the hydrocarbon chain are fully extended and closely packed. This would make the niosomal membrane more rigid and resisting to drug release (Suwakul et al., 2006). It was noticed that niosomes prepared from Span<sup>®</sup>80 which had its  $T_c$  of  $-12^\circ\text{C}$ , showed lower flux and permeability coefficients than others. This might be attributed to a possible change of the liquid crystalline state of Span<sup>®</sup>80 at the experimental temperature ( $37^\circ\text{C}$ ). Consequently, sericin might leak from niosomal vesicles at this temperature. Therefore, the formulations that composed of Span<sup>®</sup>20 had higher permeability than the formulations that composed of Span<sup>®</sup>40, Span<sup>®</sup>60 and Span<sup>®</sup>80.



Table 19 The membrane permeability coefficients of various formulation of silk sericin (mean±SD, n =3-4).

<b>Formulation</b>	<b>Slope</b> (Flux, mg/cm <sup>2</sup> /h)	<b>P<sub>app</sub> (cm/h)</b>
Silk sericin solution	0.0024±0.0005	3.23±0.07 x10 <sup>-4</sup>
silk sericin loaded in niosome-span 20	0.100±0.014	4.9±0.5 x10 <sup>-3</sup>
silk sericin loaded in niosome-span 40	0.085±0.011	4.7±0.6 x10 <sup>-3</sup>
silk sericin loaded in niosome-span 60	0.098±0.017	5.1±0.4 x10 <sup>-3</sup>
silk sericin loaded in niosome-span 80	0.083±0.046	4.3±2.7 x10 <sup>-3</sup>

From the results obtained in this study, it revealed clearly that the application of silk sericin loaded niosomes for antioxidant and anti-tyrosinase activity by skin delivery was feasible. In the in vitro study, the elastic factor such as mechanically force is the important factor for skin delivery. Thus the further in vivo investigation of niosome formulations for antioxidant and whitening effects are needed.

# CHAPTER V

## CONCLUSIONS

The present study was aimed to develop the extraction method of silk sericin from silkworm *Bombyx mori* (Nangnoi-Sisaket 1). The appropriate extraction method was selected from the investigation of silk sericin, total protein contents, and biological activities. The spray drying technique was optimized to obtain the optimal condition for preparing silk sericin powder. Afterthat, niosomes were applied for loading silk sericin. The results of the investigation were concluded as follows:

1. The extraction of silk sericin cocoons by autoclaving (method I) and basic hydrolysis (method II) were performed. From comparing the physicochemical properties and biological activities of silk sericin obtained from both methods, the method I was found superior and selected for preparing silk sericin in the study.

1.1 Method I gave higher yield of silk sericin powder 13.69% and lower moisture content of 7.31%.

1.2 Method I gave nonsignificantly higher total protein content of 22.97% than method II which exhibited 17.92% of protein content. The molecular weight distribution of sericin from method I ranged between 75-250 kDa.

1.3 Method I demonstrated significantly higher antioxidant activity of the sericin powder as shown from the  $EC_{50}$  values (0.43 mg/mL) in the superoxide scavenging assay.

1.4 Method I demonstrated significantly higher anti-tyrosinase activity of silk sericin powder as shown by  $EC_{50}$  (0.26 mg/mL) in the anti-tyrosinase test.

2. The optimization techniques were operated for spray dried condition of silk sericin solution, estimated by response surface methodology. The optimum region of the spray-drying technique by overlay plot was carried out using the optimal

formulation as inlet temperature 140°C and cocoon concentration 4.64% to evaluate the repeatability. The observed means of the responses obtained for %yield and %moisture contents were in ranged of the prediction intervals at 95% confidence level. The results clearly showed that the model fitted the experimental data well and described the region studied well.

3. The silk sericin powder which was obtained from the optimal spray drying condition had small particles size ( $7.114 \pm 0.299 \mu\text{m}$ ), bulky yellow, spherical shaped, and smooth shrinking surface.

4. The physiochemical and biological properties of silk sericin powder prepared from the optimal spray drying condition were as follows:

4.1 The total protein content was  $22.97 \pm 0.86\%$ .

4.2 The molecular weight distribution ranged 75-250 kDa.

4.3 The DSC thermograms and powder X-ray diffractograms of silk sericin powder was amorphous state.

4.4 Antioxidant activities: the  $EC_{50}$  (mg/ml) values of free radical scavenging activity was 0.82 mg/ml and The  $EC_{50}$  (mg/ml) values of superoxide radical scavenging activity was 0.43 mg/ml.

4.5 The  $EC_{50}$  (mg/ml) values for the inhibition of mushroom tyrosinase activity was 0.40 mg/ml

5. Niosomes could be prepared from Span<sup>®</sup>20, Span<sup>®</sup>40, Span<sup>®</sup>60, and Span<sup>®</sup>80 as surfactant with all surfactant:cholesterol ratios study as 1:1 and Solulan C-24 as stabilizer by reverse phase evaporation method. From the results obtained, the type of surfactant influenced the entrapment efficiency, particle size and size distribution.

6. The entrapment efficiency of silk sericin in niosome formulations prepared was ranged from 84.46-93.88%. The composition of Span<sup>®</sup>60 gave significantly highest entrapment efficiency. This formulation showed the

nonsignificant decrease of entrapment efficiency at the refrigerated temperature for 8 weeks.

7. All niosome formulations showed superoxide radical scavenging activity and anti-tyrosinase activity of silk sericin in despite of the presence in niosomal vesicular structures.

8. Niosomes formulations loaded with silk sericin showed remarkably higher permeation through the skin than silk sericin solution. This result revealed that niosomes acted as a carrier for delivery of silk sericin into the skin.

9. The permeation of silk sericin from all niosome formulations were close among four formulations. The permeability coefficients obtained ranged from 0.0043-0.0051 cm/h.

However, further studies regarding investigation of the mechanism of transdermal delivery, in vivo test of efficacy may be performed to confirm the result of this study in the future.

## REFERENCES

ภาษาไทย

สร้อยรัตน์ พ่วงบริสุทธิ์, สุพนิดา วินิจชัย, หทัยรัตน์ ริมศิริ, วิชัย หฤทัยธนาสันดี และสุคันธรส ธาดา  
กิตติสาร. 2553. ความสามารถในการต้านอนุมูลอิสระ การยับยั้งกิจกรรมเอนไซม์ไทโร  
ซิเนส สมบัติทางกายภาพและเคมีบางประการของผงโปรตีนไหมพันธุโนนถั่วเขียวที่เตรียม  
โดยการสกัดวิธีต่างๆ. ประชุมวิชาการมหาวิทยาลัยเกษตรศาสตร์ ครั้งที่ 48: สาขา  
วิทยาศาสตร์. กรุงเทพฯ: หน้า 319-327.

สุพนิดา วินิจชัย และพิลาณี ไวกนอมสัจย์. 2553. ฤทธิ์ต้านอนุมูลอิสระและยับยั้งเอนไซม์ไทโร  
ซิเนสของโปรตีนไฮโดรไลเสทจากไหมพันธุอีรี่. ประชุมวิชาการของ  
มหาวิทยาลัยเกษตรศาสตร์ ครั้งที่ 48: สาขาวิทยาศาสตร์. กรุงเทพฯ: หน้า 252-259.

หฤทัย สุวานันท์ และอริษาภรณ์ เชื้อคำจันทร์. 2552. ฤทธิ์ต้านอนุมูลอิสระของผงไหม. 35th  
Congress on Science and Technology of Thailand.

ภาษาอังกฤษ

Agarwal, R., Katare, O.P. and Vyas, S.P. 2001. Preparation and in vitro evaluation of  
liposomal/niosomal delivery systems for antipsoriatic drug dithranol.  
International Journal of Pharmaceutics. 228: 43-52.

Ahmad, J.I. 1994. Cholesterol: A Current Perspective. Nutrition and Food Science.  
94(1): 8-11.

Aramwit, P. and Sangcakul, A. 2007. The Effects of Sericin Cream on Wound  
Healing in Rats. Bioscience Biotechnology and Biochemistry. 71(10): 2473-  
2477.

- Aramwit, P., Kanokpanont, S., De-eknamkul, W. and Srichana, T. 2009. Monitoring of inflammatory mediators induced by silk sericin. Journal of Bioscience and Bioengineering. 107: 556-561.
- Aramwit, P., Damrongsakkul, S., Kanokpanont, S. and Srichana, T. 2010. Properties and antityrosinase activity of sericin from various extraction methods. Biotechnology and Applied Biochemistry.55: 91-98.
- Aramwit, P., Siritientong, T. and Srichana, T. 2011. Potential applications of silk sericin, a natural protein from textile industry by-products. Waste Management and Research. 1-8.
- Arunothayanun, P., Bernard, M.S., Craig, D.Q.M., Uchegbu, I.F. and Florence, A.T. 2000. The effect of processing variables on the physical characteristics of non-ionic surfactant vesicles (niosomes) formed from a hexadecyl diglycerol ether. International of Journal of Pharmaceutics. 201: 7-14.
- Balakrishnan, P., Shanmugam, S., Lee, W.S., Lee, W.M., Kim, J.O., Oh, D.H., Kim, D.D., Kim, J.S., Yoo, B.K., Choi, H.G. and Woo, J.S. 2009. Formulation and in vitro assessment of minoxidil niosomes for enhanced skin delivery. International Journal of Pharmaceutics. 377(1-2): 1-8.
- Balasubramaniam, A., Kumar, V.A. and Pilai, K.S. 2002. Formulation and In Vivo Evaluation of Niosome-Encapsulated Daunorubicin Hydrochloride. Drug Development and Industrial Pharmacy. 28(10): 1181-1193.
- Bali, V., Ali, M. and Ali, J. 2010. Study of surfactant combinations and development of a novel nanoemulsion for minimizing variations in bioavailability of ezetimibe. Colloids and Surfaces B: Biointerfaces. 76: 410-420.
- Biswal, S., Murthy, P.N., Sahu, J., Sahoo, P. and Amir, F. 2008. Vesicles of Non-ionic Surfactants (Niosomes) and Drug Delivery Potential. International Journal of Pharmaceutical Sciences and Nanotechnology. 1(1): 1-7.
- Brenner, M. and Hearing, V.J. 2007. The Protective Role of Melanin Against UV Damage in Human Skin. Photochemistry and Photobiology. 84(3): 539-549.

- COLIPA-The European Cosmetic, Toiletry and Perfumery Association. 1997. Guidelines for Percutaneous Absorption/Penetration [Online]. Available from: <http://www.cosmeticseurope.eu> [2011, September 10].
- Choi, E.H., Chang, H.J., Cho, J.Y. and Chun, H.S. 2007. Cytoprotective effect of anthocyanins against doxorubicin-induced toxicity in H9c2 cardiomyocytes in relation to their antioxidant activities. Food and Chemical Toxicology. 45: 1873-1881.
- Choi, M.J. and Maibach, H.I. 2005. Liposomes and Niosomes as Topical Drug Delivery Systems. Skin Pharmacology and Physiology. 18: 209-219.
- Datta, A., Ghosh, A. K. and KUNDU, S.C. 2001. Purification and characterization of fibroin from the tropical Saturniid silkworm, *Antheraea mylitta*. Insect Biochemistry and Molecular Biology. 31: 1013-1018.
- Drummy, L.F., Phillips, D.M., Stone, M.O., Farmer, B.L. and Naik, R.R. 2005. Thermally Induced  $\alpha$ -Helix to  $\beta$ -Sheet Transition in Regenerated Silk Fibers and Films. Biomacromolecules. 6: 3328-3333.
- Fan, J.B., Wu, L.P., Chen, L.S., Mao, X.Y. and Ren, F.Z. 2009. Antioxidant activities of silk sericin from silkworm *Bombyx mori*. Journal of Food Biochemistry. 33: 74-88.
- Fanun, M. 2010. Colloids in drug Delivery. Boca Raton: CRC Press. 355-364.
- Fang, J.Y., Hong, C.T., Chiu, W.T. and Wang, Y.Y. 2001. Effect of liposome and niosomes on skin permeation of enoxacin. International Journal of Pharmaceutics. 219(1-2): 61-72.
- Ebrahimzadeh, M.A., Nabavi, S.F. and Nabavi, S.M. 2009. Antioxidant Activities of Methanol Extract of *Sambucus ebulus* L. Flower. Pakistan Journal of Biological Sciences. 12(5): 447-450.
- Fernandes, E., Costa, D., Toste, S.A., Lima, J.L.F.C. and Reis, S. 2004. In vitro scavenging activity for reactive oxygen and nitrogen species by nonsteroidal

- anti-inflammatory indole, pyrrole, and oxazole derivative drugs. Free Radical Biology and Medicine. 37(11): 1895-1905.
- Genc, G., Narin, G. and Bayraktar, O. 2008. Spray drying as a method of producing silk sericin powders. Archives of Materials Science. 29: 16-18.
- Guinedi, A.S., Mortada, N.D., Mansour, S. and Hathout, R.M. 2005. Preparation and evaluation of reverse-phase evaporation and multilamellar niosomes as ophthalmic carriers of acetazolamide. International Journal of Pharmaceutics. 306: 71-82.
- Gupta, P.N., Mishra, V., Rawat, P., Mahor, S., Lain, S. chetterji, D.P. and Vyas, S. 2005. Non-invasive vaccine delivery in transfersomes, niosomes and liposomes: a comparative study. International Journal of Pharmaceutics. 293: 73-82.
- Hensley, K., Mou, S. and Pye, Q.N. 2003. Methods in Biological Oxidative Stress. New Jersey: Humana Press Inc. 185-193.
- Hino, T., Tanimoto, M. and Shimabayashi, S. 2003. Change in secondary structure of silk fibroin during preparation of its microspheres by spray-drying and exposure to humid atmosphere. Journal of Colloid and Interface Science. 266: 68-73.
- Hao, Y., Zhao, F., Li, N., Yang, Y. and Li, K. 2002. Studies on a high encapsulation of colchicine by a niosome system. International journal of Pharmaceutics. 244: 73-80.
- Ibrahim, M.A., Sammour, O.A., Hamed, M.A. and Megrab, N.A. 2008. In vitro evaluation of proniosomes as a drug carrier for flurbiprofen. AAPS PharmSciTech. 4(3): 782-789.
- Karadag, A., Ozcelik, B. and Saner, S. 2009. Review of Methods to Determine Antioxidant Capacities. Food Analytical Methods. 2: 41-60.



- Kato, N., Sato, S., Yamanaka, A., Yamada, H., Fuwa, N. and Nomura, M. 1998. Silk Protein, Sericin, Inhibits Lipid Peroxidation and Tyrosinase Activity. Bioscience Biotechnology and Biochemistry. 62(1): 145-147.
- Kaur, P. and Arora, S. 2010. Comparison of antioxidant activity of different methanol extract of Cassia and Bauhinia sp. Journal of Chinese Clinical Medicine. 5(8): 8.
- Khazaeli, P. and Pardakhty, A. 2007. Caffeine-Loaded Niosomes: Characterization and in Vitro Release Studies. Drug Delivery. 14: 447-452.
- Ki, C.S., Kim, J.W., Oh, H.J., Lee, K.H. and Park, Y.H. 2007. The effect of residual silk sericin on the structure and mechanical property of regenerated silk filament. International Journal of Biological Macromolecules. 41:346-353.
- Kim, Y.J. and Uyama, H. 2005. Tyrosinase inhibitors from natural and synthetic sources: structure, inhibition mechanism and perspective for the future. CMLS Cellular and Molecular Life Sciences. 62: 1707-1723.
- Kundu, S.C., Dash, B., Dash, R. and Kaplan, D.L. 2008. Natural protective glue protein, sericin bioengineered by silkworm: Potential for biomedical and biotechnological applications. Progress in Polymer Science. 33: 998-1012.
- Lamoolphak, W., De-eknamkul, W. and Shotipruk, A. 2008. Hydrothermal production and characterization of protein and amino acids from silk waste. Bioresource Technology. 99: 7678-7685.
- Lee, K., Kweon, H., Yeo, J. H., Woo, S. O., Lee, Y. W., Cho, C.S., Kim, K. H. and Park, Y. H. 2003. Effect of methyl alcohol on the morphology and conformational characteristics of silk sericin. International Journal of Biological Macromolecules. 33: 75-80.
- Manconi, M., Sinico, C., Valenti, D., Lai, F. and Fadda, A. M. 2006. Niosomes as carriers for tretinoin: III. A study into the in vitro cutaneous delivery of vesicle-incorporated tretinoin. International Journal of Pharmaceutics. 311: 11-19.

- Mandal, S., Hazra, B., Sarkar, R., Biswas, S. and Mandal, N. 2009. Assessment of the Antioxidant and Reactive Oxygen Species Scavenging Activity of Methanolic Extract of *Caesalpinia crista* Leaf. eCAM Advance Access. 1-11.
- Mandal, B.B. and Kundu, S.C. 2008. Non-Bioengineered Silk Fibroin Protein 3D Scaffolds for Potential Biotechnological and Tissue Engineering Applications. Macromolecular Bioscience. 8: 807-818.
- Mandal, B.B., Priya, A.S. and Kundu, S.C. 2009. Novel silk sericin-gelatin 3D scaffolds and 2D films: Fabrication and characterization for potential tissue engineering applications. Acta Biomaterialia. 5: 3007-3020.
- Manosroi, A., Boonpisuttinant, K., Winitchai, S., Manosroi, W. and Manosroi, J. 2010. Free radical scavenging and tyrosinase inhibition activity of oiks and sericin extracted from Thai native silkworms (*Bombyx mori*). Pharmaceutical Biology. 48(8): 855-860.
- Manosroi, A., Podjanasoonthon, K. and Manosroi, J. 2002. Development of novel topical tranexamic acid liposome formulations. International Journal of Pharmaceutics. 235: 61-70.
- Manosroi, A., Wongtrakul, P., Manosroi, J., Sakai, H., Sugawara, F., Yuasa, M. and Abe, M. 2003. Characterization of vesicles prepared with various non-ionic surfactants mixed with cholesterol. Colloids and Surfaces B: Biointerfaces. 30: 129-138.
- Manosroi, A., Wongtrakul, P., Manosroi, J., Midorikawa, U., Hanya, Y., Yuasa, M., Sugawara, F., Sakai, H. and Abe, M. 2005. The entrapment of Kojic oleate in bilayer vesicles. International Journal of Pharmaceutics. 298: 13-25.
- Montgomery, D.C. (2005) Design and Analysis of Experiments 6<sup>th</sup> ed. Arizona: John Wiley & Sons, Inc.
- Mokhtar, M., Sammour, O.A., Hammad, M.A. Megrab, N.A. 2008. Effect of some formulation parameters on flurbiprofen encapsulation and release rates of

- niosomes prepared from proniosomes. International Journal of Pharmaceutics. 361(1-2): 104-111.
- Molyneux, P. 2004. The use of the stable free radical diphenylpicrylhydrazyl (DPPH) and for estimating antioxidant activity. Songklanakarin Journal of Science and Technology. 26(2): 211-219.
- Mondal, M., Trivedy, K. and Kumar, S.N. 2007. The silk proteins, sericin and fibroin in silkworm, *Bombyx mori* Linn.,-a review. Caspian Journal of Environmental Sciences. 5(2): 63-76.
- Moreno, C.S. 2002. Review: Methods Used to Evaluate the Free Radical Scavenging Activity in Foods and Biological Systems. Food Science and Technology International. 8(3): 121-137.
- Nagai, N., Murao, T., Ito, Y., Okamoto, N. and Sasaki, M. 2009. Enhancing Effects of Sericin on Corneal Wound Healing in Otsuka Long-Evans Tokushima Fatty Rats as a Model of Human Type 2 Diabetes. Biological and Pharmaceutical Bulletin. 32(9): 1594-1599.
- New, R.C.C. 1990. Liposomes: A practical approach. United States: Oxford University Press.
- Owusu-Apenten, R.K. 2002. Food protein analysis: quantitative effects on processing. New York: Marcel Dekker.
- Padamwar, M.N. and Pawar, A.P. 2004. Silk sericin and its applications: A review. Journal of Scientific and Industrial Research. 63: 323-329.
- Padamwar, M.N., Pawar, A.P., Daithankar, A.V. and Mahadik, K.R. 2005. Silk sericin as a moisturizer: an in vivo study. Journal of Cosmetic Dermatology. 4(4): 250-257.
- Park, D.V. 1999. Nutritional Antioxidants and Disease Prevention: Mechanisms of Action. Antioxidants in Human Health. CAB International.

- Perron, N.R. and Brumaghim, J.L. 2009. A Review of the Antioxidant Mechanism of Polyphenol Compounds Related to Iron Binding. Cell Biochemistry and biophysics. 53: 75-100.
- Piao, L.Z., Park, H.R., Park, Y.K., Lee, S.K., Park, J.H. and Park, M.K. 2002. Mushroom Tyrosinase Inhibition Activity of Some Chromones. Chemical and Pharmaceutical Bulletin. 50(3): 309-311.
- Puangmalai, N. 2007. Anti-free radical activity and formulation of deformable liposomes loaded with silk sericin. Master's Thesis, Graduate School, Chulalongkorn University.
- Reigosa Roger, M.J. 2001. Handbook of Plant Ecophysiology Techniques. Netherlands: Kluwer Academic Publishers. 283-295.
- Ruckmani, K., Jayakar, B. and Ghosal, S.K. 2000. Nonionic Surfactant Vesicles (Niosomes) of Cytarabine Hydrochloride for Effective Treatment of Leukemias: Encapsulation, Storage, and In Vitro Release. Drug Development and Industrial Pharmacy. 26(2): 217-222.
- Sagar, G.H., Arunagirinathan, M.A. and Bellare, J. 2007. Self-assembled surfactant nano-structures important in drug delivery: A review. Indian Journal of Experimental Biology. 45: 133-159.
- Sanchez-Moreno, C. 2002. Review: Methods Used to Evaluate the Free Radical Scavenging Activity in Foods and Biological Systems. Food Science and Technology International. 8: 121-137.
- Scherer, R. and Godoy, H.T. 2009. Antioxidant activity index (AAI) by the 2,2-diphenyl-1-picrylhydrazyl method. Food Chemistry. 112:654-658.
- Schmook, F.P., Meingassner, J.G. and Billich, A. 2001. Comparison of human skin or epidermis models with human and animal skin in in-vitro percutaneous absorption. International Journal of Pharmaceutics. 215: 51-56.

- Schneider, A., Wang, X.Y., Kaplan, D.L., Garlick, J.A. and Egles, C. 2009. Biofunctionalized electrospun silk mats as a topical bioactive dressing for accelerated wound healing. Acta Biomaterialia. 5: 2570-2578.
- Schurink, M., Berkel, W.J.H., Wichers, H.J. and Boeriu, C. 2007. Novel peptides with tyrosinase inhibitory activity. Peptides. 28: 485-495.
- Shahiwala, A. and Misra, A. 2002. Studies in topical application of niosomally entrapped Nimesulide. Journal of Pharmacy and Pharmaceutical Sciences. 5(3): 220-225.
- Shatalebi, M.A., Mostafavi, S.A. and Moghaddas, A. 2010. Niosomes as a drug carrier for topical delivery of N-acetyl glucosamine. Research in Pharmaceutical Sciences. 5(2): 107-117.
- Singh, C.H., Jain, C.P. and Kumar, B.N. 2011. Formulation, characterization, stability and invitro evaluation of Nimesulide niosomes. Pharmacophore. 2(3): 168-185
- Singh, S. and Singh, R.P. 2008. In Vitro Methods of Assay of Antioxidants: An Overview. Food Reviews International. 24: 392-415.
- Sinko, P.J. 2006. Martin's physical pharmacy and pharmaceutical sciences 5<sup>th</sup> ed. Philadelphia: Lippincott Williams & Wilkins.
- Sothornvit, R., Chollakup, R. and Suwanruji, P. 2010. Extracted sericin from silk waste for film formation. Songklanakarin Journal of Science and Technology. 32(1): 17-22.
- Subodh, D., Amit, J., Metha, S.C., Pavan G., Sandeep, J. and Jagdish, S. 2012. Niosomes: The ultimate drug carrier. Drug Invention Today. 2(1): 72-77.
- Suwakul, W., Ongpipattanakul, B. and Vardhanabhuti, A. 2006. Preparation and Characterization of Propylthiouracil Niosomes. Journal of Liposome Research. 16: 391-401.

- Tamada, Y., Sano, M., Niwa, K., Imai, T. and Yoshino, G. 2004. Sulfation of silk sericin and anticoagulant activity of sulfated sericin. Journal of Biomaterials Science, Polymer Edition. 15(8): 971-980.
- Tao, W., Li, M. and Xie, R. 2005. Preparation and Structure of Porous Silk Sericin Materials. Macromolecular materials and Engineering. 290: 188-194.
- Teramoto, H., Nakajima, K. and Takabayashi, C. 2005. Preparation of Elastic Silk Sericin Hydrogel. Bioscience Biotechnology and Biochemistry. 69(4): 845-847.
- Torchilin, V. and Weissig, V. 2003. Liposomes: A practical approach. 2<sup>nd</sup> ed. United States: Oxford University Press.
- Trachootham, D., Alexandre, J. and Huang, P. 2009. Targeting cancer cells by ROS-mediated mechanisms: a radical therapeutic approach. Nature Reviews Drug Discovery. 8: 579-591.
- Tsikas, D. 2007. Analysis of nitrite and nitrate in biological fluids by assays based on the Griess reaction: Appraisal of the Griess reaction in the L-arginine/nitric oxide area of research. Journal of Chromatography B. 851: 51-70.
- Uchegbu, I. F. and Vyas, S. P. 1998. Non-ionic surfactant based vesicles (niosomes) in drug delivery. International Journal of Pharmaceutics. 172: 33-70.
- Vaithanomsat, P. and Kitpreechavanich, V. 2008. Sericin separation from silk degumming wastewater. Separation and Purification Technology. 59: 129-133.
- Vangal, A., Kirby, D., Rosenkrands, I., Agger, E.M., Andersen, P. and Perrie, Y. 2006. A comparative study of cationic liposome and niosome-based adjuvant systems for protein subunit vaccines: characterisation, environmental scanning electron microscopy and immunisation studies in mice. Pharmacy and pharmacology. 58: 787-799.
- Vepari, C. and Kaplan, D.L. 2007. Silk as a biomaterial. Progress in Polymer Science. 32: 991-1007.

- Walker, J. M. 2002. The protein protocol handbook. 2<sup>nd</sup> ed. New Jersey: Humana Press.
- Wiseman, H. and Halliwell, B. 1996. Damage to DNA by reactive oxygen and nitrogen species: role in inflammatory disease and progression to cancer. Biochemical Journal. 313: 17-29.
- Weinheimer, T. and White, D. 2003. Using Peroxidase To Demonstrate Enzyme Kinetics. The American Biology Teacher. 65(2): 116-121.
- Wu, J.-H., Wang, Z. and Xu, S.-Y. 2007. Preparation and characterization of sericin powder extracted from silk industry wastewater. Food Chemistry. 103: 1255-1262.
- Yamada, H., Nakao, H., Takasu, Y. and Tsubouchi, K. 2001. Preparation of undegraded native molecular fibroin solution from silkworm cocoons. Materials Science and Engineering C. 14: 41-46.
- Zhang, Y.-Q. 2002. Applications of natural silk protein sericin in biomaterials. Biotechnology Advances. 20: 91-100.
- Zhang, Y.Q., Tao, M.L., Shen, W.D., Zhou, Y.Z., Ding, Y., Ma, Y., Zhou, W.L. 2004. Immobilization of L-asparaginase on the microparticles of the natural silk sericin protein and its characters. Biomaterials. 25: 3751-3759.

## **APPENDICES**



## **APPENDIX A**

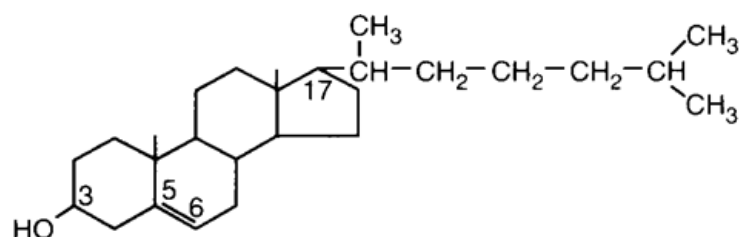
**Molecular structure and physical properties of material**

### 1. Cholesterol

Molecular formulation  $C_{27}H_{46}O$

Molecular weight 386.65

Structure



### 2. Span<sup>®</sup>20

Chemical name Sorbitan laurate; Sorbitan monododecanoate

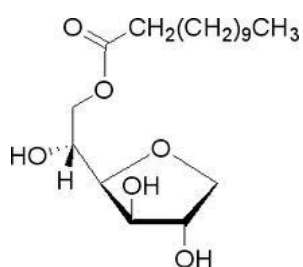
Molecular formulation  $C_{18}H_{34}O_6$

Molecular weight 346

Transition temperature 16 °C

HLB 8.6

Structure



### 3. Span<sup>®</sup>40

Chemical name Sorbitan monopalmitate

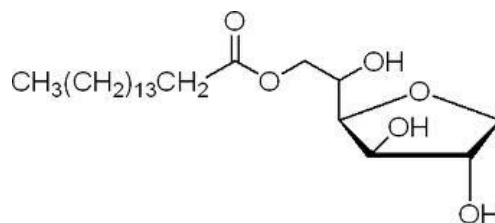
Molecular formulation  $C_{22}H_{42}O_6$

Molecular weight 403

Transition temperature 42 °C

HLB 6.7

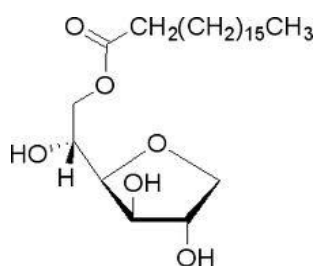
Structure



#### 4. Span<sup>®</sup>60

Chemical name	Sorbitan stearate; Sorbitan monooctadecanoate
Molecular formulation	$C_{24}H_{46}O_6$
Molecular weight	431
Transition temperature	53 °C
HLB	4.7

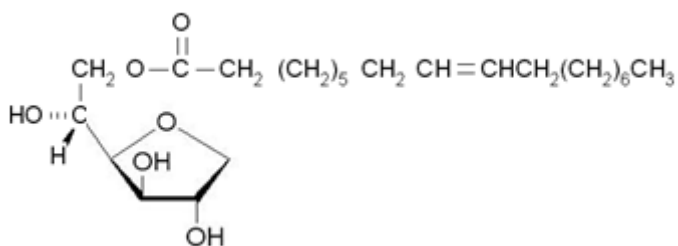
Structure



#### 5. Span<sup>®</sup>80

Chemical name	Sorbitan oleate
Molecular formulation	$C_{24}H_{44}O_6$
Molecular weight	429
Transition temperature	-12 °C
HLB	4.3

Structure

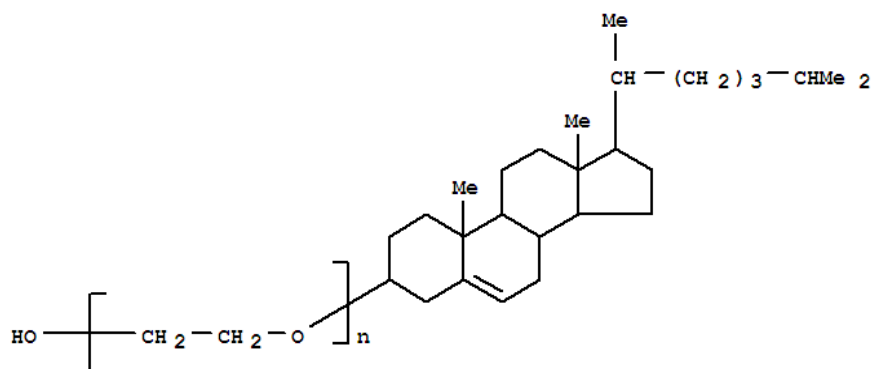


### 7. Solulan<sup>®</sup> C-24

Chemical name Polyoxyethylene-24-cholesteryl ether

Molecular weight 1443

Structure



## **APPENDIX B**

### **Comparison of extraction methods for silk sericin**

### Total protein contents

Table B1. Absorbance of BSA by Bradford assay.

BSA (mg/ml)	Absorbance 595 nm					Absorbance 595 nm		
	1	2	3	4	5	Mean	SD	SEM
0.000	0.000	0.000	0.000	0.000	0.000	0.000	0.000	0.000
0.065	0.044	0.060	0.064	0.054	0.054	0.055	0.008	0.003
0.130	0.100	0.114	0.109	0.109	0.089	0.104	0.010	0.004
0.259	0.201	0.209	0.217	0.200	0.203	0.206	0.007	0.003
0.356	0.279	0.284	0.275	0.268	0.267	0.275	0.007	0.003
0.518	0.411	0.349	0.381	0.348	0.369	0.372	0.026	0.012
0.712	0.498	0.503	0.484	0.485	0.461	0.486	0.016	0.007
1.036	0.653	0.615	0.670	0.632	0.642	0.642	0.021	0.009

Table B2. The total protein contents of silk sericin.

Samples	% Protein content						
	1	2	3	4	Mean	SD	SEM
silk sericin (Method I)	23.887	22.474	22.013	23.512	22.972	0.875	0.437
silk sericin (Method II)	17.518	18.12	18.151	17.898	17.922	0.292	0.146

Table B3. The total protein contents of silk sericin (optimization)

Samples	% Protein content						
	1	2	3	4	Mean	SD	SEM
silk sericin (optimization)	22.083	19.43	23.491	22.312	21.829	1.714	0.857

### Anti-oxidant activities of silk sericin

Table B4. The EC<sub>50</sub> values calculated from linear regression equations for DPPH radicals scavenging activity of different extraction method silk sericin, L-ascorbic acid was used as a positive control.

Samples	The half maximum effective concentration (EC <sub>50</sub> ) (mg/ml)				
	1	2	3	Mean	SD
L-ascorbic acid	0.0023	0.0025	0.0023	0.0024	0.00
Sericin (Method I)	1.936	0.883	1.070	1.30	0.56
Sericin (Method II)	2.640	2.372	2.754	2.59	0.20

Table B5. Analysis the EC<sub>50</sub> values for DPPH radicals scavenging activity of different extraction method silk sericin, L-ascorbic acid was used as a positive control by one-way ANOVA.

#### Test of Homogeneity of Variances

##### EC50

Levene Statistic	df1	df2	Sig.
8.471011717	2	6	0.0179

#### ANOVA

EC50	Sum of Squares	df	Mean Square	F	Sig.
Between Groups	10033.422	2	5016.711	42.490	0.0003
Within Groups	708.401	6	118.067		
Total	10741.823	8			

### Post Hoc Tests: Multiple Comparisons

Dependent Variable: EC50 ( $\mu\text{g/ml}$ )

	(I) Categoriis	(J) Categoriis	Mean Dif. (I-J)	Std. Error	Sig.	95% Confidence Interval	
						Lower Bound	Upper Bound
Dunnett T3	L-ascorbic	Sericin (Method I)	-1.294	0.324	0.118	-3350.73	763.26
		Sericin (Method II)	-2.586	0.113	0.004	-3304.11	-1868.49
	Sericin (Method I)	L-ascorbic	1.294	0.324	0.118	-763.26	3350.73
		Sericin (Method II)	-1.293	0.344	0.099	-3055.60	470.47
	Sericin (Method II)	L-ascorbic	2.586	0.113	0.004	1868.49	3304.11
		Sericin (Method I)	1.293	0.344	0.099	-470.47	3055.60

\*The mean difference is significant at the .05 level.

Table B6 The EC<sub>50</sub> values calculated from linear regression equations for superoxide radical scavenging activity of different extraction method silk sericin, quercetin was used as a positive control.

Samples	EC 50 (mg/ml)					
	1	2	3	Mean	SD	SEM
Quercetin	0.01	0.02	0.02	0.02	0.01	0.00
Sericin (Method I)	0.48	0.39	0.43	0.43	0.05	0.03
Sericin (Method II)	0.81	0.71	0.66	0.73	0.08	0.04

Table B7. Analysis the EC<sub>50</sub> ( $\mu\text{g/ml}$ ) values for superoxide radical scavenging activity of different extraction methods assay by one-way ANOVA.

### Test of Homogeneity of Variances

EC50 ( $\mu\text{g/ml}$ )

Levene Statistic	df1	df2	Sig.
3.960655789	2	6	0.080059577



## ANOVA

EC50	Sum of Squares	df	Mean Square	F	Sig.
Between Groups	765034.2578	2	382517.1289	144.8997	8.34567E-06
Within Groups	15839.2462	6	2639.874367		
Total	780873.504	8			

## Post Hoc Tests: Multiple Comparisons

Dependent Variable: EC50 ( $\mu\text{g/ml}$ )

## Tukey HSD

(I) Categorie	(J) Categorie	Mean Difference (I-J)	Std. Error	Sig.	95% Confidence Interval	
					Lower Bound	Upper Bound
Quercetin	Sericin (Method I)	-413.083	41.95	0.00016	-541.80	-284.37
	Sericin (Method II)	-711.06	41.95	0.00001	-839.78	-582.34
Sericin (Method I)	Quercetin	413.0833	41.95	0.00016	284.37	541.80
	Sericin (Method II)	-297.977	41.95	0.00095	-426.69	-169.26
Sericin (Method II)	Quercetin	711.06	41.95	0.00001	582.34	839.78
	Sericin (Method I)	297.9767	41.95	0.00095	169.26	426.69

\*The mean difference is significant at the .05 level.

## Homogeneous Subsets

EC50

## Tukey HSD

Categorie	N	Subset for alpha = .05		
		1	2	3
Quercetin	3	16.89333		
Sericin (Method I)	3		429.9766667	
Sericin (method II)	3			727.9533
Sig.		1	1	1

Means for groups in homogeneous subsets are displayed.

a

Uses Harmonic Mean Sample Size = 3.000.

Table B8. The EC<sub>50</sub> values calculated from linear regression equations for hydrogen peroxide radical scavenging activity of different extraction method silk sericin, quercetin was used as a positive control.

Sample	EC 50 (mg/ml)						
	1	2	3	4	Mean	SD	SEM
Quercetin	0.01	0.01	0.02	0.02	0.01	0.00	0.00
Sericin (Method I)	1.10	2.31	1.65	1.46	1.63	0.51	0.25
Sericin (Method II)	2.29	1.91	1.78	1.12	1.77	0.49	0.24

Table B9. Analysis the EC<sub>50</sub> (µg/ml) values for hydrogen peroxide radical scavenging activity of different extraction methods assay by one-way ANOVA.

#### Test of Homogeneity of Variances

##### EC50 (µg/ml)

Levene Statistic	df1	df2	Sig.
2.362293794	2	9	0.149742275

#### ANOVA

##### EC50

	Sum of Squares	df	Mean Square	F	Sig.
Between Groups	7638903.106	2	3819451.553	23.25739	0.00027813
Within Groups	1478027.618	9	164225.2908		
Total	9116930.723	11			

### Post Hoc Tests: Multiple Comparisons

**Dependent Variable: EC50**

**Tukey HSD**

(I) Categories	(J) Categories	Mean Diff. (I-J)	Std. Error	Sig.	95% Confidence Interval	
					Lower Bound	Upper Bound
Quercetin	Sericin (Method I)	-1615.83	286.553	0.00083	-2415.89	-815.77
	Sericin (Method II)	-1759.97	286.553	0.000447	-2560.03	-959.91
Sericin (Method I)	Quercetin	1615.83	286.553	0.00083	815.77	2415.89
	Sericin (Method II)	-144.14	286.553	0.871713	-944.20	655.92
Sericin (Method II)	Quercetin	1759.97	286.553	0.000447	959.91	2560.03
	Sericin (Method I)	144.14	286.553	0.871713	-655.92	944.20
* The mean difference is significant at the .05 level.						

Table B10. The EC<sub>50</sub> values calculated from linear regression equations for hydroxyl radical scavenging activity of different extraction method silk sericin, mannitol was used as a positive control.

Sample	EC 50 (mg/ml)					
	1	2	3	Mean	SD	SEM
Mannitol	0.66	0.47	0.48	0.54	0.11	0.06
Sericin (Method I)	0.82	1.01	1.00	0.94	0.11	0.06
Sericin (Method II)	0.85	1.01	1.03	0.96	0.10	0.06

Table B11. Analysis the EC<sub>50</sub> values for hydroxyl radical scavenging activity of different extraction methods assay by one-way ANOVA.

### Test of Homogeneity of Variances

#### EC50

Levene Statistic	df1	df2	Sig.
0.035502959	2	6	0.965321063

### ANOVA

#### EC50

	Sum of Squares	df	Mean Square	F	Sig.
Between Groups	0.3478	2	0.1739	16.004	0.0039
Within Groups	0.0652	6	0.0109		
Total	0.4130	8			

### Post Hoc Tests: Multiple Comparisons

#### Dependent Variable: EC50

#### Tukey HSD

(I) Categories	(J) Categories	Mean Dif. (I-J)	Std. Error	Sig.	95% Confidence Interval	
					Lower Bound	Upper Bound
Mannitol	Sericin (Method I)	-0.407	0.0851	0.0073	-0.668	-0.146
	Sericin (Method II)	-0.427	0.0851	0.0058	-0.688	-0.166
Sericin (Method I)	Mannitol	0.407	0.0851	0.0073	0.146	0.668
	Sericin (Method II)	-0.020	0.0851	0.9702	-0.281	0.241
Sericin (Method II)	Mannitol	0.427	0.0851	0.0058	0.166	0.688
	Sericin (Method I)	0.020	0.0851	0.9702	-0.241	0.281
*	The mean difference is significant at the .05 level.					

**Homogeneous Subsets****EC50****Tukey HSD**

Categories	N	Subset for alpha = .05	
		1	2
Mannitol	3	0.536667	
Sericin (method I)	3		0.943333333
Sericin (method II)	3		0.963333333
Sig.		1	0.970170523

Means for groups in homogeneous subsets are displayed.  
a Uses Harmonic Mean Sample Size = 3.000.

Table B12. The EC<sub>50</sub> values calculated from linear regression equations for nitric oxide scavenging activity of different extraction method silk sericin, quercetin was used as a positive control.

Sample	EC 50 (mg/ml)					
	1	2	3	Mean	SD	SEM
Quercetin	0.00	0.01	0.01	0.01	0.00	0.00
Sericin (Method I)	1.70	2.20	2.15	2.02	0.28	0.16
Sericin (Method II)	1.15	2.05	1.80	1.67	0.47	0.27

Table B13. Analysis the EC<sub>50</sub> (µg/ml) values for nitric oxide scavenging activity of different extraction methods assay by one-way ANOVA.

**Test of Homogeneity of Variances****EC50 (µg/ml)**

Levene	df1	df2	Sig.
Statistic			
9.969541422	2	8	0.006722199

**ANOVA****EC50**

	Sum of Squares	df	Mean Square	F	Sig.
Between Groups	9390973.797	2	4695486.899	63.9833946	1.2E-05
Within Groups	587088.1879	8	73386.02348		
Total	9978061.985	10			

**Post Hoc Tests: Multiple Comparisons****Dependent Variable: EC50**

	(I) Categories	(J) Categories	Mean Dif. (I-J)	Std. Error	Sig.	95% Confidence Interval	
						Lower Bound	Upper Bound
Dunnett T3	Quercetin	Sericin (Method I)	-2010.86	160.37	0.013	-3027.63	-994.09
		Sericin (Method II)	-1664.71	268.57	0.052	-3367.56	38.14
	Sericin (Method I)	Quercetin	2010.86	160.37	0.013	994.09	3027.63
		Sericin (Method II)	346.15	312.81	0.65	-964.67	1656.97
	Sericin (Method II)	Quercetin	1664.71	268.57	0.052	-38.14	3367.56
		Sericin (Method I)	-346.15	312.81	0.65	-1656.97	964.67

### Anti-tyrosinase activities of silk sericin

Table B14. The EC<sub>50</sub> values calculated from linear regression equations for anti-tyrosinase activity of different extraction method silk sericin, alpha-arbutin and kojic acid were used as a positive control (n=3).

Sample	The half maximum effective concentration EC 50 (mg/ml)					
	1	2	3	Mean	SD	SEM
Alpha-arbutin	0.200	0.240	0.190	0.210	0.026	0.015
Kojic acid	0.005	0.005	0.004	0.005	0.000	0.000
Sericin (Method I)	0.300	0.270	0.210	0.260	0.046	0.026
Sericin (Method II)	3.230	2.370	2.030	2.543	0.618	0.357

Table B15. Analysis the EC<sub>50</sub> values for anti-tyrosinase activity of different extraction methods assay by one-way ANOVA.

#### Test of homogeneity of variances

Levene Statistic	df1	df2	Sig.
8.477	3	8	.007

#### One-way ANOVA analysis

	Sum of Squares	df	Mean Square	F	Sig.
Between Groups	12.910	3	4.303	44.670	.000
Within Groups	.771	8	.096		
Total	13.680	11			

### Multiple Comparisons

Dependent Variable: EC<sub>50</sub>

(I) Sample			Mean Difference (I-J)	Std. Error	Sig.	95% Confidence Interval	
						Lower Bound	Upper Bound
Tukey HSD	Alpha-arbutin	Kojic acid	.205333	.253421	.848	-.6062	1.0169
		Sericin (Method I)	-.050000	.253421	.997	-.8615	.7615
		Sericin (Method II)	-2.333333*	.253421	.000	-3.1449	-1.5218
	Kojic acid	Alpha-arbutin	-.205333	.253421	.848	-1.0169	.6062
		Sericin (Method I)	-.255333	.253421	.750	-1.0669	.5562
		Sericin (Method II)	-2.538667*	.253421	.000	-3.3502	-1.7271
	Sericin (Method I)	Alpha-arbutin	.050000	.253421	.997	-.7615	.8615
		Kojic acid	.255333	.253421	.750	-.5562	1.0669
		Sericin (Method II)	-2.283333*	.253421	.000	-3.0949	-1.4718
	Sericin (Method II)	Alpha-arbutin	2.333333*	.253421	.000	1.5218	3.1449
		Kojic acid	2.538667*	.253421	.000	1.7271	3.3502
		Sericin (Method I)	2.283333*	.253421	.000	1.4718	3.0949

\*. The mean difference is significant at the 0.05 level

### Homogeneous subset

Sample	N	Subset for alpha = 0.05	
		1	2
Tukey HSD <sup>a</sup>	Kojic acid	3	.00467
	Alpha-arbutin	3	.21000
	Sericin (Method I)	3	.26000
	Sericin (Method II)	3	2.54333
	Sig.		.750

Means for groups in homogeneous subsets are displayed.

a. Uses Harmonic Mean Sample Size = 3.000.



### Particle size and size distribution of spray draying condition

Table B16. Particle size of silk sericin powder of spray draying condition.

Factor		Particle size				
%Cocoon concentration	Inlet temperature	D[4, 3]			average	SD
		1	2	3		
3	100	7.616	7.586	7.747	7.649	0.086
3	120	6.866	6.728	6.882	6.325	0.085
3	140	7.309	7.375	6.954	7.213	0.226
6.5	100	6.449	6.654	6.608	6.494	0.108
6.5	120	6.853	7.025	7.045	6.974	0.106
6.5	140	7.728	7.207	7.321	7.419	0.274
10	100	7.36	7.19	7.386	7.312	0.106
10	120	8.573	8.449	8.037	8.353	0.281
10	140	9.193	9.207	9.14	9.18	0.035
4.6	140	6.796	7.391	7.153	7.114	0.299
<b>Sericin</b>						
<b>(Method II)</b>						
3	120	5.842	5.796	5.537	5.725	0.164

Table B17. Size distribution of silk sericin powder of spray draying condition.

<b>Factor</b>		<b>Size distribution</b>				
<b>%Cocoon concentration</b>	<b>Inlet temperature</b>	<b>Span</b>				
		<b>1</b>	<b>2</b>	<b>3</b>	<b>average</b>	<b>SD</b>
3	100	1.951	1.965	1.966	1.961	0.008386
3	120	1.689	1.565	1.704	1.651	0.076291
3	140	1.546	1.585	1.506	1.543	0.039501
6.5	100	1.198	1.079	1.082	1.121	0.067855
6.5	120	1.273	1.381	1.264	1.305	0.065108
6.5	140	1.246	1.287	1.287	1.273	0.023671
10	100	1.286	1.199	1.285	1.261	0.049943
10	120	1.462	1.279	1.3	1.345	0.100145
10	140	1.393	1.391	1.393	1.392	0.001155
4.6	140	1.278	1.343	1.321	1.317	0.033061
<b>Sericin (Method II)</b>						
3	120	1.453	1.447	1.325	1.408	0.072231

## **APPENDIX C**

### **Determination of Entrapment Efficiency and Stability of Niosomes**

### Entrapment Efficiency

Table C1. The data for entrapment efficiency study (%entrapment) of niosomes at day 0 when storage in refrigerator (4-8 °C).

Formulation	%Entrapment efficiency (day 0)				
	1	2	3	Mean	SD
Span <sup>®</sup> 20	85.67	83.39	84.32	84.46	1.15
Span <sup>®</sup> 40	84.08	86.3	82.27	84.22	2.02
Span <sup>®</sup> 60	95.9	92.55	93.19	93.88	1.78
Span <sup>®</sup> 80	89.45	90.07	89.46	89.66	0.36

Table C2. Analysis the percentage of entrapment efficiency of niosomes at day 0 when storage in refrigerator (4-8 °C).

#### Test of Homogeneity of Variances

EE

Levene Statistic	df1	df2	Sig.
2.440	3	8	.139

#### ANOVA

EE

	Sum of Squares	df	Mean Square	F	Sig.
Between Groups	178.475	3	59.492	38.701	.000
Within Groups	12.298	8	1.537		
Total	190.772	11			

**EE**

Formulation		N	Subset for alpha = 0.05		
			1	2	3
Tukey	Span20	3	84.4600		
HSD <sup>a</sup>	Span40	3	84.8667		
	Span80	3		89.6600	
	Span60	3			93.8800
	Sig.		.977	1.000	1.000

Table C3. The data for entrapment efficiency study (%entrapment) of niosomes at week 1 when storage in refrigerator (4-8 °C).

Formulation	%Entrapment efficiency (week 1)				
	1	2	3	Mean	SD
<b>Span<sup>®</sup>20</b>	82.61	83.06	78.38	81.35	2.58
<b>Span<sup>®</sup>40</b>	80.43	87.1	85.45	84.33	3.47
<b>Span<sup>®</sup>60</b>	94.36	95.28	92.66	94.10	1.33
<b>Span<sup>®</sup>80</b>	87.13	73.44	80.29	80.29	6.85

Table C4. The data for entrapment efficiency study (%entrapment) of niosomes at week 2 when storage in refrigerator (4-8 °C).

Formulation	%Entrapment efficiency (week 2)				
	1	2	3	Mean	SD
<b>Span<sup>®</sup>20</b>	80.38	85.52	83.13	83.01	2.57
<b>Span<sup>®</sup>40</b>	81.76	78.35	84.92	81.68	3.29
<b>Span<sup>®</sup>60</b>	93.04	91.74	87.84	90.87	2.71
<b>Span<sup>®</sup>80</b>	61.31	83.39	71.49	72.06	11.05

Table C5. The data for entrapment efficiency study (%entrapment) of niosomes at week 4 when storage in refrigerator (4-8 °C).

Formulation	%Entrapment efficiency (week 4)				
	1	2	3	Mean	SD
Span <sup>®</sup> 20	80.56	79	76	78.52	2.32
Span <sup>®</sup> 40	85.16	79.63	80.15	81.65	3.05
Span <sup>®</sup> 60	93.44	88.56	89.67	90.56	2.56
Span <sup>®</sup> 80	70.52	65.01	79.59	71.71	7.36

Table C6. The data for entrapment efficiency study (%entrapment) of niosomes at week 8 when storage in refrigerator (4-8 °C).

Formulation	%Entrapment efficiency (week 8)				
	1	2	3	Mean	SD
Span <sup>®</sup> 20	79.27	75.85	74.32	76.48	2.53
Span <sup>®</sup> 40	83.24	84.33	83.09	83.55	0.68
Span <sup>®</sup> 60	87.51	85.96	91.5	88.32	2.86
Span <sup>®</sup> 80	69.36	72.15	66.5	69.34	2.83

Table C7. Analysis the percentage of entrapment efficiency of niosomes when storage in refrigerator (4-8 °C) for 8 week.

**Niosome that compose of Span<sup>®</sup> 20:**

**Test of Homogeneity of Variances**

EE

Levene Statistic	df1	df2	Sig.
.593	4	10	.676

## ANOVA

EE

	Sum of Squares	df	Mean Square	F	Sig.
Between Groups	127.310	4	31.827	6.030	.010
Within Groups	52.782	10	5.278		
Total	180.091	14			

## Post Hoc Tests: Multiple Comparisons

Dependent Variable:EE

	(I) Day	(J) Day	Mean Differenc e (I-J)	Std. Error	Sig.	95% Confidence Interval	
						Lower Bound	Upper Bound
Tukey HSD	Day0	Wk1	3.11000	1.87584	.497	-3.0635	9.2835
		wk2	1.45000	1.87584	.933	-4.7235	7.6235
		wk4	5.94000	1.87584	.061	-.2335	12.1135
		wk8	7.98000*	1.87584	.011	1.8065	14.1535
	Wk1	Day0	-3.11000	1.87584	.497	-9.2835	3.0635
		wk2	-1.66000	1.87584	.896	-7.8335	4.5135
		wk4	2.83000	1.87584	.580	-3.3435	9.0035
		wk8	4.87000	1.87584	.144	-1.3035	11.0435
	wk2	Day0	-1.45000	1.87584	.933	-7.6235	4.7235
		Wk1	1.66000	1.87584	.896	-4.5135	7.8335
		wk4	4.49000	1.87584	.194	-1.6835	10.6635
		wk8	6.53000*	1.87584	.037	.3565	12.7035
	wk4	Day0	-5.94000	1.87584	.061	-12.1135	.2335
		Wk1	-2.83000	1.87584	.580	-9.0035	3.3435
		wk2	-4.49000	1.87584	.194	-10.6635	1.6835
		wk8	2.04000	1.87584	.809	-4.1335	8.2135
wk8	Day0	-7.98000*	1.87584	.011	-14.1535	-1.8065	
	Wk1	-4.87000	1.87584	.144	-11.0435	1.3035	
	wk2	-6.53000*	1.87584	.037	-12.7035	-.3565	
	wk4	-2.04000	1.87584	.809	-8.2135	4.1335	

**Homogeneous Subsets****EE**

		N	Subset for alpha = 0.05	
			1	2
Tukey HSD <sup>a</sup>	Day			
	wk8	3	76.4800	
	wk4	3	78.5200	78.5200
	Wk1	3	81.3500	81.3500
	wk2	3		83.0100
	Day0	3		84.4600
Sig.			.144	.061

**Niosome that compose of Span<sup>®</sup> 40:****Test of Homogeneity of Variances**

EE

Levene Statistic	df1	df2	Sig.
1.421	4	10	.296

**ANOVA**

EE

	Sum of Squares	df	Mean Square	F	Sig.
Between Groups	21.282	4	5.320	.724	.595
Within Groups	73.445	10	7.345		
Total	94.727	14			



### Post Hoc Tests: Multiple Comparisons

Dependent Variable:EE

	(I)	(J)	Mean Differen ce (I-J)	Std. Error	Sig.	95% Confidence Interval	
						Lower	Upper
						Bound	Bound
Tukey HSD	Day0	Wk1	-.11000	2.21277	1.000	-7.3924	7.1724
		wk2	2.54000	2.21277	.779	-4.7424	9.8224
		wk4	2.57000	2.21277	.772	-4.7124	9.8524
		wk8	.66333	2.21277	.998	-6.6191	7.9457
	Wk1	Day0	.11000	2.21277	1.000	-7.1724	7.3924
		wk2	2.65000	2.21277	.753	-4.6324	9.9324
		wk4	2.68000	2.21277	.746	-4.6024	9.9624
		wk8	.77333	2.21277	.996	-6.5091	8.0557
	wk2	Day0	-2.54000	2.21277	.779	-9.8224	4.7424
		Wk1	-2.65000	2.21277	.753	-9.9324	4.6324
		wk4	.03000	2.21277	1.000	-7.2524	7.3124
		wk8	-1.87667	2.21277	.909	-9.1591	5.4057
	wk4	Day0	-2.57000	2.21277	.772	-9.8524	4.7124
		Wk1	-2.68000	2.21277	.746	-9.9624	4.6024
		wk2	-.03000	2.21277	1.000	-7.3124	7.2524
		wk8	-1.90667	2.21277	.904	-9.1891	5.3757
wk8	Day0	-.66333	2.21277	.998	-7.9457	6.6191	
	Wk1	-.77333	2.21277	.996	-8.0557	6.5091	
	wk2	1.87667	2.21277	.909	-5.4057	9.1591	
	wk4	1.90667	2.21277	.904	-5.3757	9.1891	

### Homogeneous Subsets

EE

Day		N	Subset for alpha = 0.05
			1
Tukey HSD <sup>a</sup>	wk4	3	81.6467
	wk2	3	81.6767
	wk8	3	83.5533
	Day0	3	84.2167
	Wk1	3	84.3267
	Sig.		.746

Niosome that compose of Span<sup>®</sup> 60:

### Test of Homogeneity of Variances

EE

Levene Statistic	df1	df2	Sig.
.838	4	10	.531

### ANOVA

EE

	Sum of Squares	df	Mean Square	F	Sig.
Between Groups	71.362	4	17.840	3.308	.057
Within Groups	53.930	10	5.393		
Total	125.292	14			

### Post Hoc Tests: Multiple Comparisons

Dependent Variable:EE

	(I)	(J)	Mean Difference (I-J)	Std. Error	Sig.	95% Confidence Interval	
						Lower	Upper
						Bound	Bound
Tukey HSD	Day0	Wk1	-.22000	1.89614	1.000	-6.4604	6.0204
		wk2	3.00667	1.89614	.537	-3.2337	9.2470
		wk4	3.32333	1.89614	.448	-2.9170	9.5637
		wk8	5.55667	1.89614	.087	-.6837	11.7970
	Wk1	Day0	.22000	1.89614	1.000	-6.0204	6.4604
		wk2	3.22667	1.89614	.474	-3.0137	9.4670
		wk4	3.54333	1.89614	.391	-2.6970	9.7837
		wk8	5.77667	1.89614	.073	-.4637	12.0170
	wk2	Day0	-3.00667	1.89614	.537	-9.2470	3.2337
		Wk1	-3.22667	1.89614	.474	-9.4670	3.0137
		wk4	.31667	1.89614	1.000	-5.9237	6.5570
		wk8	2.55000	1.89614	.672	-3.6904	8.7904
	wk4	Day0	-3.32333	1.89614	.448	-9.5637	2.9170
		Wk1	-3.54333	1.89614	.391	-9.7837	2.6970
		wk2	-.31667	1.89614	1.000	-6.5570	5.9237
		wk8	2.23333	1.89614	.763	-4.0070	8.4737
wk8	Day0	-5.55667	1.89614	.087	-11.7970	.6837	
	Wk1	-5.77667	1.89614	.073	-12.0170	.4637	
	wk2	-2.55000	1.89614	.672	-8.7904	3.6904	
	wk4	-2.23333	1.89614	.763	-8.4737	4.0070	

### Homogeneous Subsets

EE

	Day	N	Subset for alpha = 0.05
			1
Tukey HSD <sup>a</sup>	wk8	3	88.3233
	wk4	3	90.5567
	wk2	3	90.8733
	Day0	3	93.8800
	Wk1	3	94.1000
	Sig.		.073

**Niosome that compose of Span<sup>®</sup> 80:**

### Test of Homogeneity of Variances

EE

Levene Statistic	df1	df2	Sig.
1.819	4	10	.202

### ANOVA

EE

	Sum of Squares	df	Mean Square	F	Sig.
Between Groups	844.310	4	211.077	4.563	.024
Within Groups	462.579	10	46.258		
Total	1306.889	14			

### Post Hoc Tests: Multiple Comparisons

Dependent Variable:EE

(I) Day	(J) Day	Mean Difference (I-J)	Std. Error	Sig.	95% Confidence Interval	
					Lower Bound	Upper Bound
					Tukey HSD	Day0 Wk1
	Day0 wk2	17.59667	5.55325	.060	-.6795	35.8729
	Day0 wk4	17.95333	5.55325	.055	-.3229	36.2295
	Day0 wk8	20.32333*	5.55325	.028	2.0471	38.5995
	Wk1 Day0	-9.37333	5.55325	.481	-27.6495	8.9029
	Wk1 wk2	8.22333	5.55325	.595	-10.0529	26.4995
	Wk1 wk4	8.58000	5.55325	.559	-9.6962	26.8562
	Wk1 wk8	10.95000	5.55325	.344	-7.3262	29.2262
	wk2 Day0	-17.59667	5.55325	.060	-35.8729	.6795
	wk2 Wk1	-8.22333	5.55325	.595	-26.4995	10.0529
	wk2 wk4	.35667	5.55325	1.000	-17.9195	18.6329
	wk2 wk8	2.72667	5.55325	.986	-15.5495	21.0029
	wk4 Day0	-17.95333	5.55325	.055	-36.2295	.3229
	wk4 Wk1	-8.58000	5.55325	.559	-26.8562	9.6962
	wk4 wk2	-.35667	5.55325	1.000	-18.6329	17.9195
	wk4 wk8	2.37000	5.55325	.992	-15.9062	20.6462
	wk8 Day0	-20.32333*	5.55325	.028	-38.5995	-2.0471
	wk8 Wk1	-10.95000	5.55325	.344	-29.2262	7.3262
	wk8 wk2	-2.72667	5.55325	.986	-21.0029	15.5495
	wk8 wk4	-2.37000	5.55325	.992	-20.6462	15.9062

### Homogeneous Subsets

EE

	Day	N	Subset for alpha = 0.05	
			1	2
Tukey HSD <sup>a</sup>	wk8	3	69.3367	
	wk4	3	71.7067	71.7067
	wk2	3	72.0633	72.0633
	Wk1	3	80.2867	80.2867
	Day0	3		89.6600
	Sig.			.344

### Particle size and polydispersity index

Table C8. Particle size\* and polydispersity index\* of silk sericin loaded in noisome formulations under storage in refrigerator (4-8 °C) at day 0.

Day 0	Span <sup>®</sup> 20		Span <sup>®</sup> 40		Span <sup>®</sup> 60		Span <sup>®</sup> 80	
	Size (nm)	Pdi	Size (nm)	Pdi	Size (nm)	Pdi	Size (nm)	Pdi
1	224.47	0.342	179.90	0.365	263.00	0.521	465.60	0.619
2	200.14	0.271	232.20	0.370	225.20	0.351	297.53	0.535
3	327.30	0.670	240.90	0.440	268.00	0.448	429.20	0.329
<b>mean</b>	250.64	0.428	217.67	0.392	252.07	0.440	397.44	0.494
<b>SD</b>	67.50	0.213	32.99	0.042	23.40	0.085	88.42	0.149

Table C9. Particle size\* and polydispersity index\* of silk sericin loaded in noisome formulations under storage in refrigerator (4-8 °C) at week 1.

Week 1	Span <sup>®</sup> 20		Span <sup>®</sup> 40		Span <sup>®</sup> 60		Span <sup>®</sup> 80	
	Size (nm)	Pdi	Size (nm)	Pdi	Size (nm)	Pdi	Size (nm)	Pdi
1	220.80	0.366	224.90	0.365	219.80	0.338	279.80	0.543
2	234.40	0.358	231.00	0.398	225.10	0.360	329.70	0.577
3	218.20	0.332	240.70	0.436	230.70	0.355	283.10	0.485
<b>mean</b>	224.47	0.352	232.20	0.400	225.20	0.351	297.53	0.535
<b>SD</b>	8.70	0.018	7.97	0.036	5.45	0.012	27.91	0.047

Table C10. Particle size\* and polydispersity index\* of silk sericin loaded in noisome formulations under storage in refrigerator (4-8 °C) at week 2.

Week 2	Span <sup>®</sup> 20		Span <sup>®</sup> 40		Span <sup>®</sup> 60		Span <sup>®</sup> 80	
	Size (nm)	Pdi	Size (nm)	Pdi	Size (nm)	Pdi	Size (nm)	Pdi
<b>1</b>	304.50	0.462	354.60	0.532	273.10	0.411	352.40	0.660
<b>2</b>	307.10	0.456	486.30	0.689	267.30	0.386	382.80	0.627
<b>3</b>	309.70	0.431	334.30	0.572	299.90	0.459	362.50	0.512
<b>mean</b>	307.10	0.450	391.73	0.598	280.10	0.419	365.90	0.600
<b>SD</b>	2.60	0.016	82.52	0.082	17.39	0.037	15.48	0.078

Table C11. Particle size\* and polydispersity index\* of silk sericin loaded in noisome formulations under storage in refrigerator (4-8 °C) at week 4.

Week 4	Span <sup>®</sup> 20		Span <sup>®</sup> 40		Span <sup>®</sup> 60		Span <sup>®</sup> 80	
	Size (nm)	Pdi	Size (nm)	Pdi	Size (nm)	Pdi	Size (nm)	Pdi
<b>1</b>	243.60	0.383	285.80	0.403	315.70	0.460	405.10	0.601
<b>2</b>	299.80	0.493	357.05	0.527	333.90	0.518	441.70	0.557
<b>3</b>	294.30	0.517	354.40	0.516	316.90	0.458	414.60	0.572
<b>mean</b>	279.23	0.464	332.42	0.482	322.17	0.479	420.47	0.577
<b>SD</b>	30.98	0.071	40.39	0.069	10.18	0.034	18.99	0.022



Table C12. Particle size\* and polydispersity index\* of silk sericin loaded in niosome formulations under storage in refrigerator (4-8 °C) at week 8.

Week 8	Span <sup>®</sup> 20		Span <sup>®</sup> 40		Span <sup>®</sup> 60		Span <sup>®</sup> 80	
	Size (nm)	Pdi	Size (nm)	Pdi	Size (nm)	Pdi	Size (nm)	Pdi
<b>1</b>	232.80	0.430	321.90	0.571	306.80	0.424	332.30	0.491
<b>2</b>	214.00	0.321	356.70	0.570	298.60	0.417	390.00	0.518
<b>3</b>	230.40	0.326	312.50	0.454	308.80	0.467	449.40	0.526
<b>mean</b>	225.73	0.359	330.37	0.532	304.73	0.436	390.57	0.512
<b>SD</b>	10.23	0.062	23.28	0.067	5.40	0.027	58.55	0.018

Table C13. Analysis the Particle sizes of niosomes when storage in refrigerator (4-8 °C) for 8 week.

**Niosome that compose of Span<sup>®</sup> 20:**

**Test of Homogeneity of Variances**

Particle size

Levene Statistic	df1	df2	Sig.
7.859	4	10	.004

**ANOVA**

Particle size

	Sum of Squares	df	Mean Square	F	Sig.
Between Groups	15239.711	4	3809.928	3.340	.055
Within Groups	11405.894	10	1140.589		
Total	26645.605	14			

**Post Hoc Tests: Multiple Comparisons**

Dependent Variable: Particle size

	(I) Day	(J) Day	Mean Difference (I-J)	Std. Error	Sig.	95% Confidence Interval	
						Lower Bound	Upper Bound
Tukey HSD	Day0	Wk1	26.17000	27.57522	.871	-64.5823	116.9223
		wk2	-56.46333	27.57522	.312	-147.2157	34.2890
		wk4	-28.59667	27.57522	.833	-119.3490	62.1557
		wk8	24.90333	27.57522	.889	-65.8490	115.6557
	Wk1	Day0	-26.17000	27.57522	.871	-116.9223	64.5823
		wk2	-82.63333	27.57522	.079	-173.3857	8.1190
		wk4	-54.76667	27.57522	.338	-145.5190	35.9857
		wk8	-1.26667	27.57522	1.000	-92.0190	89.4857
	wk2	Day0	56.46333	27.57522	.312	-34.2890	147.2157
		Wk1	82.63333	27.57522	.079	-8.1190	173.3857
		wk4	27.86667	27.57522	.845	-62.8857	118.6190
		wk8	81.36667	27.57522	.085	-9.3857	172.1190
wk4	Day0	28.59667	27.57522	.833	-62.1557	119.3490	
	Wk1	54.76667	27.57522	.338	-35.9857	145.5190	
	wk2	-27.86667	27.57522	.845	-118.6190	62.8857	
	wk8	53.50000	27.57522	.358	-37.2523	144.2523	
wk8	Day0	-24.90333	27.57522	.889	-115.6557	65.8490	
	Wk1	1.26667	27.57522	1.000	-89.4857	92.0190	
	wk2	-81.36667	27.57522	.085	-172.1190	9.3857	
	wk4	-53.50000	27.57522	.358	-144.2523	37.2523	

### Homogeneous Subsets

#### Particle size

		N	Subset for alpha = 0.05
Day			1
Tukey	Wk1	3	224.4667
HSD <sup>a</sup>	wk8	3	225.7333
	Day0	3	250.6367
	wk4	3	279.2333
	wk2	3	307.1000
	Sig.		.079

#### Niosome that compose of Span<sup>®</sup> 40:

#### Test of Homogeneity of Variances

##### Particle size

Levene Statistic	df1	df2	Sig.
5.494	4	10	.013

#### ANOVA

##### Particle size

	Sum of Squares	df	Mean Square	F	Sig.
Between Groups	65279.263	4	16319.816	8.050	.004
Within Groups	20272.162	10	2027.216		
Total	85551.424	14			

**Post Hoc Tests: Multiple Comparisons**

Dependent Variable: Particle size

(I)	(J)	Mean Difference (I-J)	Std. Error	Sig.	95% Confidence Interval		
					Lower Bound	Upper Bound	
Dunnett T3	Day0	Wk1	-14.53333	19.59722	.983	-163.0580	133.9913
		wk2	-174.06667	51.31220	.219	-506.9223	158.7889
		wk4	-114.75000	30.11231	.111	-263.0563	33.5563
		wk8	-112.70000	23.31549	.060	-232.2884	6.8884
	Wk1	Day0	14.53333	19.59722	.983	-133.9913	163.0580
		wk2	-159.53333	47.86667	.274	-561.0431	241.9765
		wk4	-100.21667	23.77030	.173	-287.2956	86.8623
		wk8	-98.16667*	14.20872	.049	-195.8329	-.5005
	wk2	Day0	174.06667	51.31220	.219	-158.7889	506.9223
		Wk1	159.53333	47.86667	.274	-241.9765	561.0431
		wk4	59.31667	53.04638	.900	-256.6708	375.3041
		wk8	61.36667	49.50534	.850	-299.8064	422.5397
	wk4	Day0	114.75000	30.11231	.111	-33.5563	263.0563
		Wk1	100.21667	23.77030	.173	-86.8623	287.2956
		wk2	-59.31667	53.04638	.900	-375.3041	256.6708
		wk8	2.05000	26.91817	1.000	-147.2704	151.3704
wk8	Day0	112.70000	23.31549	.060	-6.8884	232.2884	
	Wk1	98.16667*	14.20872	.049	.5005	195.8329	
	wk2	-61.36667	49.50534	.850	-422.5397	299.8064	
	wk4	-2.05000	26.91817	1.000	-151.3704	147.2704	

**Niosome that compose of Span® 60:****Test of Homogeneity of Variances**

Particle size

Levene Statistic	df1	df2	Sig.
4.242	4	10	.029

**ANOVA**

Particle size

	Sum of Squares	df	Mean Square	F	Sig.
Between Groups	18370.737	4	4592.684	22.678	.000
Within Groups	2025.180	10	202.518		
Total	20395.917	14			

### Post Hoc Tests: Multiple Comparisons

Dependent Variable: Particle size

	(I) Day	(J) Day	Mean Difference (I-J)	Std. Error	Sig.	95% Confidence Interval	
						Lower Bound	Upper Bound
Dunnett T3	Day0	Wk1	26.86667	13.87231	.579	-79.0778	132.8111
		wk2	-28.03333	16.83304	.665	-112.9740	56.9073
		wk4	-70.10000	14.73348	.098	-162.4344	22.2344
		wk8	-52.66667	13.86635	.204	-158.7485	53.4151
	Wk1	Day0	-26.86667	13.87231	.579	-132.8111	79.0778
		wk2	-54.90000	10.52220	.098	-129.3441	19.5441
		wk4	-96.96667*	6.66642	.003	-135.1438	-58.7896
		wk8	-79.53333*	4.43183	.000	-100.8814	-58.1852
	wk2	Day0	28.03333	16.83304	.665	-56.9073	112.9740
		Wk1	54.90000	10.52220	.098	-19.5441	129.3441
		wk4	-42.06667	11.63405	.156	-106.1874	22.0540
		wk8	-24.63333	10.51433	.443	-99.2167	49.9500
	wk4	Day0	70.10000	14.73348	.098	-22.2344	162.4344
		Wk1	96.96667*	6.66642	.003	58.7896	135.1438
		wk2	42.06667	11.63405	.156	-22.0540	106.1874
		wk8	17.43333	6.65399	.334	-20.8133	55.6800
	wk8	Day0	52.66667	13.86635	.204	-53.4151	158.7485
		Wk1	79.53333*	4.43183	.000	58.1852	100.8814
		wk2	24.63333	10.51433	.443	-49.9500	99.2167
		wk4	-17.43333	6.65399	.334	-55.6800	20.8133

**Niosome that compose of Span<sup>®</sup> 80:****Test of Homogeneity of Variances**

Particle size

Levene Statistic	df1	df2	Sig.
3.171	4	10	.063

**ANOVA**

Particle size

	Sum of Squares	d f	Mean Square	F	Sig.
Between Groups	26685.681	4	6671.420	2.642	.097
Within Groups	25251.491	10	2525.149		
Total	51937.172	14			

**Post Hoc Tests: Multiple Comparisons**

Dependent Variable: Particle size

	(I)	(J)	Mean Difference (I-J)	Std. Error	Sig.	95% Confidence Interval	
						Lower Bound	Upper Bound
						Day	Day
Tukey HSD	Day0	Wk1	99.91000	41.02966	.183	-35.1220	234.9420
		wk2	31.54333	41.02966	.934	-103.4886	166.5753
		wk4	-23.02333	41.02966	.978	-158.0553	112.0086
		wk8	6.87667	41.02966	1.000	-128.1553	141.9086
	Wk1	Day0	-99.91000	41.02966	.183	-234.9420	35.1220
		wk2	-68.36667	41.02966	.493	-203.3986	66.6653
		wk4	-122.93333	41.02966	.079	-257.9653	12.0986
		wk8	-93.03333	41.02966	.232	-228.0653	41.9986
	wk2	Day0	-31.54333	41.02966	.934	-166.5753	103.4886
		Wk1	68.36667	41.02966	.493	-66.6653	203.3986
		wk4	-54.56667	41.02966	.681	-189.5986	80.4653
		wk8	-24.66667	41.02966	.972	-159.6986	110.3653
	wk4	Day0	23.02333	41.02966	.978	-112.0086	158.0553
		Wk1	122.93333	41.02966	.079	-12.0986	257.9653
		wk2	54.56667	41.02966	.681	-80.4653	189.5986
		wk8	29.90000	41.02966	.945	-105.1320	164.9320
wk8	Day0	-6.87667	41.02966	1.000	-141.9086	128.1553	
	Wk1	93.03333	41.02966	.232	-41.9986	228.0653	
	wk2	24.66667	41.02966	.972	-110.3653	159.6986	
	wk4	-29.90000	41.02966	.945	-164.9320	105.1320	



### Homogeneous Subsets

#### Particle size

Day		N	Subset for alpha = 0.05
			1
Tukey	Wk1	3	297.5333
HSD <sup>a</sup>	wk2	3	365.9000
	wk8	3	390.5667
	Day0	3	397.4433
	wk4	3	420.4667
	Sig.		.079

## **APPENDIX D**

### **Skin permeation study**

### Skin permeation study

Table D1. The percentage of cumulative amount of silk sericin solution (n=3).

Time (h)	Cumulative per area (mg/cm <sup>2</sup> )				
	1	2	3	Mean	SD
0.5	0.13	0.03	0.04	0.07	0.06
1	0.13	0.13	0.04	0.10	0.05
1.5	0.14	0.13	0.13	0.14	0.01
2	0.15	0.13	0.13	0.14	0.01
4	0.15	0.14	0.14	0.14	0.01
6	0.14	0.15	0.14	0.14	0.00
8	0.15	0.16	0.15	0.15	0.00
10	0.16	0.16	0.15	0.15	0.01
12	0.16	0.15	0.15	0.15	0.00
14	0.15	0.15	0.15	0.15	0.00
16	0.17	0.16	0.15	0.16	0.01
18	0.16	0.15	0.15	0.16	0.00
20	0.17	0.17	0.15	0.17	0.01
22	0.18	0.16	0.16	0.16	0.01
24	0.19	0.16	0.15	0.17	0.02

Table D2. The percentage of cumulative amount of silk sericin loaded in niosome-Span<sup>®</sup>20 (n=3).

Time (h)	Cumulative per area (mg/cm <sup>2</sup> )				
	1	2	3	Mean	SD
0.5	0.57	0.17	0.34	0.36	0.20
1	0.57	0.31	0.34	0.41	0.14
1.5	0.76	0.31	0.65	0.57	0.23
2	0.76	0.31	0.65	0.57	0.23
4	0.97	0.31	0.97	0.75	0.38
6	1.12	0.67	0.97	0.92	0.23
8	1.20	0.82	1.37	1.13	0.28
10	1.20	0.84	1.37	1.14	0.27
12	1.20	1.01	1.37	1.20	0.18
14	1.29	1.10	1.87	1.42	0.40
16	1.55	1.51	1.99	1.69	0.27
18	2.20	2.06	2.17	2.15	0.07
20	2.39	2.38	2.61	2.46	0.13
22	2.45	2.43	2.93	2.60	0.28
24	2.74	2.56	3.23	2.84	0.34

Table D3. The percentage of cumulative amount of silk sericin loaded in niosome-Span<sup>®</sup> 40 (n=4).

<b>Time (h)</b>	<b>Cumulative per area (cm<sup>2</sup>)</b>					
	<b>1</b>	<b>2</b>	<b>3</b>	<b>4</b>	<b>Mean</b>	<b>SD</b>
0.5	0.43	0.75	0.48	0.63	0.57	0.14
1	0.43	0.75	0.50	0.64	0.58	0.14
1.5	0.70	0.75	0.68	0.65	0.70	0.04
2	0.70	0.75	0.68	0.65	0.70	0.04
4	1.09	1.38	0.94	0.71	1.03	0.28
6	1.09	1.38	0.94	0.71	1.03	0.28
8	1.36	1.72	1.35	0.99	1.35	0.30
10	1.36	1.72	1.39	1.02	1.37	0.28
12	1.36	1.72	1.39	1.02	1.37	0.28
14	1.57	2.21	1.76	1.36	1.73	0.36
16	1.70	2.44	1.76	1.43	1.83	0.43
18	1.97	2.58	2.27	1.63	2.11	0.40
20	2.00	2.77	2.27	2.31	2.34	0.32
22	2.18	2.84	2.44	2.50	2.49	0.27
24	2.18	2.93	2.46	2.57	2.53	0.31

Table D4. The percentage of cumulative amount of silk sericin loaded in niosome-Span<sup>®</sup> 60 (n=4).

<b>Time (h)</b>	<b>Cumulative per area (cm<sup>2</sup>)</b>					
	<b>1</b>	<b>2</b>	<b>3</b>	<b>4</b>	<b>Mean</b>	<b>SD</b>
0.5	0.61	0.34	0.31	0.76	0.50	0.215
1	0.78	0.34	0.33	0.76	0.55	0.248
1.5	0.83	0.48	0.37	0.76	0.61	0.217
2	0.83	0.48	0.42	0.93	0.66	0.252
4	1.02	0.77	0.69	0.93	0.85	0.147
6	1.03	0.90	0.86	1.11	0.97	0.116
8	1.17	1.29	1.24	1.52	1.30	0.152
10	1.17	1.29	1.24	1.52	1.30	0.152
12	1.29	1.29	1.49	1.52	1.40	0.126
14	1.32	1.32	1.93	1.73	1.58	0.306
16	1.54	1.47	2.09	1.89	1.75	0.291
18	2.36	2.17	2.14	2.02	2.17	0.141
20	2.64	2.63	2.65	2.14	2.51	0.250
22	2.80	2.67	3.00	2.40	2.72	0.249
24	2.85	2.77	3.06	2.87	2.89	0.124

Table D5. The percentage of cumulative amount of silk sericin loaded in niosome-Span<sup>®</sup> 80 (n=4).

Time (h)	Cumulative per area (mg/cm <sup>2</sup> )				
	1	2	3	Mean	SD
0.5	0.34	0.52	0.34	0.40	0.10
1	0.33	0.52	0.55	0.47	0.12
1.5	0.57	0.77	0.66	0.67	0.10
2	0.30	0.77	0.44	0.50	0.24
4	0.39	0.85	0.99	0.74	0.32
6	0.51	0.85	0.88	0.75	0.20
8	0.76	1.15	1.44	1.12	0.34
10	0.53	1.20	1.67	1.13	0.57
12	0.47	1.26	1.86	1.19	0.70
14	0.48	1.33	2.39	1.40	0.96
16	0.61	1.46	2.49	1.52	0.94
18	1.18	1.61	2.82	1.87	0.85
20	1.40	1.95	3.17	2.17	0.90
22	1.43	2.18	3.30	2.30	0.94
24	1.52	2.37	3.33	2.41	0.90

Table D6. The flux (mg/cm<sup>2</sup>/h) of silk sericin all niosomes formulation.

Formulation	Slope (Flux, mg/cm <sup>2</sup> /h)					
	1	2	3	4	mean	SD
Silk sericin solution	0.002	0.0029	0.0025	-	0.002433	0.000503
Span <sup>®</sup> 20	0.0847	0.1036	0.1112	-	0.099833	0.013646
Span <sup>®</sup> 40	0.0724	0.0988	0.0867	0.082	0.084975	0.010971
Span <sup>®</sup> 60	0.0909	0.1023	0.1199	0.0798	0.098225	0.017123
Span <sup>®</sup> 80	0.0464	0.0695	0.1342	-	0.083367	0.045513

Table D7. The permeability coefficient (cm/h) of silk sericin all niosomes formulation.

Formulation	Papp (cm/h)					
	1	2	3	4	mean	SD
Silk sericin solution	0.000	0.000316	0.000323	-	0.000323	0.000007
Span <sup>®</sup> 20	0.0046494	0.004604	0.005548	-	0.004934	0.000532
Span <sup>®</sup> 40	0.0042421	0.00569	0.00474	0.004317	0.004747	0.00067
Span <sup>®</sup> 60	0.0049557	0.004988	0.005616	0.004757	0.005079	0.000372
Span <sup>®</sup> 80	0.0024662	0.004006	0.006521	-	0.004331	0.002047

Table D8. Analysis the flux of all niosomes formulation.

### Test of Homogeneity of Variances

Slope (flux)

Levene Statistic	df1	df2	Sig.
5.239	4	12	.011

### ANOVA: Slope (flux)

	Sum of Squares	df	Mean Square	F	Sig.
Between Groups	.020	4	.005	10.632	.001
Within Groups	.006	12	.000		
Total	.026	16			



**Post Hoc Tests: Multiple Comparisons**

Dependent Variable:Slope (flux)

	(I) Type	(J) Type	Mean Difference (I-J)	Std. Error	Sig.	95% Confidence Interval	
						Lower Bound	Upper Bound
Dunnett T3	Solution	Span20	-.09740*	.00788	.024	-.16477	-.03003
		Span40	-.08254*	.00549	.003	-.11434	-.05075
		Span60	-.09579*	.00857	.008	-.14550	-.04609
		Span80	-.08093	.02628	.315	-.30615	.14428
	Span20	Solution	.09740*	.00788	.024	.03003	.16477
		Span40	.01486	.00960	.721	-.03267	.06239
		Span60	.00161	.01163	1.000	-.04887	.05209
		Span80	.01647	.02743	.995	-.18025	.21318
	Span40	Solution	.08254*	.00549	.003	.05075	.11434
		Span20	-.01486	.00960	.721	-.06239	.03267
		Span60	-.01325	.01017	.841	-.05668	.03018
		Span80	.00161	.02684	1.000	-.20755	.21076
	Span60	Solution	.09579*	.00857	.008	.04609	.14549
		Span20	-.00161	.01163	1.000	-.05209	.04887
		Span40	.01325	.01017	.841	-.03018	.05668
		Span80	.01486	.02764	.998	-.17757	.20729
Span80	Solution	.08093	.02628	.315	-.14428	.30615	
	Span20	-.01647	.02743	.995	-.21318	.18025	
	Span40	-.00161	.02684	1.000	-.21076	.20755	
	Span60	-.01486	.02764	.998	-.20729	.17757	

Table D9. Analysis the permeability coefficient of all niosomes formulation.

**Test of Homogeneity of Variances**

Permeability coefficient

Levene Statistic	df1	df2	Sig.
4.370	4	12	.021

**ANOVA**

Permeability coefficient

	Sum of Squares	df	Mean Square	F	Sig.
Between Groups	.000	4	.000	14.395	.000
Within Groups	.000	12	.000		
Total	.000	16			

### Post Hoc Tests: Multiple Comparisons

Dependent Variable: Permeability coefficient

(I) Type	(J) Type	Mean Difference (I-J)	Std. Error	Sig.	95% Confidence Interval		
					Lower Bound	Upper Bound	
Dunnett T3	Span20	Solution	-.00457*	.00030	.016	-.00714	-.00200
		Span40	-.004402*	.00034	.005	-.00639	-.00241
		Span60	-.00478*	.00017	.001	-.00578	-.00377
		Span80	-.00401	.00117	.264	-.01401	.00599
	Span 20	Solution	.00457*	.00030	.016	.00200	.00715
		Span40	.00017	.00046	1.000	-.00179	.00214
		Span60	-.00020	.00035	.998	-.00208	.00168
		Span80	.00056	.00120	.999	-.00843	.00956
	Span 40	Solution	.00440*	.00034	.005	.00241	.00639
		Span20	-.00017	.00045	1.000	-.00214	.00179
		Span60	-.00037	.00038	.953	-.00212	.00137
		Span80	.00039	.00121	1.000	-.00836	.00914
Span 60	Solution	.00477*	.00017	.001	.00377	.00578	
	Span20	.00020	.00034	.998	-.00168	.00208	
	Span40	.00037	.00038	.953	-.00137	.00212	
	Span80	.00077	.00118	.991	-.00885	.01038	
Span 80	Solution	.00401	.00117	.264	-.00599	.01401	
	Span20	-.00057	.00120	.999	-.00957	.00843	
	Span40	-.00039	.00121	1.000	-.00914	.00836	
	Span60	-.00077	.00118	.991	-.01038	.00885	



### Chulalongkorn University Animal Care and Use Committee

<b>Certificate of Project Approval</b>	<input type="checkbox"/> Original	<input type="checkbox"/> Renew
<b>Animal Use Protocol No. 12-33-001</b>	<b>Approval No. 12-33-001</b>	
<b>Protocol Title</b> Formulation of spray-dried silk sericin loaded in niosomes and evaluation of biological activities		
<b>Principal Investigator</b> Suchada Chutimaworapan, Ph.D.		
<b>Certification of Institutional Animal Care and Use Committee (IACUC)</b> This project has been reviewed and approved by the IACUC in accordance with university regulations and policies governing the care and use of laboratory animals. The review has followed guidelines documented in Ethical Principles and Guidelines for the Use of Animals for Scientific Purposes edited by the National Research Council of Thailand.		
<b>Date of Approval</b> January 30, 2012	<b>Date of Expiration</b> January 30, 2015	
<b>Applicant Faculty/Institution</b> Faculty of Pharmaceutical Sciences, Chulalongkorn University, Phyathai Rd., Pathumwan BKK-THAILAND. 10330		
<b>Signature of Chairperson</b> 	<b>Signature of Authorized Official</b> 	
<b>Name and Title</b> THONGCHAI SOOKSAWATE, Ph.D. Chairman	<b>Name and Title</b> PARKPOOM TENGAMNUAY, Ph.D. Associate Dean (Research and Academic Service)	
<p><i>The official signing above certifies that the information provided on this form is correct. The institution assumes that investigators will take responsibility, and follow university regulations and policies for the care and use of animals.</i></p> <p><i>This approval is subjected to assurance given in the animal use protocol and may be required for future investigations and reviews.</i></p>		

## VITA

Miss Panida Kethip was born on June 9, 1982 in Sisaket, Thailand. She received her Bachelor's degree in Pharmacy from the Faculty of Pharmaceutical Sciences, Prince of Songkla University, Songkla, Thailand in 2005. Since graduation, she has worked at the Pharmacy Department, Siriraj Hospital, Bangkok. She enrolled the Master's degree program in Pharmacy at Chulalongkorn University in 2009.